ESTIMATION OF PLANE OF MAXIMUM CURVATURE FOR ENHANCEMENT OF ORTHOTIC MANAGEMENT OF ADOLESCENT IDIOPATHIC SCOLIOSIS (AIS)

WU HUIDONG

PhD

The Hong Kong Polytechnic University

This programme is jointly offered by The Hong Kong Polytechnic University and Sichuan University

2022

The Hong Kong Polytechnic University
Department of Biomedical Engineering

Sichuan University
Department of Rehabilitation Medicine

Estimation of Plane of Maximum Curvature for Enhancement of Orthotic Management of Adolescent Idiopathic Scoliosis (AIS)

WU Huidong

A thesis submitted in partial fulfilment of the requirements of the Degree of Doctor of Philosophy

June 2021

CERTIFICATE OF ORIGINALITY

I hereby declare that this thesis is my own work and that, to the best of my knowledge and belief, it reproduces no material previously published or written, nor material that has been accepted for the award of any other degree or diploma, except where due acknowledgement has been made in the text.

_____ (Signed)

WU Huidong (Name of student)

ABSTRACT

Adolescent idiopathic scoliosis (AIS) is a complex three-dimensional (3D) spine deformity in adolescents with unknown causes. Coronal-Cobb angle (coronal-Cobb) measured from radiograph serves as the golden standard in assessing patients with AIS.. However, it may underestimate the severity of AIS and not fully reflect the 3D features of spinal deformity. Therefore, 3D descriptors, including the best-fit plane (BFP), end-apical-end plane (EAEP), and plane of maximum curvature (PMC), were proposed. However, these descriptors were not commonly used in assessing AIS due to the complexity of their acquisition methods. The BFP and EAEP are regarding the three axes of the human coordinate system, and the PMC only uses the vertical axis. By comparison, the PMC seems closer to the coronal-Cobb as both reveal the spinal curvature in a vertical plane. The PMC is a vertical plane between the sagittal and coronal planes and presents the maximum spinal curvature. Its parameters include the maximum Cobb angle (PMC-Cobb) and PMC orientation (PMC-orientation, the angle between the sagittal plane and PMC).

Radiographic and ultrasound techniques have been applied for PMC assessments. However, they are operated with special software/skills (e.g., 3D reconstruction), further validations are being explored. Therefore, Part I of this study was to develop a more user-friendly computational method (CM) for estimating the PMC (PMC-Cobb; PMC-orientation) and verify its results with computed tomography (CT). In the proposed CM, PMC was estimated via an anti-trigonometric function based on the 3D coordinates of 8 points located at the upper-end vertebra's superior endplate and the lower-end vertebra's inferior endplate of the spinal curve in the coronal and sagittal CT images. The users identified the 8 points manually. In the CT method, the PMC was determined via rotating a vertical plane, where the scoliotic spine was projected onto, with 5^{o} increments, and measuring the Cobb angle in each rotated plane. Twenty-nine subjects with AIS were recruited, and two well-trained raters collected the data. The results of this study demonstrated high intra- & inter-rater reliability for the PMC obtained using the CM (intra- & inter-rater intraclass correlation coefficient ≥0.87). The PMC acquired using the CM was strongly correlated with those obtained using the CT method (ICC ≥0.84, Pearson correlation coefficient (r)

≥0.72, linear regression analysis (R^2) ≥0.69). To conclude, the CM provided reliable and valid PMC information for patients with AIS. The contribution of PMC in 3D assessment and classification of AIS was reported earlier. Compared with the coronal-Cobb, the PMC appeared to be more informative since it provides both the maximum curve magnitude (PMC-Cobb) and the rotation of the spinal curve towards the coronal plane (PMC-orientation). In the sagittal plane of a normal spine, curves are present in the thoracic and lumbar regions. However, the thoracic and/or lumbar curve(s) are/is abnormally rotated towards the coronal plane in a scoliotic spine, accompanying with or without changes in the original curvature. This indicates that the coronal-Cobb was only a component of the spinal curvature. In orthotic treatment, if only the correction of coronal-Cobb is considered, the sagittal curve may go beyond physiological range, likely causing thoracic hyper-kyphosis and lumbar hyper-lordosis. Thus, employing the PMC as a supplement of the coronal-Cobb in managing AIS would be necessary. Due to the complexity of the PMC method, it was not considered in managing AIS in the past. The CM has been developed and converted into comprehensible software in this study. A preliminary study demonstrated high reliability of the PMC obtained using this software (ICC ≥0.91), and further study is going on. With continuous effort, it believes that the CM would potentially serve as a useful tool for the 3D assessment of AIS. Additionally, Part I of this study was first to investigate CT usage in assessing the PMC and the prone-standing difference/correlation of PMC. The results could establish a foundation for future relevant studies.

In current practice, spinal orthosis was designed empirically. The pressure-pad shape and correcting-force direction vary among orthoses designed by different orthotists. There were 5 most common pressure-pad shapes (A, B, C, D, and E) applied inside orthoses according to Society on Scoliosis Orthopedic and Rehabilitation Treatment (SOSORT) investigation. It is ambiguous what pressure-pad shape and correcting-force direction would provide an optimal correction. The PMC could be a promising descriptor for reflecting 3D characteristics of AIS, which may make it valuable for orthosis design. Thus, Part II of this study was to investigate (I) what pressure-pad shape and (II) correcting-force direction could produce a better clinical efficacy, and (III) whether the PMC concept would improve

the clinical efficacy of orthosis designed (correcting force in the PMC zone, PMC-orientation ±15° of the thoracic curves or perpendicular to the plane located in the PMC zone of the thoraco/lumbar curves). The pressure-pad shape and correcting-force direction would be estimated based on the modified models of patients' trunks in the Computer-Aided Design /Computer-Aided Manufacturing system (CAD/CAM). The PMC was estimated using the CM proposed in part I based on patients' EOS images (biplanar X-rays). The optimal correcting-force direction was analysed by evenly diving the left and right posterior quadrants into 4 zones, respectively: zone 1(0° to ±22.5°), zone 2 (22.5° to 45.0° or -22.5º to -45.0º), zone 3 (45.0º to 67.5º or -45.0 to -67.5º), and zone 4 (67.5° to 90º or -67.5° to -90º) (the sagittal plane=0° and coronal plane=+/-90º; clockwise and counter-clockwise rotation from the sagittal plane to coronal plane was recorded as "+" and "-", respectively, in top view). The outcome measurements included PMC (PMC-Cobb; PMC-orientation), coronal-Cobb, thoracic kyphosis, and lumbar lordosis at the pre-orthosis, immediate in-orthosis, and follow-up off-orthosis (6-12 months). The clinical efficacy was analysed using the immediate in-orthosis correction and the success rate of progression control. Based on the inclusion and exclusion criteria proposed by the Scoliosis Research Society (SRS), 81 consecutive patients with AIS were selected from the database of a local hospital. This study's results suggested that pressure-pad shape A appeared superior clinical efficacy for the spinal curves accompanied by the thoracic hyper-kyphosis. In contrast, shape E produced superior clinical efficacy for the curves combined with thoracic hypo-/normal kyphosis. The correcting force with the direction in zone 2 could provide superior correction of curves combined with thoracic hyper-kyphosis. By comparison, those with direction in zone 3 were more effective for controlling curves accompanied by thoracic hypo-/normal kyphosis. The orthoses designed with the PMC concept did not show superior to those designed without the PMC concept in correcting the spinal curvature. It may be because of some confounding factors. For instance, only considering correcting-force direction on the convex side of the spinal curve was involved in analysis while neglecting correcting-force level and counter-forces. Still, it first applied the PMC for enhancing orthotic design and would create a base for continuous study. Based on the biomechanical analyses of all results, correcting force with direction at 30°–40° regarding the sagittal plane may be more effective in controlling curves with thoracic hyper-kyphosis;

correcting force with direction over 50°may be more helpful for controlling curves with thoracic hypo-/normal kyphosis. Additionally, rotation of the spinal curve (PMC-orientation) was not significantly corrected after orthosis fitting, which was in line with the earlier reports. This may be associated with the correcting forces and anatomical structures of the spine and rib cage. A primary limitation should be noted. This study only involved the correcting-force direction on the convex side of the spinal curve in analysis while ignoring some potential confounding factors, such as correcting-force level and counter-forces. Nevertheless, this study initiated a starting point in understanding the 3D correction of orthoses designed with different pressure-pad shapes, correcting-force directions, and the PMC concept, which would help optimize the orthotic management of AIS. A future prospective study with more potential confounding factors controlled was suggested to further confirm the findings of this study.

PUBLICATIONS ARISING FROM THE THESIS

Peer-reviewed journal papers

Hui-Dong Wu, Chen He, Winnie Chiu-Wing Chu, Man-Sang Wong. Estimation of Plane of Maximum Curvature for the Patients with Adolescent Idiopathic Scoliosis via A Purpose-design Computational Method. European Spine Journal, 2021; 30(3):668-675.

Hui-Dong Wu, Wei Liu, Man-Sang Wong. Reliability and Validity of Coronal Curvature Assessments using Clinical Ultrasound for the Patients with Scoliosis: A Systematic Review. European Spine Journal 2020; 29:717-725.

Hui-Dong Wu, Winnie Chiu-Wing Chu, Cheng-Qi He, Man-Sang Wong. Estimation of Plane of Maximum Curvature for Patients with Adolescent Idiopathic Scoliosis via Computed Tomography. Prosthetics and Orthotics International 2020; 44: 298-304.

Hui-Dong Wu, Man-Sang Wong. Assessment of Maximum Spinal Deformity in Scoliosis: A Literature Review. Journal of Medical and Biological Engineering 2020; 40: 621-629.

Peer-reviewed conference papers

Hui-Dong Wu, Cheng-Qi He, Man-Sang Wong. Estimation of The Plane of Maximum Curvature (PMC) for the Patients with Adolescent Idiopathic Scoliosis (AIS) via a Purpose Design Computational Method. In: Proceedings of Hong Kong Prosthetic and Orthotic Scientific Meeting 2018, Hong Kong, 23th September 2018.

Hui-Dong Wu, Cheng-Qi He, Man-Sang Wong. Reliability and Validity of a Purpose Design Computational Method in the Estimation of Plane of Maximum Curvature (PMC) for Patients with Adolescent Idiopathic Scoliosis (AIS). In: Proceedings of Asian Prosthetic and Orthotic Scientific Meeting 2018 in Bangkok, Thailand, 7th-9th November 2018.

Hui-Dong Wu, Cheng-Qi He, Man-Sang Wong. Reliability and Validity Study of a Purpose-Designed Computational Method for Estimation of Plane of Maximum Curvature of Adolescent Idiopathic Scoliosis. In: Proceedings of International Society of Prosthetic and Orthotic World Congress 2019 in Kobe, Hyogo, Japan, 5th-8th October 2019.

Hui-Dong Wu, Man-Sang Wong. Concept of Plane of Maximum Curvature (PMC) in Orthotic Management of Adolescent Idiopathic Scoliosis (AIS). In: Proceedings of International Society of Prosthetic and Orthotic World Congress 2019 in Kobe, Hyogo, Japan, 5th-8th October 2019.

Hui-Dong Wu, Man-Sang Wong. Investigation of Optimal Biomechanical Design of Spinal Orthosis for AIS. In: proceeding of International Society of Prosthetic and Orthotic World Congress (virtual version), 4th Nov. 2021.

ACKNOWLEDGEMENTS

I would like to express my great gratitude to my chief supervisor Dr. Man-Sang Wong for his patient guidance and strong support to my Ph.D. research work and this thesis preparation. I also would like to thank my co-supervisor Prof. Cheng-qi He for his kind support during my Ph.D. research.

I would especially thank Prof. Winnie Chiu-Wing Chu for her kind suggestions to my research work and arrangements for the collection of CT and EOS images for this project. I am also thankful to Miss Min Deng and her colleagues for the collection of CT and EOS images in the Prince of Wales Hospital, Chinese University of Hong Kong.

I am grateful to Mr. Sai-Wing Sin, Mr. Wing-Kwan Kwok, Mr. Hon Man Kee, and Mr. Choi-Kam Au Yang for their kind comments/suggestions to my research work and their arrangements for subjects screening in database and CAD data collection in the Prince of Wales Hospital, Chinese University of Hong Kong.

I am thankful to Dr. Babak Hassan Beygi, Dr. Chen He and Miss Syeda Aimen Abbasi for their kind help and comments/suggestions in my research work and support for data collection. I also would like to thank Dr. Yu Zheng, Dr. Yangmin Lin, Dr. Chengfei Gao, and Mr. Zhaojian Meng for their kind help and suggestions on my research work.

Thanks to all the subjects who were involved in this project.

I would also like to thank the Hong Kong Jockey Club for providing the Scholarship to support my Ph.D. study in Hong Kong.

I would like to thank my family for their love, understanding, and support during the pursuit of a Ph.D. degree.

TABLE OF CONTENTS

LIST OF FIGURES

LIST OF TABLES

LIST OF ABBREVIATIONS

Abbreviation	Full Spelling
AIS	Adolescent idiopathic scoliosis
AP	Antero-posterior
BFP	Best fit plane
CM	Computational method
CI	Confidence interval
CT	Computed tomography
EAEP	End-apical-end vertebrae plane
ICC	Intraclass correlation coefficient
LTLs/LLs	left (thoraco)lumbar curves
MAD	Mean absolute difference
MD	Mean difference
MRI	Magnetic resonance imaging
PA	Posteroanterior
PMC	Plane of maximum curvature
RTs	Right thoracic curves
SD	Standard deviation
SEM	Standard error of measurement
VAR	Vertebral axial rotation

CHAPTER 1 INTRODUCTION

1.1 Background

Adolescent idiopathic scoliosis (AIS) is a complicated three-dimensional (3D) deformity of the spine characterized by lateral curvature of at least 10° and vertebral axial rotation (VAR) and may accompany by sagittal thoracic hypo-kyphosis [1-3] and lumbar hyper-lordosis [4]. AIS is a common disease observed in adolescents with an overall prevalence of 0.47–5.2% [5] and unknown causes. The prevalence is higher in females than males and increases with age [5]. It could cause discontent with body image [6,7], higher incidence of low back pain [6,7], asymmetrical gait patterns [8,9], higher energy cost of walking [9], higher prevalence of osteopenia [10], and even respiratory impairment [6,11-13] and/or cardiovascular compromise [12] in a severe case.

Part I

Coronal Cobb angle (coronal-Cobb) measured from the posteroanterior (PA) radiograph is commonly used to assess AIS, including initial diagnosis and subsequent progression monitor [14-16]. However, the coronal-Cobb may underestimate the spinal curvature [17-20] and not fully reflect the curve pattern [21]. Sangole, C E Aubin (21) reported that two distinct curve types with remarkably different maximum curvature and thoracic kyphosis could present almost the same coronal-Cobb. Thus, the 3D assessment was increasingly recognized clinically [22], and the plane of maximum curvature (PMC) was proposed [23] (Figure 1.1). PMC is a vertical plane that positions between the sagittal and coronal planes and presents the maximum spinal curvature when a scoliotic spine is projected onto it [23]. The parameters include PMC-Cobb (the maximum Cobb angle measured in the PMC) and PMC-orientation (the angle between the PMC and sagittal plane [23]). PMC was considered as a promising descriptor for reflecting 3D features of the scoliotic spine [24] and differentiating curve types three-dimensionally [21], which may decrease the unknown variability of the current two-dimensional (2D) classification. It has been recommended for the 3D assessment and classification of scoliosis by the 3D Classification Committee

under the Scoliosis Research Society (SRS) [24].

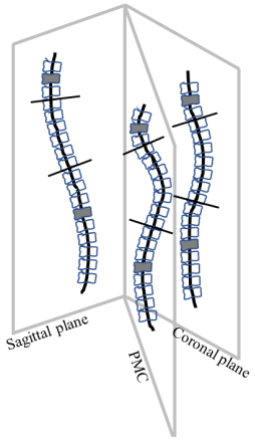

Figure 1.1 Plane of maximum curvature [25]

Several approaches allow PMC assessment in either standing or recumbent (prone/supine) position [18,26,27]. With the aid of fluoroscopy, Lindahl and Movin (18) acquired the PMC via rotating a platform, where the patients stood until the maximum spinal curvature was found. Computed tomography (CT) and magnetic resonance imaging (MRI) allow PMC assessment in recumbent position by rotating a vertical plane with a certain increment until the maximum spinal curvature was measured. However, the recumbent and standing deformities could be remarkably different because of the gravitational effect. Besides, CT would expose an individual to high radiation [28], which has been the main concern of patients and their families. These limitations make CT and MRI inappropriate for routine assessment of PMC for immature patients, especially those with mild to moderate curves. Recently, an EOS (stereo radiography) system and 3D ultrasound have also been developed for PMC assessment. For the EOS system, a 3D model of the scoliotic spine was reconstructed from the standing bi-planar EOS images, and the PMC-orientation was determined using the projection of apical vertebra on the transverse plane. Regarding the ultrasound, 3D images of a scoliotic spine were established from ultrasound data, based on which a vertical plane was rotated along the axial axis to a position with the orientation equalling to the maximum VAR (±2°/4°) [27]. However, both the EOS system and ultrasound needed further validation before clinical application (e.g., comparing to

CT/MRI). Also, the need for 3D reconstruction software/skills makes these two modalities a bit time-consuming and not that user-friendly for clinical users. The use of the EOS system and 3D ultrasound for PMC assessment was limited to the research stage. Thus, it was attractive to propose alow-dose radiation, more user-friendly, and less time-consuming method.

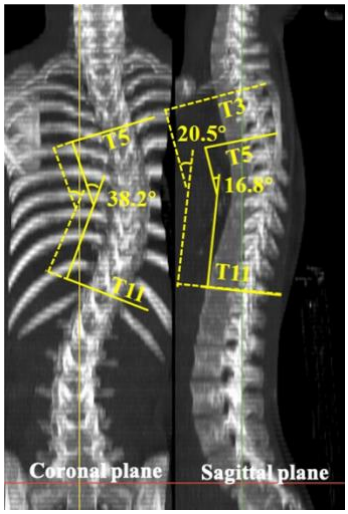

Figure 1.2 Constrained (solid lines) and unconstrained (dashed lines) Cobb methods

Due to the complicated global, regional, and local deformity of the scoliotic spine [23,29-31], it was unknown if the end-vertebrae most tilted in the coronal plane would always be most tilted in any other vertical planes. Hence, PMC assessed based on the end-vertebrae selected from the coronal plane may be or may not be the "actual" PMC (presenting the "actual" maximum spinal curvature). There were different degrees of discrepancies between PMC measurements based on the end-vertebrae selected from the coronal plane and based on the end-vertebrae selected from the plane where the Cobb angle was measured [32,33].

As shown in Figure 1.2, the constrained Cobb method is to measure the Cobb angle in any other vertical planes different from the coronal plane but using the upper and lower end-vertebrae selected from the coronal plane at the beginning of the measurement [23,33]. The unconstrained Cobb method is to measure the Cobb angle in any other vertical planes using the upper and lower end-vertebrae identified from that plane, where the Cobb angle is

measured [32]. Although possible discrepancies of PMC assessment using these two methods were observed, they were not studied primarily. With the increasing recognition of PMC in the assessment of AIS, understanding the difference and correlation of PMC measurements acquired using these two methods might benefit the selection of PMC assessment methods.

Because of the gravitational effect, the spinal deformities in recumbent (prone/supine) and standing positions could be notably different. Understanding the difference of spinal-deformity parameters in recumbent and standing positions may benefit the management of AIS. The standing-prone/supine differences/correlations of coronal-Cobb [34-44], sagittal thoracic kyphosis [35,39,41,42], sagittal lumbar lordosis [35,39,41,42] and VAR [41-44] have been studied. PMC was recognized as a comprehensive 3D descriptor. However, the standing-prone/supine difference and correlation have not been investigated yet.

Part II

Orthotic bracing is a typical conservative intervention for immature patients with a primary curve of 20°–40°, alone or in association with exercises [45]. Apart from some negative reports [46,47], the orthotic intervention has been demonstrated to positively affect the prevention of curve progression and reduction of surgical incidence in most studies [48-52]. However, the positive effect was mainly observed on the lateral curvature (e.g., coronal-Cobb) barely on the VAR and rib hump [48,49]. The importance of 3D correction has been long recognized and emphasized. However, the correction mechanism could be remarkably different among orthoses designed by different orthotists [53]. So far, there has not been a consistent document for guiding the orthosis design specifically, and, in general, orthoses are designed empirically. It was unclear which shape of pressure-pad inside the orthosis and which direction of correcting force provided by the orthosis would provide better clinical efficacy for patients with AIS.

Besides, during clinical practice, the correction mechanism of the orthosis is commonly designed based on the curve type identified from the coronal plane. However, it has been reported to may not fully reflect the "actual" curve types. On the other hand, PMC was considered as a promising descriptor for reflecting the 3D features of the scoliotic spine and differentiating curve types [23]. Its importance in 3D assessment and classification of scoliosis has been reported [33,54-57]. However, it is barely considered when making orthotic strategies.

1.2 Study Objectives

Part I

1) To develop a more user-friendly and less time-consuming computational method (CM) for PMC estimation merely based on the coronal and sagittal planes (PA & lateral CT images) of the scoliotic spine.
2) To investigate the inter- & intra-rater reliability of PMC obtained using the CM and validate it with CT.
3) To evaluate the feasibility of using CT to obtain PMC and the comparability of PMC acquired using the constrained and unconstrained Cobb methods.
4) To analyze the difference and correlation between the PMC in prone and standing positions.

Part II

5) To investigate which shape of pressure-pad inside orthosis would provide superior clinical efficacy to other shapes;
6) To evaluate which direction of correcting force would produce superior clinical efficacy to other directions;
7) To investigate whether orthosis designed with the PMC concept would provide superior clinical efficacy to those designed with the non-PMC concept.

1.3 Organization of the Thesis

Chapter 2 briefs the current status of parts I and II, and the remaining chapters were organized as shown in Figure 1.3. Part I included chapters 3, 4, and 5. Chapter 1 was to propose a computational method (CM) for PMC estimation and verify its PMC with those acquired using CT; chapter 4 analyzed the reliability of PMC acquired using the CT which served as the reference for the validation of PMC obtained using the CM; and in chapter 5, the PMC in prone and standing positions were estimated and compared, which may benefit the understanding of gravitational impact on the AIS. Part II investigated the application of PMC in enhancement of orthotic management of AIS, including biomechanical design of spinal orthosis and 3D correction evaluation of orthotic treatment. Chapter 7 provided a summary and recommendations regarding the findings of this project.

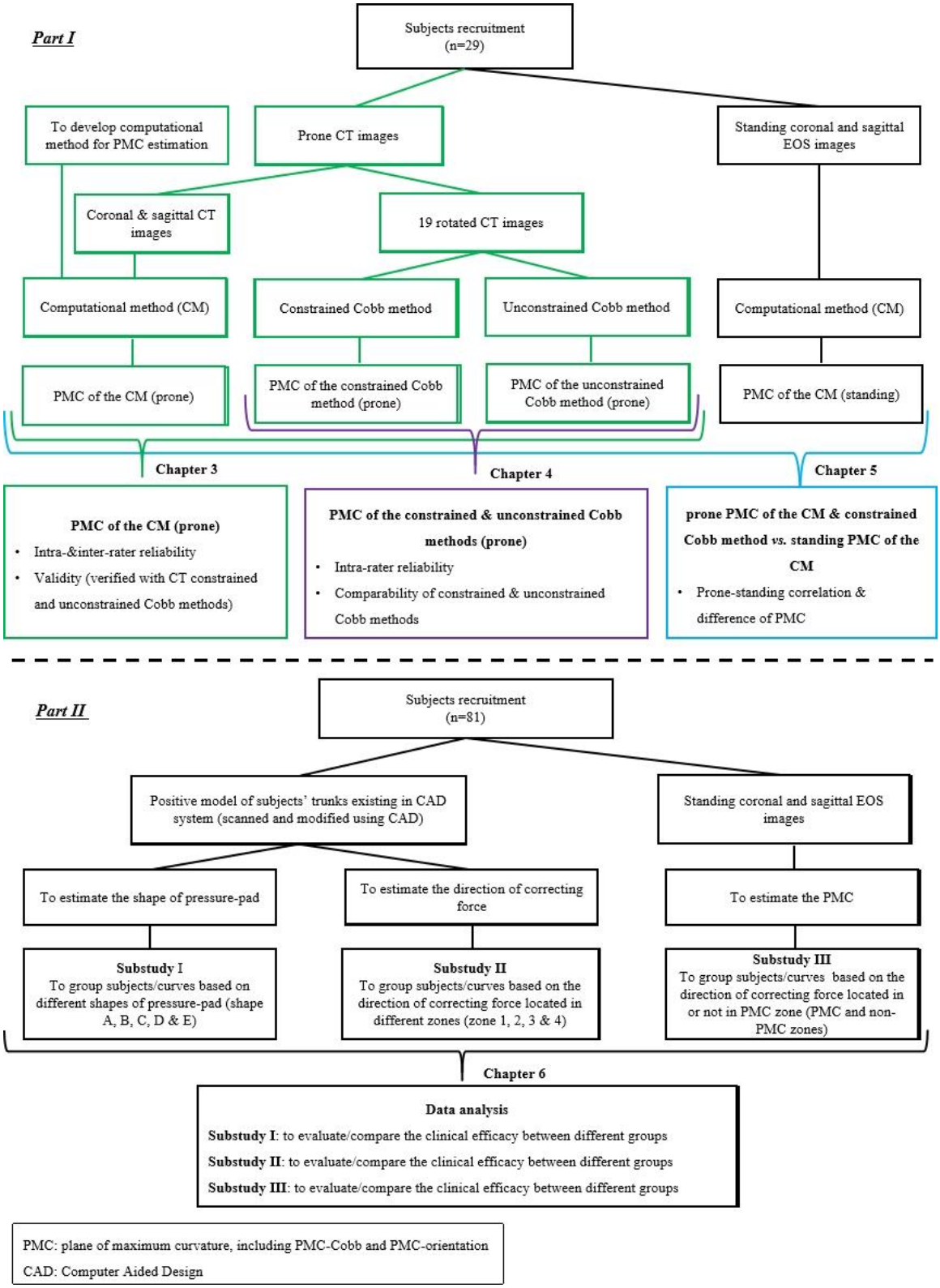

Figure 1.3 Organization of the thesis

CHAPTER 2 LITERATURE REVIEW

2.1 Spine and Vertebra

The terminologies of anatomical planes, the global axis system (x, y, z), and structures related to the spine and vertebra in this thesis are introduced. As shown in Figure 2.1, the anatomical planes contain: (1) the coronal (or frontal) plane, a vertical plane that divides the human body into anterior and posterior parts; (2) the sagittal plane, a vertical plane that divides the human body into left and right parts; (3) the transverse (or axial) plane, a horizontal plane that divides the human body into superior and inferior parts. These three imaginary planes are perpendicular to each other.

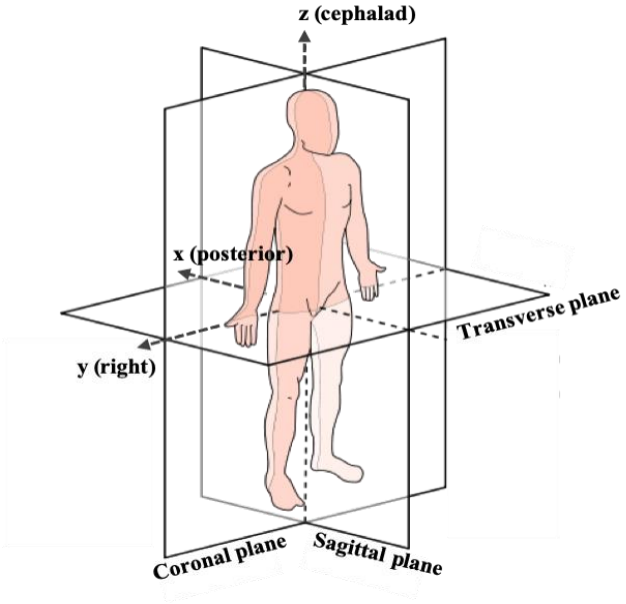

Figure 2.1 Anatomical planes [58]

As shown in Figure 2.1, the global axis system (x, y, z) of the human body has its origin placed at the center of the superior endplate of the first sacral vertebra (S1) [23]. Axis x, paralleling to the sagittal plane, points towards the posterior; axis y, paralleling to the coronal plane, points towards the right; and axis z, perpendicular to the transverse plane,

points towards the cephalad direction. These three imaginary axes were perpendicular to each other.

Figure 2.2 A normal spine in coronal and sagittal views [59]

The spine is a vertebral column that extends from the pelvis to the skull base, protecting the spinal cord, supporting the human body's upright posture, and providing functional movements. The spine consists of the cervical vertebrae (C1–C7), thoracic vertebrae (T1–T12), lumbar vertebrae (L1–L5), fused sacral vertebrae (S1–S5), and coccyx (Figure 2.2). These bony structures are connected by intervertebral discs and facet joints and stabilized by attached ligaments and muscles. Generally, an individual vertebra comprise a vertebral body anteriorly, a vertebral arch posteriorly, and superior & inferior endplates. The vertebral arch contains two pedicles, two laminae, two transverse processes, two inferior articular processes, two superior articular processes, and one spinous process (Figure 2.3) [60].

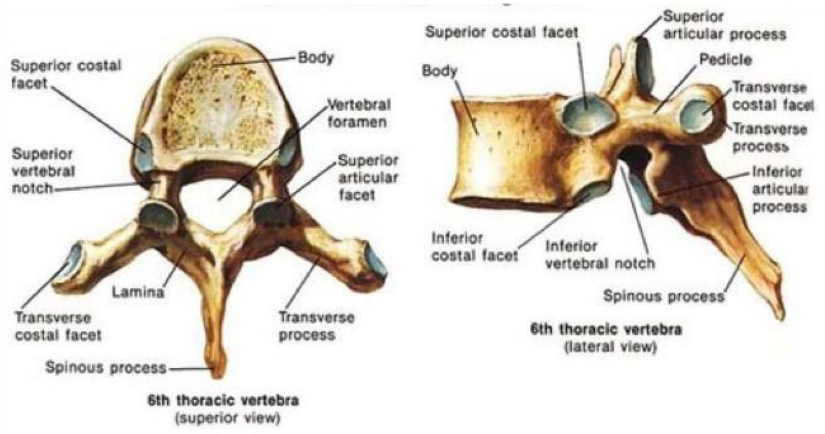

Figure 2.3 Thoracic vertebra [61]

2.2 Scoliosis

Scoliosis is a general term, firstly defined by Vasiliadis, Grivas (62), meaning an abnormal spinal lateral curvature (Cobb angle ≥10°) and VAR [63]. Scoliosis can be structural or functional. This thesis focused on structural scoliosis (called scoliosis in the followings) differentiated from functional scoliosis. Functional scoliosis is commonly induced by extra causes, such as shortening a lower extremity or asymmetric tone of paraspinal muscles, and is partially/completely reduced after elimination of causes. Scoliosis can be subclassified into congenital, syndromic, and idiopathic [64]. The congenital mainly results from deformed vertebrae; the syndromic is usually caused by the disorder of neuromusculoskeletal/connective tissue systems or neurofibromatosis; and the idiopathic, introduced by Kleinberg (65), is associated with unknown causes or probably several causes, and accounts for about 85% of all the scoliosis cases [63].

Based on the standing coronal-Cobb, idiopathic scoliosis can be subcategorized into low (10°–20°), moderate (21°–35°), moderate to severe (36°–40°), severe (41°–50°), severe to very severe (51°–55°) and very severe (≥56°) [63]. According to the level of the apical vertebra in the coronal plane, idiopathic scoliosis can also be subclassified into cervical (apex: C1 to Disc C6-7), cervicothoracic (apex: C7–T1), thoracic (apex: Disc T1–2 to Disc

T11–12), thoracolumbar (apex: T12–L1) and lumbar (apex: Disc L1-2 to L5) [63]. Also, according to the age of onset, idiopathic scoliosis is sub-divided into infantile (<3 years), juvenile (4–10 years), adolescent (10–17 years), and adult (≥18 years) [63,66]. This thesis is going to introduce adolescent idiopathic scoliosis.

2.3 Adolescent Idiopathic Scoliosis (AIS)

Adolescent idiopathic scoliosis (AIS) is a complicated 3D deformity of the spine, including a lateral curvature of ≥10° in the coronal plane and VAR in the transverse, and may be accompanied by thoracic hypo-kyphosis [1-3] and/or lumbar hyper-lordosis [4]. The reasons are unknown. This section was going to introduce the prevalence, symptoms, and progression of AIS.

2.3.1 Prevalence of AIS

The overall prevalence of AIS was 0.47%–5.2% [5]. Its prevalence is associated with race or genetic factors. Of patients with AIS, 97% are associated with other family members who suffered from AIS [67], and 40% of Prader-Willi syndrome patients experience scoliosis [68]. Kamtsiuris, Atzpodien (69) reported that scoliosis is more frequent in German children than in other immigrant children (5.5% *vs.* 3.5%). Ratahi, Crawford (70) found a higher prevalence in Europeans than in Polynesians. Additionally, according to an investigation conducted in Singapore, Chinese girls had a higher prevalence than Malay and Indian girls [71].

Age is another factor affecting higher prevalence was found in patients older than 15 years [5]. Daruwalla, Balasubramaniam (71) also reported similar results: 0.12% for 6–7 years, 1.0% for 11–12 years, and 3.12% for 16–17 years (only girls in the last), and by Kamtsiuris, Atzpodien (69): 6.5% for 11–13 years and 11.1% for 14–17 years.

Prevalence was higher in females than in males with an overall ratio of 2: 1 [5,71], which

increased with age [5,69] and severity [5]. Prevalence ratio reached 10: 1 when the standing coronal-Cobb was more than 30° [5]. However, a higher prevalence of atypical curve types was found in males than in females when the standing coronal-Cobb was greater than 20° [72].

Generally, a single thoracic curve is the most common curve type (48%), followed by a single (thoraco)lumbar curve (40%) [5], a double curve (9%), and double thoracic curve (3%) [73]. By comparison, the (thoraco)lumbar curve appears more frequent in males, while the thoracic and double curves are more common in females [73].

2.3.2 Symptoms and Progression of AIS

As mentioned previously, AIS could result in discontent with body image [6,7], higher incidence of low back pain [6,7], asymmetrical gait patterns [8,9], the higher energy cost of walking [9], higher prevalence of osteopenia [10], and even respiratory impairment [6,11-13] and cardiovascular compromise [12] in severe case.

Curve progression is associated with the degree of skeletal maturity and curve severity [64,74]. Weinstein, Dolan (75) reported that the younger the patients are and/or the greater the curves are, the higher the risk of curve progression. Curve progression notably increases during the period of the growth spurt while remarkedly slowing or ceasing after completion of growth (skeletal maturity) [76-78]. A growth spurt usually lasts about 2.5–3.0 years [79], with a velocity peak of progression at a mean age of 14 and 12 years in males and females, respectively [80]. Additionally, Charles, Daures (81) found that the risk of surgery was 16% for a curve of 20°, however, 100% for curves ≥30° at the onset of puberty [81]. Skeletal age is an accurate marker of maturity or immaturity, usually identified using the Risser sign [82]. The likelihood of progression of untreated AIS is correlated with the Risser sign and curve severity [83]. It could reach 68% when a curve was 20°–29°, and a Risser sign was 0 or 1 while reducing to 1.6% when a curve was ≤19° and a Risser sign was ≤2 [83]. For a curve of ≥19° with Risser sign <2 and a curve of 20°–29° with Risser sign ≥2, the incident

of progression was similar (22% *vs.* 23%) [83].

2.3.3 Assessment of AIS

Adam's Forward Bend Test

Adam's forward bend test, described by William Adams in 1865 [84] (Figure 2.4), is considered as a simple, reliable, and inexpensive way to assess trunk asymmetry related to scoliosis. An individual is required to bend forward with knees straight and palms together and locate between the knees. Examiner looks down the possible asymmetries in the rib cage (rib hump) and deformities along the back. Scoliometer is an instrument used to quantify the degree of trunk axial rotation and it is placed on the back and moved along the spine when the patient performs the forward bend test. Coté, Kreitz (85) conducted a study with 105 subjects recruited to investigate the diagnostic accuracy and reliability of the forwards bend test and scoliometer, and verify them with the Cobb method. The results showed that the forward bend test was more sensitive in detecting scoliosis and remained a non-invasive clinical test to assess scoliosis.

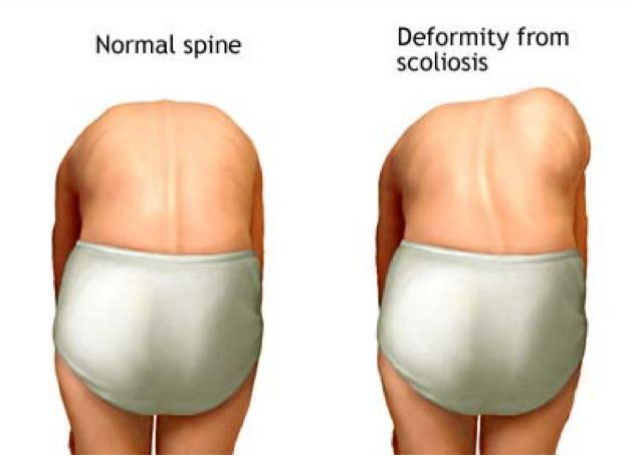

Figure 2.4 Adam's forward bend test [86]

Quality of Life

Quality of life (QoL) is an important aspect of the assessment/treatment of scoliosis [63]. A series of instruments were developed for the assessment of QoL, such as scoliosis

research society-22 patient questionnaires (SRS-22) [87-91], brace questionnaire (BrQ) [92], bad Bernheim stress questionnaires (BBSQ-Deformity [93], and BSSQ-Brace [94-96]). These instruments generally have good inter- & intra-rater reliability (Cronbach's alpha coefficient=0.5–0.92, ICC=0.78–0.93 for the SRS-22 [87-91]; Cronbach's alpha coefficient=0.72–0.88 for the BrQ [92]; Cronbach's alpha coefficient=0.97 for the BSSQbrace [95]).

2.4 Imaging Assessment of AIS

This section was going to introduce the imaging methods used in assessing AIS, containing plain radiograph, EOS system (stereo radiography), CT, MRI, ultrasound, and surface topography. The plain radiograph is the most common imaging modality used for assessing AIS, and the EOS system is characterized by micro-dose radiation and has been widely used in the clinic. CT and MRI allow the coronal and transverse assessment of spinal deformities with the same image-set. Due to the high-radiation exposure and only recumbent assessment, they are generally recommended for patients suffering from severe AIS or scheduled with surgery. Both ultrasound and surface topography are non-invasive modalities that allow repeated assessment within the short term.

2.4.1 Plain Radiograph

Coronal-Cobb measured from the PA plain radiographs is the gold standard for the assessment of AIS. Posture for radiographing is upright standing, looking straight ahead with feet being shoulder-width apart, elbows bending and knuckling in the supraclavicular fossa bilaterally (Figure 2.5) [97]. Curve magnitude is measured using the Cobb method as shown in Figure 2.6.

Figure 2.5 Radiographic posture [97]

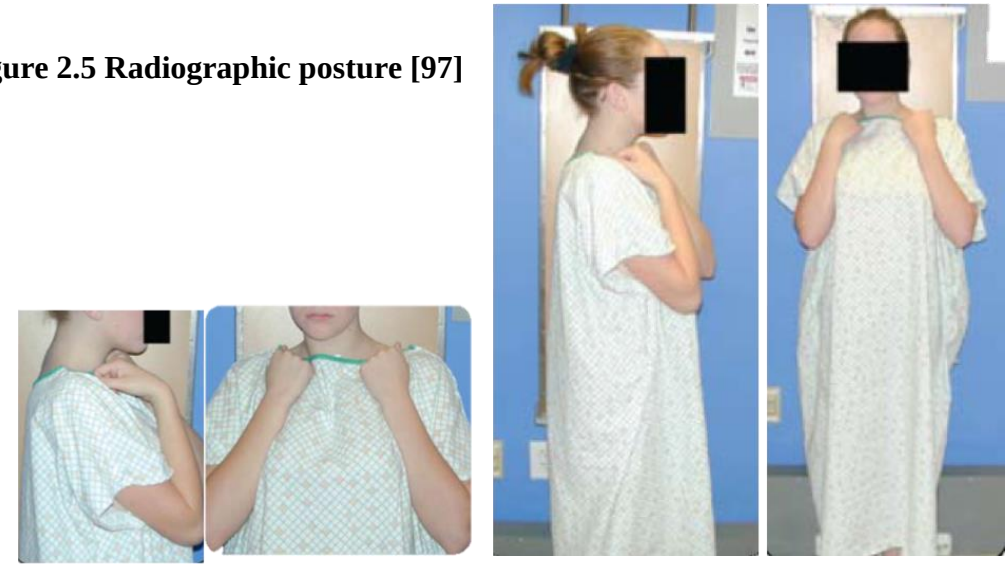

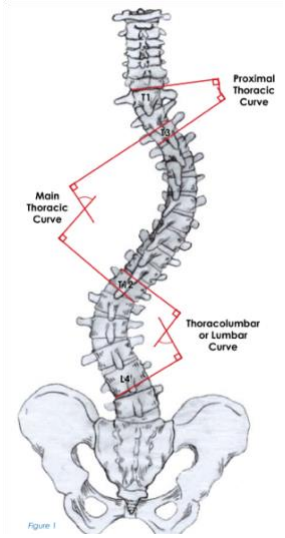

Figure 2.6 Cobb method [97]

According to the Society on Scoliosis Orthopedic and Rehabilitation Treatment (SOSORT) recommendations, a radiograph should be taken at the first visit, and then every 6–12 months afterward [63]. An individual is expected to take a radiograph regularly throughout treatment and follow-up [98]. An individual may have an average of 22.9 times' radiograph taken [99] during the whole course. Considering the potential oncogenic effects of radiation, there is a general agreement to avoid inappropriate use of radiographs in children to reduce exposure. Follow-up radiographs should be taken using the lowest dose while avoiding the lateral radiograph if unnecessary [98]. Besides, SOSORT suggested a PA radiograph, if

possible, to reduce the radiation exposure to the thyroid and breast tissue [98]. Delayed radiographing is also recommended to reduce exposure times if possible [98]. However, it should be aware that delayed imaging may impede scoliosis treatment. Nevertheless, although there is an overall increase in cancer risk, it can be minimized if reducing the radiographing frequency as little as possible and positioning benefits an individual safely. In this case, it is crucial to balance the risk and benefit during clinical practice.

2.4.2 EOS System

EOS system is a bi-planar imaging system developed in 2000 and has been accessible to clinical use since 2007. It allows the coronal and sagittal images to be obtained simultaneously in an upright weight-bearing position (Figure 2.7). It is characterized by remarkably micro-dose radiation exposure compared to the traditional radiography [100], computed radiography (by 8–10 times), and CT (by up to 100 times) [101]. The image quality is comparable to or even better than that of traditional radiographs [100], computed radiographs [101], and digital radiographs [102].

Figure 2.7 EOS system [103]

As shown in Table 2.1, coronal-Cobb obtained from the EOS images were very reliable (intra-rater intraclass correlation coefficient (ICC) =0.70–1.00 [104-108]; inter-ICC=0.68–0.98 [104,106-108]). Reliable VAR could be also achieved (intra-ICC=0.55–0.99 [106-

108]; inter-ICC=0.65–0.99 [105-108]). Moreover, the intra- & inter-rater mean absolute difference (MAD) of VAR was 0.3°–13.0° and 0.1°–12.4°, respectively [106,109]. The coronal-Cobb acquired from EOS system was comparable to that obtained from the traditional manual method (correlation coefficient (r)=0.70–0.95 [104,109], MAD=5.4° [109]). Additionally, EOS system has been also used for assessing spinal flexibility [110] and evaluating effectiveness of surgical [111,112] and orthotic [113] treatments.

Table 2.1 Reliability of measurements obtained from the EOS system

Reference	Study sample	Coronal-Cobb		Vertebral axial rotation	
		Intra-ICC	Inter-ICC	Intra-ICC	Inter-ICC
Somoskeoy, Tunyogi-Csapo (104)	n=201 Coronal-Cobb=2.4°-117.5°	0.999-1.000	0.971	-	-
Al-Aubaidia, Lebelb (105)	n=7 age=15±0.4 yrs	0.880		-	0.880
Bagheri, Liu (106)	n=15 age=6-15 yrs Coronal-Cobb=32.5°±11.4°	0.720-0.970	0.680-0.880	0.55-0.75	0.650-0.800
Tabard-Fougere, Bonnefoy-Mazure (109)	n=35 age=13.1±2.0 yrs Coronal-Cobb=32.5°±11.4°	0.700-0.720	0.840	0.850-0.900	0.970
Gille, Champain (107)	n=30 Age=13 (7-19) yrs Coronal-Cobb=16° (5°-38°)	0.980	0.980	0.930	0.880
Carreau, Bastrom (108)	n=30 Coronal-Cobb=67.2°±12.5°	0.981-0.996	0.975-0.984	0.974-0.994	0.985-0.986

yrs: years

2.4.3 Computed Tomography

Computed tomography (CT) produces cross-sectional images of the spine and projection images of the whole spine in a recumbent position, allowing the coronal and transverse assessment of spinal deformity at the same image-set. Curve angle is measured using the Cobb method [114]; VAR is measured using the Perdriolle method is in the coronal plane while Aaron and Dahlborn method in the transverse plane [115].

CT showed similar variability for Coronal-Cobb in comparison with a plain radiograph (error of measurement ≤2.7°) [114]. High reliability was found for VAR of CT obtained from the coronal and transverse planes (ICC≥0.83), being similar to that of plain radiographs (ICC=0.76) [115]. CT is commonly used for pre-operative planning, intro-operative determination, post-operative assessment [116-118], and the accuracy and safety evaluation of pedicle screw placement during the intro-operative period [119]. Because of high radiation exposure [28], CT is generally recommended for patients suffering from severe AIS and/or scheduled with operation while rarely suggested for those with mild and moderate AIS.

2.4.4 Magnetic Resonance Imaging

Magnetic resonance imaging (MRI) is characterized by radiation-free and allows coronal/sagittal and transverse assessment of spinal deformities in a recumbent position at the same image set. Similarly, the curve angle is measured using the Cobb method in the coronal/sagittal plane, and VAR is determined using Aaro and Dahlborn method in the transverse plane.

MRI can provide very reliable curvature measurements (intra- & inter-ICC>0.99 [120]; intra- and inter-variation ≤1.8° [120,121]), and reliable AVR measurements (intra- & inter-ICC>0.99 [122]). Besides being used for pre-operative assessment [123,124], it is also suggested for evaluating the abnormality of bony structure [125] and soft tissue [123,126,127] as well as neurological abnormality [123,126,127]. Due to the high cost and

only allowing recumbent assessment, MRI was not recommended for routine assessment of AIS, especially the mid to moderate.

2.4.5 Ultrasound

Ultrasound is characterized by radiation-free, cost-effective, and user-friendly. It allows AIS assessment in both recumbents (prone/supine) and standing positions. These advantages make ultrasound promising in the assessment of AIS. Curve angle is measured using the center of lamina (COL) [120,128-132], spinous process (SP) [133-135], accumulating spinous process (SP*) [136,137], transverse process (TP) [133-135,138], or transverse process-superior articular process (TP-AP) [133-135,138] methods according to different ultrasound systems and the corresponding image analysis software (Figure 2.8; Table 2.2). VAR is measured using the COL method [122,139-141] (Figure 2.9).

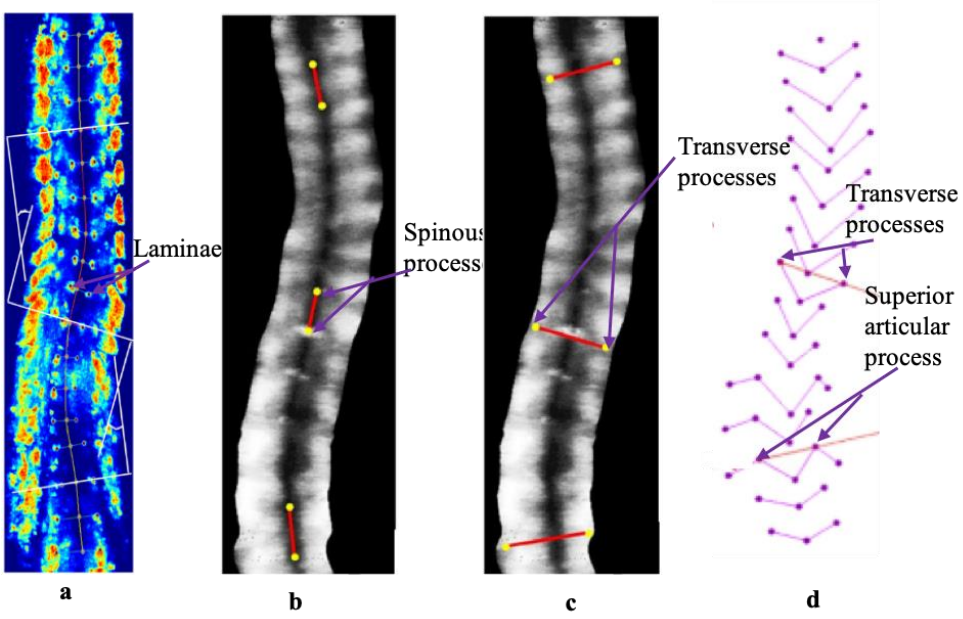

Figure 2.8 Ultrasound anlge measure : (a) COL method [120]; (b) SP method [142]; (c) TP [142]; (d) TP-SAP [133]

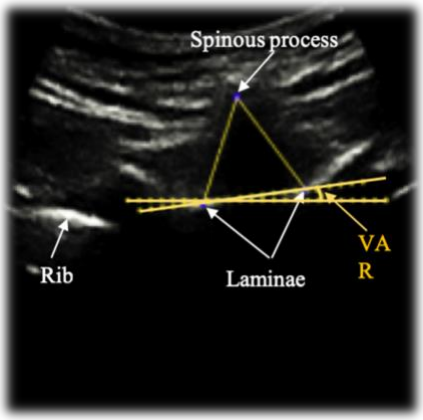

Figure 2.9 VAR measure using COL method [122]

There were three main ultrasound systems used most frequently in assessing scoliosis, including SonixTablet system, Scolioscan system, and Esaote Technos MPX ultrasound unit (Table 2.2). These ultrasound systems are commonly combined with self-developed image analysis software, which allows measuring curve angle and AVR.

Table 2.2 Curve measure methods

Measure method	Method description	Ultrasound system
Center of lamina (COL) method	To measure the angle between the two most tilted COL lines (between the left and right COL) of the upper and lower regions of spinal curve [128-132].	SonixTABLET US
Spinous process (SP) method	To measure the accumulating angle formed by every two lines joining three neighbouring spinous processes of a spinal curve [133-135].	Scolioscan system
Accumulating spinous process (SP*) method	To measure the accumulating angle formed by every two lines joining three neighbouring spinous processes of a scoliotic spine [136,137].	Esaote Technos MPX ultrasound unit
Transverse process (TP) method	To measure the angle between two most tilted TP lines (between the tips of left and right TPs) of the upper and lower regions of spinal curve [133,135,138].	Scolioscan system
Transverse process-superior articular process (TP-SAP) method	To measure the angle between two most tilted TP/SAP lines (between the tips of left and right TP or SAP) of the upper and lower regions of spinal curve [138].	Scolioscan system

Note: The ultrasound systems were used for taking ultrasound images only while the relevant measurements were obtained via their corresponding software.

As shown in Table 2.3, the coronal curvature measurements acquired from ultrasound presented high intra- & inter-rater reliability (intra-ICC=0.57–0.99 [120,128-131,133-138,140], inter-IC =0.80–0.99 [120,129-131,133-135,138,140]). The measurements were strongly correlated to those obtained from the radiograph/MRI (r=0.70–0.99 [120,128-130,133-138,140]). Moreover, high intra- & inter-rater reliability was also observed for the VAR measurements (intra-ICC>0.98 [122,139,140], inter-ICC>0.89 [122,141]). Strong correlation (r=0.88–0.94) and good agreement between the VAR measurements of ultrasound and MRI were also demonstrated [122]. In addition, ultrasound was used to evaluate the spinal flexibility [131,143-145] and monitor curve progression [146] as well as to assist orthosis casting [147] and fitting [136]. It has potential to be used as a useful tool for screening scoliosis, monitoring curve progression and assisting orthosis fitting.

Table 2.3 Reliability and validity of coronal curvature measurements obtained using ultrasound

Reference	Curvature measurements	Reliability		Validity
		Intra-ICC	Inter-ICC	Correlation coefficient (r)
Li, Ng (136), 2012	SP* angle *vs.* radiological Cobb	0.91	n/a	0.81
Cheung, Zhou (133), 2015	SP angle *vs.* radiological Cobb	0.99	0.92	0.89
	TP angle *vs.* radiological Cobb	0.98	0.96	0.88
Li, Cheng (137), 2015	SP* angle *vs.* radiological Cobb	0.91	n/a	0.79
Cheung, Zhou (138), 2015	TP-SAP angle *vs.* radiological Cobb	0.93	0.89	0.93
	TP angle *vs.* radiological Cobb	0.57	0.75	0.82
Young and Lou (128), 2015	COL angle *vs.* radiological Cobb	0.86-0.9	n/a	0.70-0.72*
Wang, Li (132), 2015	COL angle *vs.* MRI Cobb	0.99	0.99	0.997
Rui Zheng, Chan (129), 2015	COL angle *vs.* radiological Cobb	>0.8	0.80-0.90	0.78-0.84
Zheng, Young (130), 2015	COL angle *vs.* radiological Cobb	0.86	0.83	0.76
Zheng, Lee (134), 2016	SP angle *vs.* radiological Cobb	0.97	0.90	0.87
Rob C. Brink, Wijdicks (135), 2018	SP angle *vs.* radiological Cobb	0.97	0.95	0.99
	TP angle *vs.* radiological Cobb	0.96	0.93	0.99
Khodaei, Hill (131), 2018	COL angle *vs.* radiological Cobb	0.94	0.95	n/a

Intra-/inter-ICC: intra-rater/inter-rater intraclass correlation coefficient; *: ICC value

2.4.6 Surface Topography

Surface topography extrapolates back contour by projecting a grid onto an individual's back and presenting a deviation color map (Figure 2.10). Its earliest form was Moiré technology reported in 1970 [148] and was first used to assess back contour for patients with scoliosis in the 1980s to 1990s [98]. With the advantage of no radiation, surface topography has been an increasingly viable alternative for the assessment and progression monitoring of scoliosis. Currently, raster technology has been applied to the surface topography systems, including InSpeck, Integrated Shape Imaging System (ISIS), Quantec, and Frometric. These four systems showed high reproducibility and had a strong correlation with radiographs in the assessment of scoliosis [98,149-152].

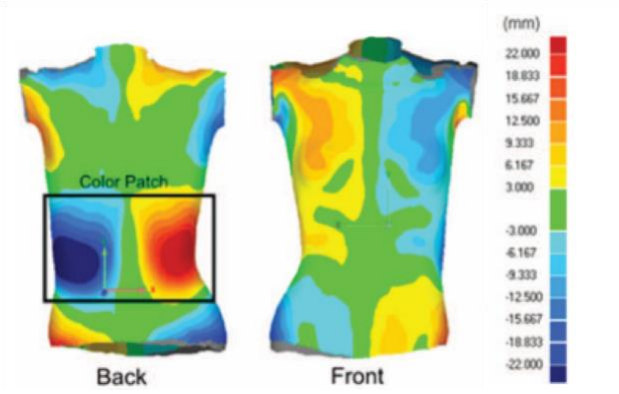

Figure 2.10 Deviation color map viewed from the back and front [153]

InSpeck system was developed in 2002, containing two/four optical digitizers and a light projector. Pazos, Cheriet (150) found that InSpeck system could provide reliable anatomic and clavicle positions (ICC=0.85–0.99). It, combined with standard radiographs, could be used to reconstruct an accurate 3D geometric model of the scoliotic rib cage (accuracy=1.1±0.9 mm for trunk surface and an error =1.4° for surface rotation [151]). InSpeck system was used to assist the positioning of pressure pads inside orthosis properly [154]. Labelle, Bellefleur (155) found that the curve correction was significantly improved when using the InSpeck system to assist the orthotic design and adjustment compared to using the traditional method.

ISIS was developed between 1984 and 1988. In Zubovic, Davies (152)'s study, good repeatability of curvature measurements obtained from ISIS was found compared to a traditional radiograph. The lateral asymmetry was highly correlated with radiological Cobb (r=0.84), while the error of the Cobb angle predicted from the lateral asymmetry was ≤10° in comparison with radiological Cobb [156]. Additionally, lateral asymmetry detected using ISIS was limited in patients who were extremely obese or muscular [156].

Quantec system has been used since 1994 and was characterized by high portability. It was found to have a variation of <5° for Q angle (an equivalent of Cobb angle) in coronal curvature measurements [149] and an average standard deviation (SD) of 3.8° for the measurements of sagittal thoracic kyphosis [157]. However, Klos, Liu (149) pointed out that Q angle may not be sufficient for monitoring curve progression since the predicted Cobb angle changed more when there was an increase of <5° in Q angle, contrarily, it changed less when there was an increase of >5° in Q angle.

Frometric system showed comparable reproducibility (an equivalent of Cobb angle) in coronal curvature measure to the standard radiography with Cronbach alpha of 0.99 [158] and average SD of 3.2° [159] to 3.4° [158]. The coronal curvature measurements of these two modalities were also strongly correlated (r=0.76–0.87) [158]. Mohokum, Mendoza (160) reported that the reproducibility of coronal curvature measurements obtained from the Prometric system was not affected by BMI. Contrarily, Knott, Mardjetko (161) pointed out that the variability of curvature measurements increased at greater BMIs while within ± 4.6° at the highest BMIs (=29) in their study. Hackenberg, Hierholzer (162) used the Frometric system to compare the axial trunk rotations in standing and forward bending positions and found a significant difference but the poor correlation between the trunk axial rotation in the two positions (MAD=3.2°, $p<0.05$; $R^2=0.41$).

Although surface topography does not provide an exact curve magnitude compared to traditional radiography, multiple studies have provided data supporting the accuracy and

reproducibility of coronal curvature measurements (the equivalent of Cobb angle). These findings suggested that surface topography can be used for assessing scoliosis, decreasing the frequency of radiographing.

2.5 Maximum Spinal Deformity

Coronal-Cobb measured from the AP/PA radiograph is the gold standard for assessing AIS. However, because of the 3D deformity of AIS, it may underestimate the curve severity [14,15,163] and not fully reflect the curve type [18,19,21,164]. 3D assessment of AIS has been increasingly recognized and emphasized in the clinic. PMC, end-apical-end vertebrae plane (EAEP), and best-fit plane (BFP) were the common 3D descriptors considered to reflect the maximum spinal deformity. These descriptors have been applied for the 3D assessment of AIS [24] and are increasingly recognized in the orthopedic operation of the spine [22]. This section was to introduce: (1) definitions of PMC, EAEP & BFP; (2) techniques for obtaining PMC, EAEP & BFP; (3) and relevant applications of PMC, EAEP & BFP in the management of scoliosis.

2.5.1 Definitions of Maximum Spinal Deformity

For a specific spinal curve, (1) PMC refers to a vertical plane, where the scoliotic spine is projected onto, presents the maximum spinal curvature by a specified method (Cobb method) (Figure 2.11: a) [23]; (2) EAEP refers to a plane formed by three lines connecting the body centroids of the two end and apical vertebrae of the curve (Figure 2.11: b) [165,166]; (3) BFP refers to a plane best accommodating the vertebrae within the curve segment (Figure 2.11: c) [23,55]. According to the definitions, PMC-orientation is regarding to axis z of the global axis system [167] with a corresponding Cobb angle on the PMC (PMC-Cobb); by contrast, orientation of EAEP/BFP (EAEP/BFP-orientation) is with respect to axis x, y and z, containing orientation components of EAEP(x)/BFP(x)-, EAEP(y)/BFP(y)- and EAEP(z)/BFP(z)-orientation with different corresponding Cobb angles (EAEP(z)/BFP(z)-, EAEP(x)/BFP(x)- and EAEP(y)/BFP(y)-Cobb). Additionally, PMC/EAEP(z)/BFP(z)-orientation presented in the following was concerning the sagittal

plane unless additional information was given.

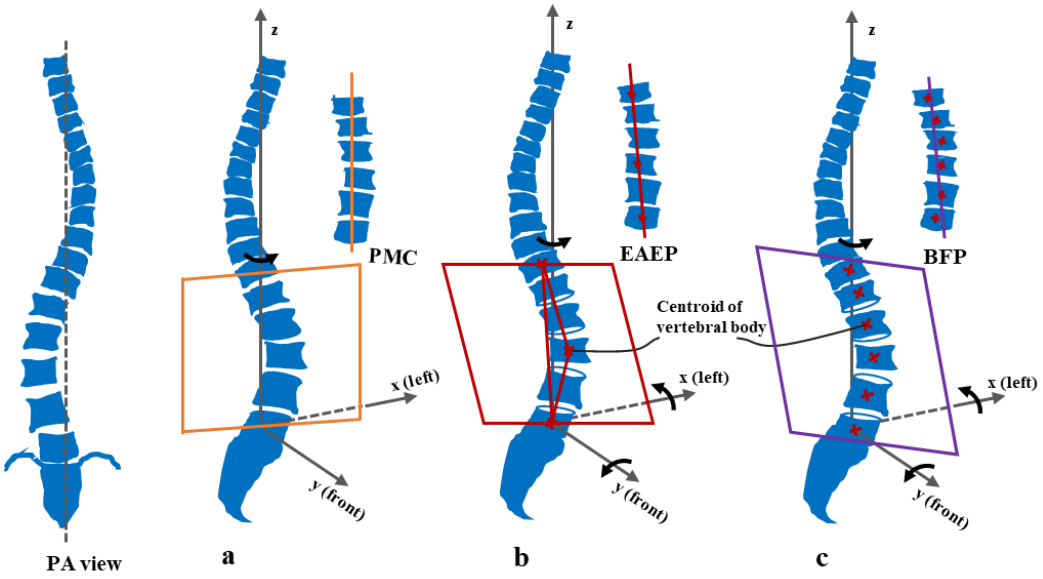

Figure 2.11 A scoliotic spine with PA view. (a) PMC, plane of maximum curvature; (b) EAEP, end-apical-end vertebrae plane; (c) BFP, best fit plane [168]

For a normal spine, there commonly is one unique global PMC, EAEP & BFP, and they generally present the same/similar Cobb angle and orientation.Due to the complication of global, regional, and local deformities for a scoliotic spine, there might be one unique global, but mostly several regional PMC, EAEPs & BFPs connected at their adjacent zones [55,169,170]. These regional planes could present notably different Cobb angles and/or orientations. Since PMC, EAEP & BFP separately take (two end vertebrae), (end and apical vertebrae), and (vertebrae within the curve segment) into account, BFP may have the potential to better reflect the deformity of a curve and would be followed by EAEP and PMC orderly. However, only one (EAEP(z)/BFP(z)-orientation [21,55,56,171,172]) or two orientation components (BFP(z)/(x)-orientation [169,173]) of EAEP and BFP were considered in most studies for reasonable variable number for analysis and understanding. It was found that BFP(z)- [173] and EAEP(z)-orientation [174] were superior to PMC-orientation in 3D classification of scoliosis (differentiating sub-types within Lenk type-1). Apart from this, it was unclear if the superiority of BFP and EAEP to PMC in the

description of maximum deformity would change or not when their orientations were simplified.

2.5.2 Techniques for Acquisition of Maximum Spinal Deformity

PMC

Two main techniques allow PMC assessment, including radiographic and ultrasound techniques. The radiographic technique was based on the 3D reconstruction of the scoliotic spine or spinal curve, which was established from the calibrated PA and lateral (or PA with a bitch angle of 20°) radiographs obtained from the radiographing system (e.g., EOS system) [19,33,57,155,164,166,173,175-183]. Based on the reconstructed model of the spine or spinal curve, PMC was determined by rotating a vertical plane along the vertical axis with a certain increment (such as 2.5° [33]) until the maximum curvature was found using the conventional [175,176] or computerized Cobb method [19,33,57,155,164,166,173,177-183]. Unlike the conventional Cobb method, the computerized Cobb method measures the Cobb angle by calculating the angle formed by two intersection lines being separately perpendicular to the reconstructed curve at its upper and lower inflection points [33,177]. Deacon, Flood (184) obtained the PMC by rotating a scoliotic phantom along the vertical axis 180° with an interval of 10° and taking a radiograph at each interval. PMC was then determined by measuring the Cobb angle in each interval plane. Because of radiation exposure, this approach did not apply to patients. Moreover, Kumar, Nayak (175) obtained PMC via rotating a vertical plane to an orientation equalling to the maximum VAR. The sagittal plane served as the reference plane for PMC-orientation in most studies [19,33,57,155,164,166,180,181,183].

Two studies focused on using ultrasound to acquire PMC. Based on 3D ultrasound images established using ultrasound data, PMC was identified by rotating a vertical plane along the vertical axis to a position with an orientation equalling to the maximum VAR, as reported by Kumar, Nayak (175), and confirmed by locating the vertical plane to maximum VAR ±2°, ±4° [27] or ±5° [185] by COL method (Figure 2.8: a). Unlike the most

radiographic studies mentioned previously [19,33,57,155,164,166,180,181,183], these two studies set the coronal plane as the reference plane for PMC-orientation [27,185].

Ultrasound is radiation-free, low-cost, and user-friendly, allowing standing and recumbent assessment of AIS. It was found very reliable and accurate for the assessment of coronal curvature [120,140,142,186-188] and VAR [122,139,141]. It was also used for assessing the spinal flexibility [131,143-145]. monitoring curve progression [146], and assisting spinal orthosis casting [147] and fitting [136]. Currently, only one study, which focused on the reliability of PMC measurements acquired from ultrasound, was found [27]. Although the PMC (PMC-Cobb; PMC-orientation) of ultrasound showed high intra- & inter-reliability (intra- & inter-ICC >0.92) and were strongly correlated to those of the EOS system (PMC-orientation only) (R^2=0.88), further validation was necessary before clinical application.

EAEP

Similarly, 3D reconstruction of the scoliotic spine or spinal curve established from the calibrated bi-planar radiographs was essential to acquiring EAEP. Based on the reconstructed model of the spine or spinal curve, EAEP was determined by establishing a triangle plane based on the three intersection lines connecting the body centroids of two end vertebrae and the apex of the curve (or connecting the upper and lower limits and apical limit of the reconstructed curve) [21,54,56,169,189]. DaVinci representation was a helpful approach for acquiring EAEP [21,170]. The body centroids of end and apical vertebrae (or the end and apical limits) were projected onto the transverse plane, generating corresponding tracks. For being easily understood, DaVinci representation replaced the projected tracks with an arrow emitting originally from the CHVA (central hip vertical axis) to the projected track of the centroid of the apex (or apical limit) on the transverse plane [21,170]. The direction of the arrow represents the EAEP(z)-orientation, and the length of the arrow is proportional to the magnitude of the EAEP(z)-Cobb. Most studies only considered the EAEP(z)-orientation for ensuring a reasonable variable number for analysis [21,56,170-172].

The daVinci representation provides a very intuitional vision for the EAEP(z)-orientation on the top view. However, it should be noted that the daVinci representation, especially the simplified daVinci representation, remains only the EAEP(z)-orientation while ignoring the EAEP(x)/(y)-orientation. Thus, the EAEP obtained through the daVinci representation could be interpreted as a vertical plane that passes through the axis z (CHVA) and body centroid of the apex. Also, daVinci representation may only provide the EAEP(z)-orientation while not giving an exact EAEP(z)-Cobb. As mentioned, it was unknown if the superiority of EAEP to PMC in the description of maximum deformity would be changed or not when its orientation was simplified.

BFP

Similarly, a 3D model of the spine or spinal curve reconstructed from the calibrated bi-planar radiographs was a basic condition for obtaining BFP. Based on the reconstructed spine or spinal curve, BFP was determined by minimizing the sum of square linear distances [173] or linear distances [55,169] from the specific 3D curve to a plane. The fitting degree between the curve and that plane (BFP) was evaluated using the linear fitting coefficient, which referred to a maximum normal distance from a curve to that plane [55]. The number of BFP in a scoliotic spine depends on if the maximum linear distance from the curve to that plane (potential BFP) was greater than 10 mm or not [55]. If the linear distance ≤10 mm, one unique global BFP was determined; otherwise, separate regional BFPs might exist. Besides, some studies identified the BFP by isolating the apical vertebrae (5 or 7 vertebrae) within the curve segment and establishing their plane, on which the isolated vertebrae showed unique flexion, regarding the body [190-192]. Being similar to EAEP, simplification of BFP-orientation was also observed in most studies, retaining BFP(z)-orientation [55] or BFP(z)- & BFP(x)-orientation [169,173].

3D reconstruction of the scoliotic spine or spinal curve was essential to acquiring PMC, EAEP & BFP. Although the accuracy and reproducibility of the 3D reconstruction model

have been demonstrated in most studies [182,190,193-198], apart from a few studies, the PMC, EAEP & BFP measurements were rarely studied explicitly. In these studies, the variability of PMC measurements was reported (PMC-Cobb: MD=0.7°–1.6°; PMC-orientation: MD=1.5°–2.7°, intra- & inter-rater root-mean-square=6.0°–14.0° & 9.3°–20.4°) [182,197]. Additionally, although CT and MRI allow 3D assessment, they were not used to assess PMC, EAEP & BFP or verify the radiographic (e.g., EOS system) and ultrasound techniques.The latter may be due to the use of recumbent (prone/supine) position in CT/MRI scan while radiographs (e.g., EOS images) or ultrasound images are mostly taken in standing position. There were relationships between PMC/EAEP/BFP and coronal/sagittal Cobb, and between coronal-Cobb and sagittal Cobb in standing and recumbent positions. These relationships may provide a link to indirectly validate the standing PMC, EAEP & BFP measurements with the corresponding recumbent measurements of CT/MRI.

It was worthwhile to note two points. PMC/EAEP/BFP-Cobb measured using the computerized Cobb method tended to gently overestimate the curve magnitude by average 11%–12% as compared to the conventional Cobb method [199,200]. Furthermore, except for a few studies, most studies set the sagittal plane, instead of the coronal plane, as the reference plane for the PMC/EAEP(z)/BFP(z)-orientation [19,33,57,155,164,166,180,181,183]. By setting the sagittal plane as the reference plane, it may be easier to understand the degree of a curve rotated towards the coronal plane (PMC/EAEP(z)/BFP(z)-orientation). This may contribute to the sagittal plane being the original plane, where PMC / EAEP / BFP should lie. In a normal spine, the PMC / EAEP / BFP generally overlap with the sagittal plane (PMC/EAEP(z)/BFP(z)-orientation = orientation of sagittal plane =0°); in a scoliotic spine, PMC/EAEP/BFP commonly lies in an abnormal position different from the sagittal, with a certain orientation concerning the sagittal plane.

2.5.3 Applications of Maximum Spinal Deformity

Applications in 3D Assessment, Progression Monitoring, and Classification of Scoliosis

The PMC, EAEP & BFP of thoracic and (thoraco)lumbar curves commonly position in the posterolateral and anterolateral quadrants of the axis system, respectively [19,33,164,180,181,183,201,202]. Interdependent relationships between PMC/EAEP/BFP and coronal/sagittal Cobb were observed. The PMC/EAEP(z)-Cobb was greater than or equal to the coronal/sagittal Cobb [33,54-56], while no significant correlation was found [56]. There existed a correlation between PMC/EAEP(z)-orientation and the ratio of coronal-Cobb to sagittal-Cobb (coronal thoracic/lumbar curvature to sagittal thoracic kyphosis/lumbar lordosis) [21,33,174]. Moreover, PMC-orientation was also correlated to ($r=0.64–0.71$) and was 1.27–1.7 times coronal-Cobb in degree [33,57]. Also, PMC-orientation was found to be correlated to but generally greater than the maximum VAR, rotation of rib hump, and back surface orderly ($r=0.56, 0.48, 0.69$) [57], and linked to the geometric torsion [202].

PMC, EAEP & BFP can better reflect the 3D features of scoliosis. PMC/EAEP/BFP-Cobb represents the maximum/"actual" spinal curvature, and PMC/EAEP/BFP-orientation reflects the degree of the curve rotated towards the coronal plane. The coronal-Cobb and sagittal-Cobb could be interpreted as the components of PMC/EAEP/BFP-Cobb since they were affected by the combined effect of both the PMC/EAEP(z)/BFP(z)-Cobb and PMC/EAEP(z)/BFP(z)-orientation.

A greater (or smaller) PMC/EAEP(z)/BFP(z)-Cobb could result in a greater (or smaller) coronal-Cobb and sagittal-Cobb when PMC/EAEP(z)/BFP(z)-orientation did not change; a greater (or smaller) PMC/EAEP(z)/BFP(z)-orientation could result in a greater (or smaller) coronal-Cobb,and a smaller (or greater) sagittal-Cobb when PMC/EAEP(z)/BFP(z)-Cobb did not change. The impact of EAEP(x)/BFP(x)-orientation and EAEP(y)/BFP(y)-orientation on the coronal-Cobb and sagittal-Cobb angles was unclear. Nonetheless, these interdependent relationships revealed that PMC, EAEP & BFP

seemed to be superior to the coronal-Cobb and sagittal-Cobb in describing the 3D deformities of scoliosis.

Villemure, Aubin (19) found that 71% of subjects with AIS (n=28) had progression in PMC-orientation during 22.8±10.8 months. Because of the interdependent relationships between PMC-Cobb/orientation and coronal-/sagittal-Cobb, progression in Cobb angle in any plane could cause progression in the corresponding PMC [19,184]. Moreover, PMC-orientation was significantly higher in progressive AIS than in non-progressive AIS at the initial visit (MD=12.1°, $p<0.05$) [176] and tended to increase with the severity of AIS [19,176]. These findings indicate that PMC-orientation may be a risk factor for the AIS progression.

PMC, EAEP & BFP have been applied to the 3D classification of scoliosis. Previous studies demonstrated that the Lenke type-1 curves could be further split into different sub-types based on PMC [173,183], EAEP [21,56,172,174] or BFP [170,173]. According to the results reported by Thong, Parent (172) and Stokes, Sangole (174), EAEP(z)-orientation was superior to coronal-Cobb, sagittal-Cobb (sagittal thoracic kyphosis and lumbar lordosis), and VAR in differentiating sub-types within all the Lenk types. Moreover, both BFP(z)/(x)- [173] and EAEP(z)-orientation [174] were superior to the PMC-orientation in the differentiation of sub-types within the Lenk type-1. Currently, most relevant studies focused on differentiating the sub-types within Lenke type-1 based on the PMC [173,183], EAEP [21,56,172,174], or BFP [173]. However, the differentiation of sub-types with other Lenke types remained studied. The sub-types should be considered when making clinical decisions since different sub-types may require different orthotic/surgical strategies.

Applications in Effectiveness Evaluation of Surgical and Orthotic Treatments

The 3D correction of different surgical instrumentations was evaluated using the PMC/EAEP. Generally, 19%–73% while mostly 25%–41% correction in PMC-orientation

[164,178,180,181], and 57%–62% correction in BFP(z)-orientation were found [190,191]. Correction in PMC-Cobb was between 24% and 51% [164,178]. By contrast, correction tended to be greater in coronal-Cobb than in PMC-Cobb (50% *vs.* 24% [178], 49%–65% *vs.* 32%–51% [164]. This may be because that correction in coronal-Cobb resulted from the combined effect of correction in both the maximum/"actual" curve magnitude (PMC-Cobb) and degree of a curve rotated towards the coronal plane (PMC-orientation). Additionally, there was a loss of 30% and 25% correction in PMC-orientation and coronal-Cobb, respectively, during a long-term follow-up of an average of 2.5 years [180]. This suggested that the correction should be followed up on a long-term basis.

Only two studies referred to the 3D correction evaluation of the orthotic intervention. Correction in PMC-Cobb was 17%–39%, and a similar correction was observed in coronal-Cobb (17%–33%) [155]. However, significant correction in PMC-orientation (38%) was only found for lumbar curves induced by the orthosis designed and adjusted with a computer-assisted tool [155]. Mostly, PMC-orientation in the thoracic curves tended not to change or even increase (37% [179], 24% [155]) after fitting orthosis. This indicated that the thoracic curve segment was not pushed towards the sagittal plane as expected but rotated towards the coronal plane even more after wearing the orthosis. Thus, correction merely in coronal-Cobb might not be enough to reflect the "actual" correction of spinal deformity, and this also demonstrated the importance of PMC/EAEP/BFP in evaluating the correction effect of treatments.

2.6 Treatments of AIS

According to the indications for treatment recommended by SRS [203]: patients with primary curve <20° are prescribed with the observation while a regular follow-up is necessary; patients suffered from primary curve >45° are commonly recommended with surgical intervention, and patients with a primary curve of 20°–40° are generally suggested with conservative interventions.

According to the recommendations of SOSORT [63], a regular clinical evaluation was recommended with a follow-up interval of 2–3 to 36–60 months according to an individual's specific clinical situation during observation. Moreover, radiographic examination is usually unnecessary for each evaluation but recommended during alternate evaluation. Conservative interventions include rehabilitation therapy (physiotherapeutic scoliosis-specific exercises and special inpatient rehabilitation [63]) and orthosis.

2.7 Rehabilitation Therapy

2.7.1 Physiotherapeutic Scoliosis-Specific Exercises

Physiotherapeutic Scoliosis-Specific Exercises (PSSE) contain all forms of physiotherapies proved efficacy for outpatients [204]. **Relevant recommendations were proposed by** SOSORT [63].

PSSE is proposed by therapists from scoliosis treatment teams and should be with proper cooperation between team members. PEES is based on 3D auto-correction, training in ADL, corrected posture stabilization, and patient education, which is usually recommended as the first step to prevent the progression of AIS. A specific form of PSSE varies from individual to individual and depends on an individual's need, curve type, treatment phase, and preference of a single therapist (usually select the program he/she was trained in school). The PSSE-dose commonly relies on the techniques and patients' compliance to carry out the treatment. Its frequency can be daily or several times per week, but usually, 2–4 times per week for long-term outpatients who are willing to co-operate fully. Moreover, during treatment, PSSE should be conducted regularly at home or in a small group to achieve optimal effectiveness. For patients with skeletal immaturity and a primary curve >25°, PSSE alone is not recommended unless prescribed by a scoliosis physician.

Several systematic reviews reported that PSSE is promising in slowing scoliosis progression, but its effectiveness cannot be confirmed as lacking high-quality evidence [204-208]. It was found to positively affect parameters concerning neuromotor control,

respiratory function, back muscle strength, mobility, postural balance, and cosmetic appearance in patients with AIS [204,205,209,210]. Moreover, PSSE could efficiently reduce the orthotic prescription [204] and was more effective in preventing scoliosis progression than electrostimulation, traction, and postural training [208]. The option of treating AIS with PSSE can be discussed with patients and their families based on the possible effectiveness and costs, and the final decision should be made by their preference [205].

2.7.2 Special Inpatient Rehabilitation

Special inpatient rehabilitation (SIR) commonly adopts an individualized exercise program, a combination of the corrective behavioral pattern(s) and physiotherapeutic method(s). An individual prescribed with SIR is usually requested to accept several hours (such as 6-hour [211]) intensive PSSE treatment daily for several weeks (generally, 3–6 weeks) at a specialized health center (or hospital department, sanatorium, a similar form of health care) [63]. It is recommended for patients with a primary curve of 20°–30°, combining or non-combining with orthotic treatment, which depends on prognosis [212]. Previous studies pointed out that SIR was promising in treating signs and symptoms of scoliosis [212] and reducing the progression [211]. However, a systematic review reported that SIR was inferior to the PSSE of outpatients in cost effect [21].

2.8 Orthotic Treatment of AIS

An orthosis is a clinically recognized intervention for patients with a primary curve of 25°–40°. This section was going to introduce the biomechanical principle of orthosis, common orthosis types, and the effectiveness of orthotic treatment.

2.8.1 Biomechanical Design of Orthosis

According to “SOSORT consensus paper on brace action: TLSO biomechanics of correction (investigating the rationale for force vector selection)” [53], the relevant biomechanical principle of orthosis was introduced.

Thoracic Curve

(1) Placement of thoracic pad, it recommended to place it on the convex side of a thoracic curve; (2) level of the thoracic pad (Figure 2.12: a), 11 out of 21 specialists selected to place it at the level of apex while the rest 10 chose to pace it below the apex level but at the apical rib; (3) direction of correcting force for thoracic convexity (Figure 2.12: b), a high percentage of the agreement described it as a 'dorsolateral to ventromedial' vector force; (4) shape of the thoracic pad, there was no consistent agreement on it currently; (5) 'three-point system' principle, it was given 95% of high priority; (6) "three-point system" correction, the preference of correction and over-correction counted for almost the same percentage from the specialists (48% *vs.* 52%); (7) derotation of rib hump (Figure 2.12: c), 85% of the 21 specialists gave it a high priority, and 57% preferred "the pads acting on the ventral and dorsal rib hump produce a pair of forces countering with each other".

Lumbar Curve

(1) Placement of lumbar pad, it recommended to place it on the convex side of lumbar curve; (2) vector force for lumbar convexity (Figure 2.12: d & e), 76% of the 21 specialists preferred a force reaching the apex and 66% recommended a "dorsolateral to ventromedial" force.

Abdominal Area

37% of the 21 specialists did not recommend an abdominal pad to push ventrally, while 10% and 14% preferred an asymmetric pad on the left and right, respectively.

Pelvic Area

32% of the 21 specialists selected bilaterally closed and symmetric pelvic area design, while 24% suggested semi-open and asymmetrical pelvic area design pushing on the left (or right) side and leaving room on the right (or left) side.

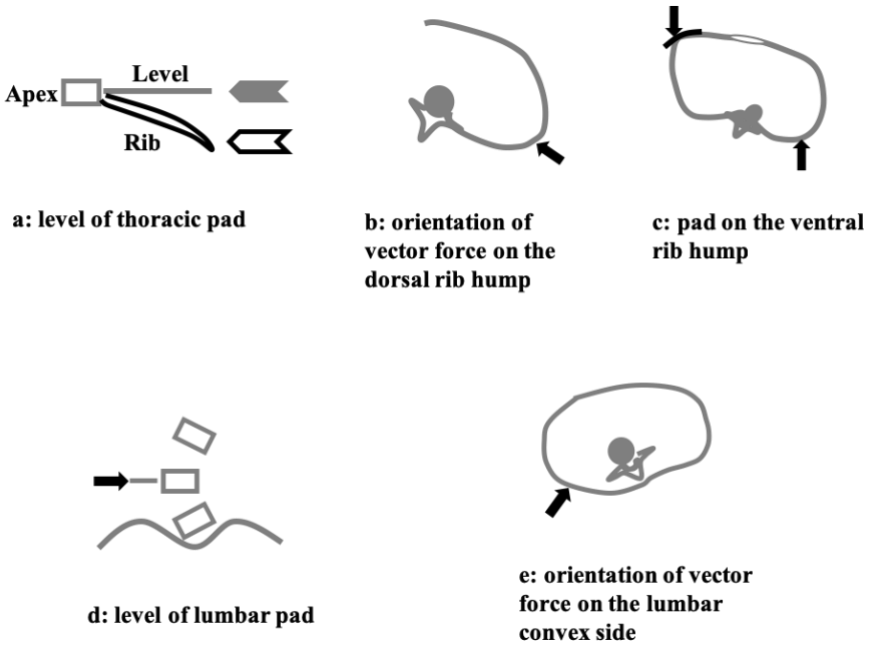

Figure 2.12 Biomechanical design of orthosis [53]

2.8.2 Orthosis Types

According to the wearing time, the spinal orthosis is classified into (1) night-time rigid orthosis, wearing mainly in bed for 8–12 hours per day; (3) part-time rigid orthosis, wearing mainly outdoor and in bed for 12–20 hours per day; (4) and full-time rigid orthosis, wearing outside and in bed for 20–24 hours per day [63]. Based on the material characteristics of the orthosis, the orthosis can be categorized into rigid and flexible. This section introduced common orthosis types, including Milwaukee, Chêneau, Boston, Charleston/ Providence night-time bending, and flexible (e.g., SpineCor) orthosis.

Milwaukee Orthosis (Full-time, Cervico-Thoraco-Lumbo-Sacral Orthosis, CTLSO)

As shown in Figure 2.13, Milwaukee orthosis is commonly prescribed for patients with high-level AIS [213]. It consists of throat mold, occipital pad, shoulder slings, anterior and posterior uprights, axillary sling, thoracic pad, lumbar pad, and pelvic girdle. The throat mold, occipital pad, and pelvic girdle fix and somewhat elongate the spinal column. The

auxiliary sling and thoracic and lumbar pads generate horizontal correcting forces. The combination of horizontal and longitudinal forces forms the biomechanical mechanism of correction. The magnitude and direction of forces acting in the horizontal plane were affected by the strap tension and the direction of strap being pulled [214]. Mulcahy, Galante (215) evaluated the changes of a longitudinal tractive force of Milwaukee orthosis in different situations. They found that the longitudinal tractive force was higher when removing the thoracic pad while lower in a standing position than in a supine or right recumbent position.

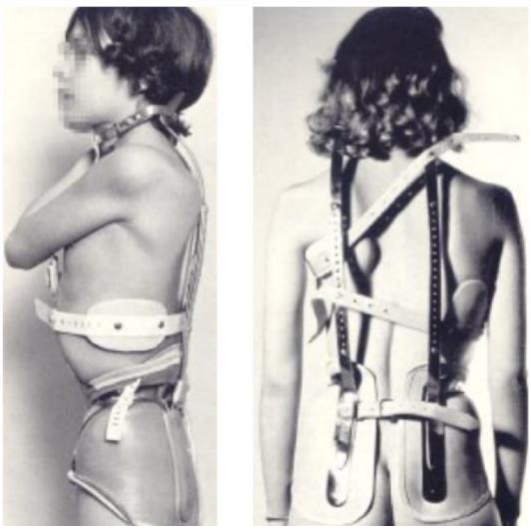

Figure 2.13 Milwaukee orthosis [216]

Chêneau Orthosis (Full-time, Thoraco-Lumbo-Sacral Orthosis, TLSO)

Chêneau orthosis is designed with a frontal opening and straps for closing (Figure 2.14). Symmetrical design is the typical characteristic that aims to provide a remodeling effect. The symmetrical design accompanies the whole body towards correction. It emphasizes the combination of proper pressure areas and free rooms, pushing the convex side and leaving room on the concave side to provide space for respiratory movements and spinal column remodeling [217-219]. The correction is realized through two mechanisms, containing the passive and active [218,220,221]. The passive mechanism derives from the pressure pads inside the orthosis, and the active mechanism works based on the combined actions of passive forces deriving from pads and active forces generated from respiratory movements. In turn, this active mechanism would asymmetrically guide the respiratory

movements, shortening the elongated axis of the thorax cage and elongating the shortened axis of the thorax cage, respectively. Additionally, the concave side of vertebral growth-plates would be unloaded when the spinal curve is corrected, which facilitates the growth of the concave side of vertebral growth-plates and ultimately remodels the spinal column.

Figure 2.14 Chêneau orthosis [103]

Boston Orthosis (Full-time, Thoraco-Lumbo-Sacral Orthosis, TLSO)

Boston orthosis is constructed from the basis of a scoliotic model that is realigned to be straight and close to normal, opening at the back and closing with straps (Figure 2.15). Boston orthosis emphasizes keeping a patient's trunk symmetrical and balanced and is usually suggested for patients with an apex of the primary curve at or below T8 level. Boston orthosis. Inside a Boston orthosis, a "three-point system" is formed by a correcting force generating from a pad at or below apical level and two counter-forces acting at the upper and lower ends of the curve. The correcting forces acting on the rib cage, which separately push the rib cage dorsally and ventrally, form a pair of horizontal forces countering with each other to de-rotate the rib cage. Pads located at the trochanters and anterior superior ilia are also recommended to re-align/stabilize the pelvis to/in a normal position, which would benefit the re-alignment of the spinal column. Additionally, an abdominal pad that pushes the trunk ventrally is also helpful for enhancing the re-alignment of the spinal column.

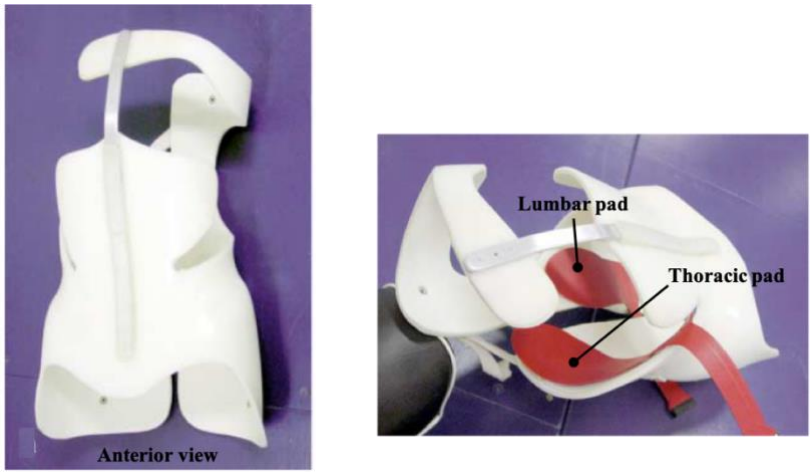

Figure 2.15 Boston orthosis [222]

Providence/Charleston Night-time Bending Orthosis (Thoraco-Lumbo-Sacral Orthosis, TLSO)

Providence /Charleston bending orthosis (Figure 2.16) is designed with a frontal opening and straps for closing and is the most common nighttime orthosis. Providence/Charleston bending orthosis positions an individual's trunk in an over-correction recumbent position during the night in bed. It is recommended for patients with primary single (thoraco)lumbar curves less than 35° [223,224] and was reported to be helpful in the control of a primary curve with an apex as high as T6 [225].

Figure 2.16 Providence night-time bending orthosis [153]

Figure 2.17 SpineCor orthosis [226]

Flexible Orthosis (SpineCor)

SpineCor is a typical flexible orthosis (Figure 2.17) developed by Sainte-Justine Hospital in 1992-1993 according to the principle of "mechanical biofeedback therapy" [227]. It consists of a pelvic belt, including three thermoformable plastic pieces stabilized by two thigh bands and two crotch bands, a cotton bolero, and four corrective elastic bands. The placement and adjustment of four elastic bands are based on a specific curve type, aiming to reproduce and enhance the corrective movement. The harnesses offer dynamic control of the shoulders, thorax, and pelvic girdles, constrain adverse movements and correct the 3D postural geometry while reserving body movement and growth.

2.8.3 Effectiveness of Orthotic Treatment

The positive effect of orthotic treatment in patients with AIS has been demonstrated in previous studies. The effectiveness of orthotic treatment is commonly evaluated via criteria proposed by SRS [74]: success refers to a primary curve progression ≤5° while failure is primary curve progression ≥6°, curve ≥45°, or surgery being recommended/undertaken at

orthotic discontinuation (skeletal maturity).

As shown in Table 2.4, the success rate varied widely from 8% to 100% among different orthoses, different follow-up period and different severities of AIS [51,52,224,226-242]. Milwarkee (CTLSO) and Boston/Chêneau/Lyon (TLSO) orthoses provided similar success rate (74%–93.7% [51,52] *vs.* 65.4%–100% [224,226,230,236-238,241,242] at ≥1 year follow-up).

In comparison with full-time rigid orthosis, Providence/Charleston night-time orthosis showed a relatively lower success rate (73%–88.2% at > 1-year follow-up [224,232-235]). The success rate of Charleston orthosis notably decreased at 2-year follow-up (29% for mild curves of 15°–25°) [231]. However, Charleston orthosis was useful for preventing mild AIS progression compared to observation alone.

For the SpineCor orthosis, the success rate was 8%–93% [226-230], but most studies showed 33%–73% [226,228,229] and were relatively lower as compared to the full-time (Milwaukee/Boston/Chêneau/Lyon orthosis) or night-time (Providence/Charleston bending orthosis) rigid orthosis. Although a high success rate of SpineCor orthosis was observed in some studies, its effectiveness was controversial. In a study conducted by Weiss and Weiss (230), the effectiveness of SpineCor and Chêneau orthosis was compared at 2-year and 3.5-year follow-up. The results showed that the success rate for SpineCor orthosis was significantly lower than that for Chêneau orthosis (33% *vs.* 93% at 2-year follow-up; 8% *vs.* 80% at 3.5-year follow-up). Wong, Cheng (226) also reported similar result (SpineCor: 68% *vs.* full-time rigid TLSO: 95% at 3.8-year follow-up). Additionally, Wong, Cheng (226) pointed out that the patients' compliance for SpineCor orthosis was not superior to that for full-time rigid TLSO.

A positive effect of orthotic treatment was demonstrated on the coronal-Cobb, while limited effectiveness was found in parameters related to the sagittal and transverse planes

[48,49,243], such as sagittal thoracic kyphosis/lumbar lordosis, VAR, and rib hump. The importance of 3D correction was increasingly recognized and emphasized, as recommended by SOSORT, that scoliosis correction should be evaluated in all three anatomical planes (the coronal, sagittal, and transverse planes) [244].

Table 2.4 Effectiveness evaluation of orthotic treatment for patients with AIS

Reference	Study design	Study sample	Orthosis type	Success rate	Failure rate
				Curve correction or curve progression ≤ 5°	Curve progression ≥ 6°, curve > 45° or surgery recommended/undertaken
Aulisa, Guzzanti (51)	Prospective	n=113 Cobb=29.6±7.5°	PASB, Lyon or Milwaukee orthosis	93.7% at 2-yr follow-up	6.2% at 2-yr follow-up
Nachemson and Peterson (52)	Prospective	n=88 Age=immaturity Cobb= 25-35°	Milwarkee orthosis	74% at maturity	-
Wiley, Thomson (242)	Retrospective	n=24 Age =12.8 yrs Cobb=38.0° (35-45°)	Boston orthosis	1. 75% 2-yr follow-up after cessation of treatment	1. 25% at 2-yr follow-up after cessation of treatment
				2. 65.4% at 9.7 (6.2-13.2)-yr follow-up after cessation of treatment	2. 24.8% at 9.7 (6.2-13.2)-yr follow-up after cessation of treatment (9.8% out of orthotic treatment at follow-up)
Giorgi, Piazzolla (241)	Retrospective	n=48 Age =11.3±2.0 (10-15) yrs Cobb=27±6.7° (20-45°)	Cheˆneau orthosis	100% at 5.4-yr follow-up	-
Negrini, Donzelli (240)	Prospective	n=73 Age =12.8±1.4 yrs Cobb= 34.4±4.4°	Sibilla, Lyon and SpineCor for 61.6%, 13.7% and 6.8% of subjects, respectively	83.5% at 3.3±1.7-yr follow-up	16.5% at 3.3±1.7-yr follow-up

Table 2.4 (cont.)

Reference	Study design	Study sample	Orthosis type	Success rate	Failure rate
				Curve correction or Curve progression ≤ 5°	**Curve progression ≥ 6°, curve > 45° or surgery recommended/undertaken**
Aulisa, Guzzanti (239)	Prospective	n=50 Age =11.8 ± 0.5 yrs Cobb=29.3 ± 5.2°	A progressive action short brace	100% at 2-yr follow-up	-
Weinstein, Dolan (238)	Prospective	n=105	Rigid TLSO	72% at maturity	-
Lusini, Donzelli (237)	Prospective multicentered	n=39 Age =15.3±1.8 yrs Cobb=52.5° (45-93°)	Lyon/Sforzesco orthosis	79.5% at 5.3-yr follow-up	20.5% at 5.3-yr follow-up
Aulisa, Guzzanti (236)	Prospective	n=69 Age =12.3±1.3 (10-12) yrs Cobb=31.5±4.3° (25-40°)	Lyon orthosis	98.5% at 2-yr follow-up after end of weaning (3.5±2.6 yrs)	1.5% at 2-yr follow-up after end of weaning (3.5±2.6 yrs)
Lee, Hwang (235)	Prospective	n=95 Age =10+ yrs Cobb=25-40°	Charleston bending orthosis	77.9% at maturity	22.1% at maturity
Price, Scott (234)	Prospective multicentered	n=139 Age =immaturity Cobb>25°	Charleston bending orthosis	83% at 1-yr follow-up	17% at 1-yr follow-up

Table 2.4 (cont.)

Reference	Study design	Study sample	Orthosis type	Success rate	Failure rate
				Curve correction or Curve progression ≤ 5°	**Curve progression ≥ 6°, curve > 45° or surgery recommended/undertaken**
Gepstein, Leitner (233)	Prospective	n_1=85, n_2=37 Age $_1$=12.8±1.7 yrs Age $_2$=13±1.8 yrs Cobb=30.4°	1. Charleston bending orthosis 2. Boston orthosis	1. 88.2% at 1-1.9-yr follow-up 2. 86.5% at 1-1.9-yr follow-up	1. 11.8% at 1-1.9-yr follow-up 2. 13.5% at 1-1.9-yr follow-up
Yrjonen, Ylikoski (224)	Prospective$_1$ + retrospectively$_2$	n_1=36, n_2=36 Age =12.3±1.3 (10-12) yrs Cobb=28.4°	1. Providence nighttime orthosis 2. Boston orthosis	1. 73% at 1.8-yr follow-up after cessation of treatment 2. 78% at 1.8-yr follow-up after cessation of treatment	1. 27% at 1.8-yr follow-up after cessation of treatment 2. 22% at 1.8-yr follow-up after cessation of treatment
d'Amato, Griggs (232)	Prospective	n=102 Age =10+ yrs Cobb=20-42°	Providence nighttime orthosis	74% at 2.6-yr follow-up after cessation of orthotic treatment	26% at 2.6-yr follow-up after cessation of treatment
Wiemann, Shah (231)	Prospective	n_1=21, n_2=16 Age $_1$=12.0±1.3 yrs Age $_2$=11.9±1.2 yrs Cobb=15-25°	1. Charleston bending orthosis 2. Observation	1. 29% at 2-yr follow-up 2. 0% at 2-yr follow-up	1. 71% at 2-yr follow-up 2. 100% at 2-yr follow-up
Coillard, Leroux (227)	Prospective	n=29 Age =13±1 yrs Cobb=29±7°	SpineCor orthosis	93% at 2-yr follow-up	7% at 2-yr follow-up

Table 2.4 (cont.)

Reference	Study design	Study sample	Orthosis type	Success rate	Failure rate
				Curve correction or Curve progression ≤ 5°	**Curve progression ≥ 6°, curve >45° or surgery recommended/undertaken**
Weiss and Weiss (230)	Prospective	n_1=12, n_2=15 Age $_1$=12.0±1.3 yrs Age $_2$=11.9±1.2 yrs $Cobb_1$=21.3° (16-32°) $Cobb_2$=33.7° (20-52°)	1. SpineCor orthosis 2. Cheˆneau orthosis	1. 33% at 2-yr follow-up, 8% at 3.5-yr follow-up 2. 93% at 2-yr follow-up, 80% at 3.5-yr follow-up	-
Coillard, Circo (229)	Prospective RCT	n=32 Age =12±2 yrs Cobb=22±4.9° (15-30°)	SpineCor	73.1% at 5-yr follow-up	26.9% at 5-yr follow-up
Coillard, Vachon (228)	Prospective	n=170 Age=premenarchal or less than 1yr postmenarchal Cobb=25-40°	SpineCor	59.4% at 2-yr follow-up beyond maturity	24.1% at 2-yr follow-up beyond maturity
Wong, Cheng (226)	Prospective	n_1=22, n_2=21 Age=10-14 yrs Cobb=20-30°	1. SpineCor 2. Rigid orthosis	1. 68% at 3.8-yr follow-up 2. 95% at 3.8-yr follow-up	-

2.9 Summaries of Literature Review

AIS is a complicated 3D deformity of the spine characterized by lateral curvature and vertebral axial rotation, usually combining with rib hump, sagittal thoracic hypo-kyphosis, and/or lumbar hyper-lordosis.

Adam's forward bend test is the first step to assessing spinal deformity, while imaging modality is necessary to diagnose scoliosis. QoL is an essential aspect of the treatment goal, so it should be involved in assessing AIS and evaluated using relevant tools. The applications of the plain radiograph, EOS system, CT, MRI, ultrasound, and surface topography in assessing scoliosis were reviewed. Plain radiograph serves as the gold standard for the imaging assessment of scoliosis. CT and MRI are commonly recommended for patients with severe scoliosis and/or scheduled with surgery. The EOS system is characterized by micro-dose radiation compared to traditional radiographic modalities (e.g., plain radiography and CT) and has been widely applied in the clinic. Ultrasound and surface topography are recognized as non-invasive and user-friendly modalities, which make them promising in assessing AIS to reduce the times of radiographing.

Coronal-Cobb is a primary parameter for the assessment of AIS. However, it may underestimate the AIS severity and not fully reflect the curve type. Thus, 3D assessment is increasingly valued in routine clinical practice. PMC, EAEP, and BFP were recognized as typical 3D descriptors that reflect the maximum spinal deformity. This literature review gives an insight into their definitions, techniques for obtaining them, and their applications in the management of scoliosis. According to the definitions, BFP appears to consider more vertebrae of a curve than the EAEP and PMC; however, BFP and EAEP were usually simplified in orientation to ensure a reasonable number of variables for analysis in most studies. From a clinical view, coronal-Cobb serves as the golden standard in diagnosis, clinical decision-making, and prognosis. The PMC concept seems closer to the coronal-Cobb as they reflect the spinal curvature in a vertical plane. This may make

clinicians/orthotists easier to understand the PMC concept and produce more meaningful applications than the EPE and BFP, which attracted this project to focus on the PMC. Nevertheless, this did not mean that the EAEP and BFP are not meaningful in clinical application. With the more profound understanding of scoliosis and the development of assessment techniques, it would be worthwhile into give an insight to these two descriptors.

The 3D model of the spine or spinal curve reconstructed from calibrated bi-planar radiographs (e.g., EOS images) is the basis for obtaining PMC, EAEP & BFP. Although the reconstructed models were reproducible and accurate, the PMC, EAEP, and BFP measurements obtained from these models were not studied explicitly. Ultrasound has been available for acquiring PMC, while further validation is necessary before clinical application. Because of the need for 3D reconstruction and special tools/skills, these modalities were still limited to research use. Thus, it was attractive to develop a more user-friendly, less time-consuming, and low-cost method to obtain PMC, EAEP, or BFP.

PMC, EAEP & BFP have been applied to 3D assessment, progression monitoring, classification, and correction evaluation of surgical and orthotic treatments, while barely considered when making clinical decisions. Thus, it may be worthwhile to explore the possible application of these 3D descriptors in surgical/orthotic strategy making.

According to the indications for treatment of AIS, patients with primary curve <20° or >45° are commonly prescribed with observation and surgery, respectively, while for those with a primary curve of 20°–40°, conservative treatments are generally prescribed.

PSSE, SIR, and orthosis are common conservative interventions. The effectiveness of the PSSE and SIR was lack of more high-quality evidence to support. Thus, a discussion with patients and their families should be made before treatment. An orthosis is a clinically recognized conservative intervention and works by using external correcting forces produced from pressure pads inside orthosis to correct/control the curve (progression). The

positive effect of orthotic treatment has been demonstrated while mainly on the corona-Cobb barely on VAR, rib hump, sagittal thoracic kyphosis, and lumbar lordosis.

Apart from some general principles proposed by SOSORT, there are no consistent documents to guide the orthosis design. In this case, an orthosis is usually designed empirically. The shape of the pad inside the orthosis and direction of correcting force could vary obviously among orthoses designed by different orthotists. Thus, it may benefit orthotic design to investigate which shape of pressure-pad and which direction of correcting force was superior to others in the control/correction of scoliosis. Also, it may be worthwhile to explore the application of the concept of PMC (or EAEP/BFP) in orthotic design.

CHAPTER 3 RELIABILITY AND VALIDITY OF PLANE OF MAXIMUM CURVATURE OBTAINED USING A PURPOSE-DESIGN COMPUTATIONAL METHOD FOR PATIENTS WITH ADOLESCENT IDIOPATHIC SCOLIOSIS

3.1 Introduction

Adolescent idiopathic scoliosis (AIS) is a complex three-dimensional (3D) deformity of the spine characterized by lateral curvature (≥10°) and vertebral axial rotation (VAR) [23]. The measured from the standing radiograph is the gold standard for the assessment of scoliosis [163], but it may underestimate the severity of spinal curvature and may not fully reflect the curve type three-dimensionally [19,21]. The importance of three-dimensional (3D) assessment was increasingly valued. Society on Scoliosis Orthopaedic and Rehabilitation Treatment (SOSORT) [63] pointed out that the assessment should be conducted in all three anatomical planes (coronal, sagittal, and transverse). Plane of maximum curvature (PMC) was a helpful descriptor that could reflect the maximum spinal deformity and the 3D features of scoliosis [24].

PMC was defined as a vertical plane that positions between the sagittal and coronal planes and presents the maximum spinal curvature [23]. Parameters include the maximum Cobb angle measured in PMC (PMC-Cobb) and orientation of PMC (PMC-orientation, the angle between the PMC and the sagittal or coronal plane [245]. The PMC-orientation was concerned with the sagittal plane in this study. PMC has been used to assess [21,33,54-57,174] and classify [173,183] AIS as well as evaluate the correction of surgical and orthotic treatments [164,178,180,181].

Several approaches allow PMC assessment. 3D model of the scoliotic spine (or spinal curve) reconstructed from the calibrated bi-planar radiographs (e.g., EOS images) is the essential requirement for PMC assessment. Based on the reconstructed model, PMC could be

estimated by rotating a vertical plane, where the scoliotic spine was projected onto, from the sagittal to coronal plane with a particular increment (e.g., 2.5° [33]), and measuring the Cobb angle in each rotated plane until the maximum spinal curvature was found [19,27,33,175,176]. Reproducibility and accuracy of the 3D reconstruction of the scoliotic spine have been demonstrated, while the PMC was barely studied. Besides, this method was mainly limited to the research use due to the need for special software/skills and the time consumption for the 3D reconstruction and PMC identification. The ultrasound technique has been available for PMC assessment [27,185]. With the 3D ultrasound images established from ultrasound data, PMC was identified by rotating a vertical plane to a position with an orientation equalling to the maximum VAR and was confirmed by placing the vertical plane to the maximum VAR ±2°, ±4° [27] or ±5° [185] using the center of laminae (COL) method. The PMC (PMC-Cobb; PMC-orientation) measurements of ultrasound showed high reliability (intra-class correlation coefficient >0.92), and the PMC-orientation measurements were strongly correlated to those of the EOS system (R^2=0.88) [27]. However, further validation was required before clinical application. Moreover, CT and MRI systems, which are recognized as the reference methods for 3D assessment of AIS, can also be used to obtain the PMC. However, because of high-radiation exposure and only recumbent assessment, they are commonly indicated for severe AIS other than mild to moderate AIS.

This study aimed to develop a more user-friendly computational method (CM) to estimate the PMC merely based on the coronal and sagittal images of the spine and to verify it with CT.

3.2 Methodology

3.2.1 Study flowchart

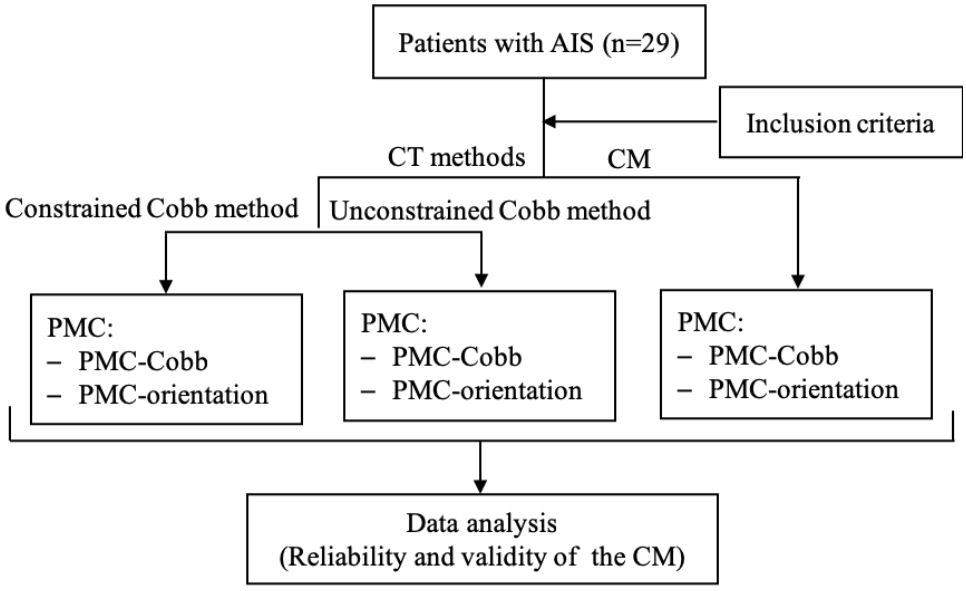

Figure 3.1 Study flowchart

3.2.2 Subjects

Inclusion criteria included: (1) diagnosed with AIS; (2) age: ≥10 years; (3) coronal-Cobb: ≥10°; (4) no prior surgical treatment; (5) with original pre-operative CT image of the whole spine; (6) no other diseases affecting the spinal morphology. The human ethical approval was granted from the authors' Institutional Review Board (Ref. HSEARS20170807003).

The sample size was 15 calculated in G*Power 3.1.9.7 with a power of 0.8, an alpha error of 0.05, and an effect size of 0.8 estimated based on a previous study of imaging measurements [137]. According to the inclusion criteria, 29 consecutive subjects (27 females / 2 males with mean age: 15.8±3.5 years) were selected from the database of a local scoliotic center. All the recruited subjects were imaged pre-operatively in the prone position with a CT scanner (LightSpeed®16, GE Healthcare with parameters set at 400 mA s, 120 kVp, 0.625 mm thicknesses, and 5 mm gap between slices) between 2015 and 2017 (all CT scans were taken for subjects' own assessment/treatment purpose).

3.2.3 Computational Method

As shown in Figure 3.2, the computational method (CM) is based on the global axis system (x, y, z) of the human body with an origin at the center of the superior endplate of the first sacral vertebra [167]. For a specific curve, the upper end-vertebra's superior endplate and the lower end-vertebra's inferior endplate are assumed to be a plane, respectively, that can be extended outward infinitely. A vertical plane positioning between or overlapping the coronal and sagittal planes intersects with the superior and inferior endplates at their intersection line $L_{vertical\text{-}superior}$ and $L_{vertical\text{-}inferior}$, respectively. The angle (β) formed by $L_{vertical\text{-}superior}$ and $L_{vertical\text{-}inferior}$ is the Cobb angle of the specific curve on the vertical plane. The vertical plane is rotated 360° counter-clockwise along axis z with an increment of 1° to determine the maximum Cobb angle (β_{max}). The Cobb angle (β) on each interval vertical plane is calculated, and the maximum Cobb angle (β_{max}) can then be determined. The vertical plane presenting the maximum Cobb angle is the PMC with an orientation of θ concerning the sagittal plane. As shown in Figure 3.4, the Cobb angle (β) is calculated according to the following steps:

(1) The normal vector to the superior and inferior endplates: as shown in Figure 3.3, eight points (C_1, C_2, C_3, C_4, C_5, C_6, C_7, and C_8) are identified orderly on the superior/inferior endplates of the upper/lower end-vertebrae in the coronal and sagittal planes (coronal and sagittal CT images) in an imaging analysis software (Digimizer, version 4.3.5, MedCalc Software bvba, Belgium). The software automatically provides the 2D coordinates of the eight points, which are converted into the 3D coordinates using a direct algorithm (Figure 3.4: a1 & c1). The vectors are obtained based on these 3D coordinates, as shown in Figure 3.4: a2 & c2. With the assumption of these vectors being in the truly superior and inferior endplates of the end-vertebrae, the normal vectors to these two endplates can be presented as those shown in Figure 3.4: a3 & c3.

(2) The normal vector to the vertical plane: with the assumption of the magnitude equal to 1 without loss of generality, the normal vector to the vertical plane can be presented as shown in Figure 3.4: b2.

(3) To calculate the Cobb angle (β) of the specified curve: based on the normal vectors to the superior endplate, vertical plane, and inferior endplate (Figure 3.4: a3, b2 & c3), the Cobb angle (β) can be calculated via a formula based on inverse trigonometric function as shown in Figure 3.4: d.

The orientation of the vertical plane (θ) is recorded as a negative value (-), and equal to 0°/-180° and -90°/-270° when overlapping with the sagittal and coronal plane separately. According to the quadrants that different curve types located in, the orientation of the vertical plane ranges from (Figure 3.5): (1) -270° to -359° and 0° to -90° for left and right thoracic curves (LTs and RTs), respectively; (2) -180° to -270° and -90° to -180° for left and right (thoraco)lumbar curves (LTLs/LLs and RTLs/RLs), respectively. After pre-defining the absolute value of the orientation (θ) at 0°,1°,2° … 358° and 359°, the Cobb angle in each vertical plane can be calculated using the Excel software (Microsoft Office 365, USA) based on the formula shown in Figure 3.4: d, and the maximum Cobb angle can be determined.

3.2.4 PMC Estimation using Computational Method

Currently, the CM relied on a third party's software to realize the calculation, and the steps are shown below:

(1) To import the coronal and sagittal CT images of the whole spine into the Digimizer and identify the eight points (Figure 3.3).

(2) To convert the 2D coordinates of the eight points obtained from Digimizer into corresponding 3D coordinates (Figure 3.4: a1 & c1).

(3) To calculate the Cobb angle (β) in each interval vertical plane using Excel software based on the formula shown in Figure 3.4: d.

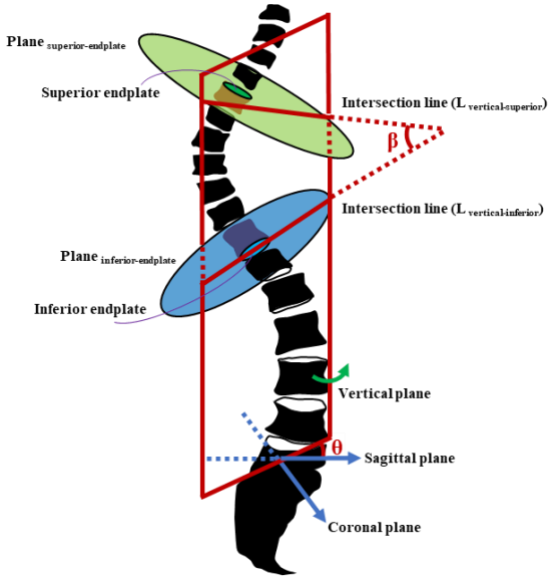

Figure 3.2 The principle of the computational method. The upper-end vertebra's superior endplate and the lower-end vertebra's inferior endplate of a specific spinal curve are assumed to be on the planes that can be extended outward named $Plane_{superior\text{-}endplate}$ and $Plane_{inferior\text{-}endplate}$, respectively. A vertical plane intersects with $Plane_{superior\text{-}endplate}$ and $Plane_{inferior\text{-}endplate}$ at $L_{vertical\text{-}superior}$ and $L_{vertical\text{-}inferior}$, respectively; and the angle (β) formed by the intersection lines is the Cobb angle of the spinal curve in that vertical plane

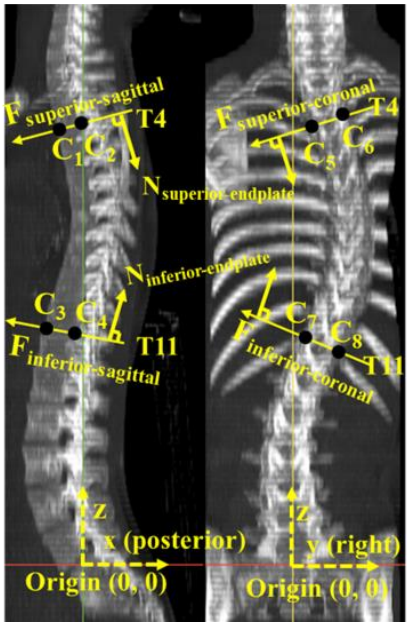

Figure 3.3 Eight points identification. Eight points in the upper-end vertebra's superior endplate and the lower-end vertebra's inferior endplate were identified in the sagittal and coronal CT images

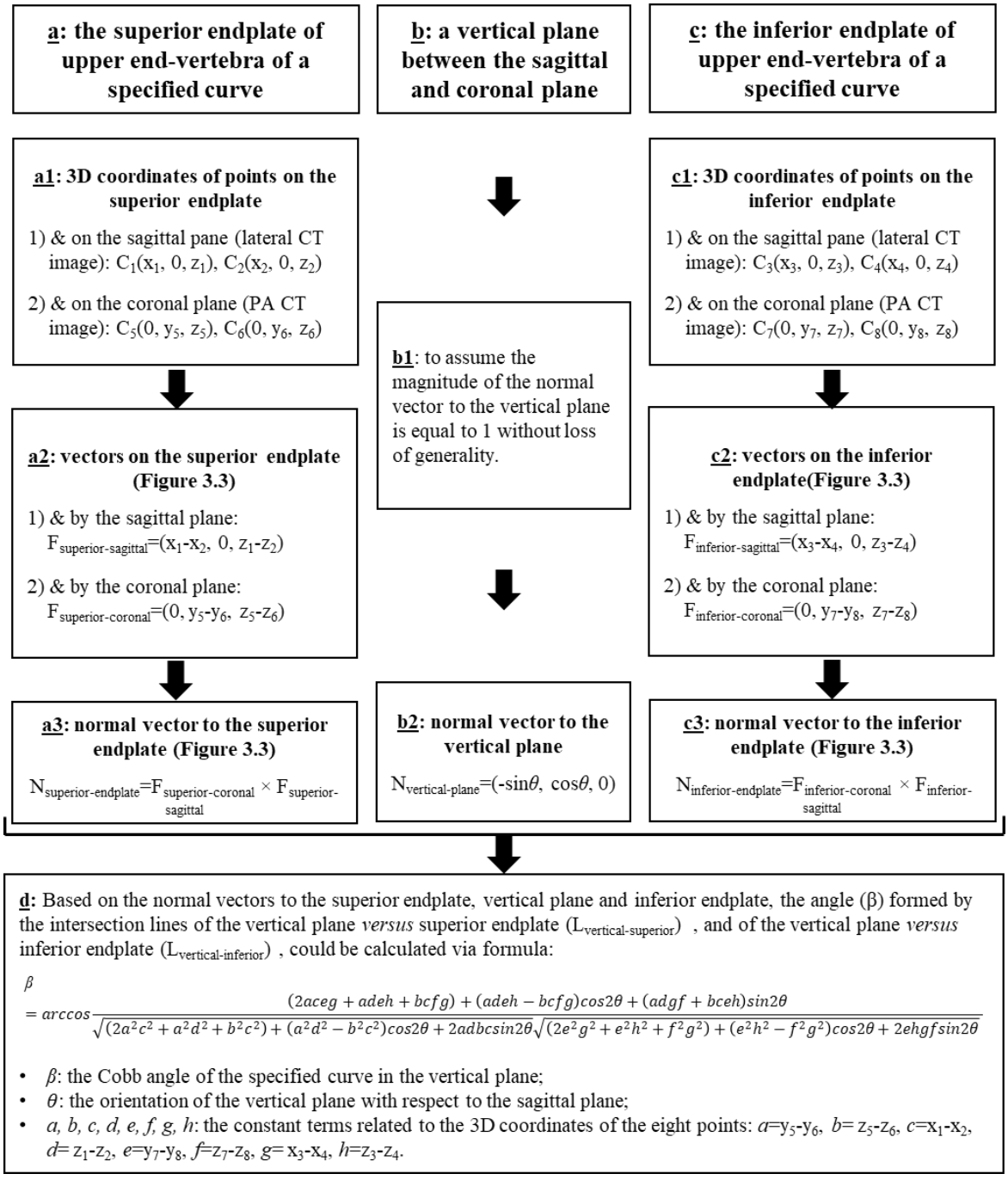

Figure 3.4 Procedures of Cobb angle (*β*) calculation. The vectors ($F_{superior-sagittal}$, $F_{superior-coronal}$, $F_{inferior-sagittal}$ and $F_{inferior-coronal}$ in a2 and c2) obtained based on the eight points identified on the projected sagittal and coronal planes were assumed to be on the actual upper-end vertebra's superior endplate and the lower-end vertebra's inferior endplate

3.2.5 PMC Estimation using Computed Tomography

(1) To import original CT images (Dicom format) into 3Dslicer (version 4.8.1, 3DSlicer Platform: www.slicer.org), which allows 3D visualization of the CT images. A vertical plane, where the spine was projected onto, was rotated 90° along the vertical axis with an increment of 5° originally from the sagittal to the coronal plane. The quadrant, where the vertical plane was rotated within, was determined according to the curve type described in "section 3.2.3" and shown in Figure 3.5. In the 3Dslicer, each interval plane was saved for the Cobb angle measure, totally generating 19 images for each curve.

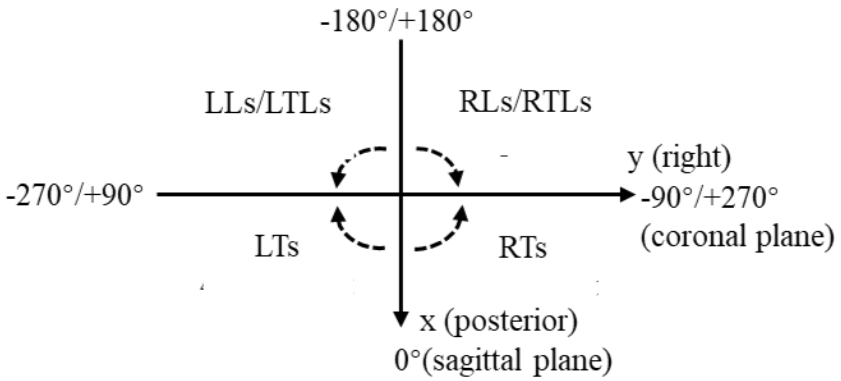

Figure 3.5 Quadrants where the orientation of the vertical plane varies according to different curve types

(2) To import the 19 images to the Digimizer one by one and measure the Cobb angle on each of them (Figure 3.6) using the constrained and unconstrained Cobb methods as described as follows:

Because of the complex global, regional, and local deformity of scoliosis [23,29,31], it is unknown if the end-vertebrae most tilted in the coronal plane would always be most tilted in any other vertical planes. Thus, the constrained and unconstrained Cobb methods were proposed. As shown in Figure 1, the constrained Cobb method measures the Cobb angle in any other vertical planes different from the coronal plane with upper and lower end-

vertebrae selected from the coronal plane at the beginning of the measurement [23,32]. The unconstrained Cobb method measures the Cobb angle in any vertical planes with upper and lower end-vertebrae determined from that plane, where the Cobb angle is measured [33]. Because it was unclear if the PMC measurements of the CT constrained and unconstrained Cobb methods were comparable or not, this study selected both methods as the reference methods to verify the CM.

(3) To determine the maximum Cobb angle among the 19 Cobb angles separately measured using the constrained and unconstrained Cobb methods.

(4) To determine the PMC of constrained and unconstrained Cobb methods according to the maximum Cobb angle.

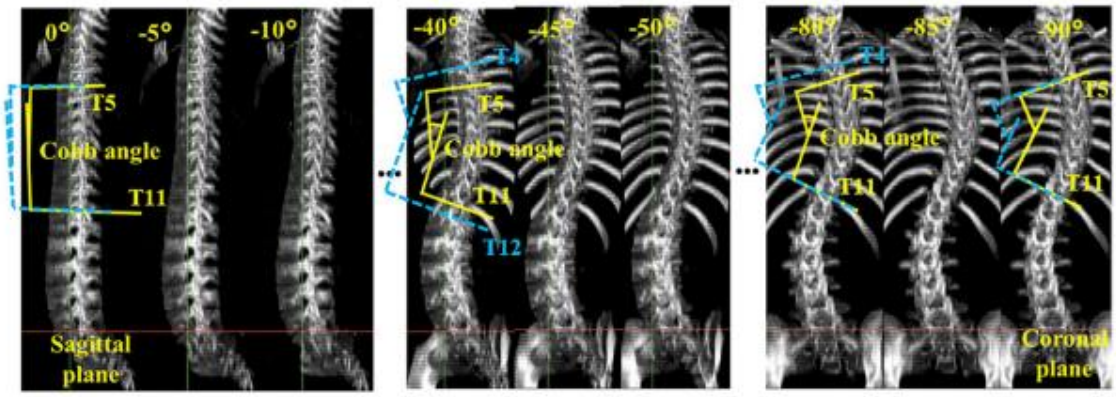

Figure 3.6 Cobb angle measured in different CT rotated images. Constrained (solid lines) and unconstrained (dashed lines) Cobb methods (the rotated planes, n=19) were generated by rotating a vertical plane 90° around axially from the sagittal to coronal plane with an increment of 5°; counter-clockwise rotation was for a right thoracic curve and recorded as negative (−))

3.2.6 Data Collection

Two raters (H & D), who had experience of 3+ years in Cobb angle measurements, were trained for PMC (PMC-Cobb; PMC-orientation) estimation using the CM in this study. As shown in Figure 3.7, based on the same sets of the coronal and sagittal images, each rater estimated the PMC three times using the CM with a one-week interval each time to reduce possible recalling bias. Rater D measured the PMC three times using the CT constrained and unconstrained Cobb methods based on the same rotated images (19 rotated images with an orientation interval of 5°) with the same protocol. The mean of three repeated PMC of CM was compared to those of the CT Cobb methods, respectively.

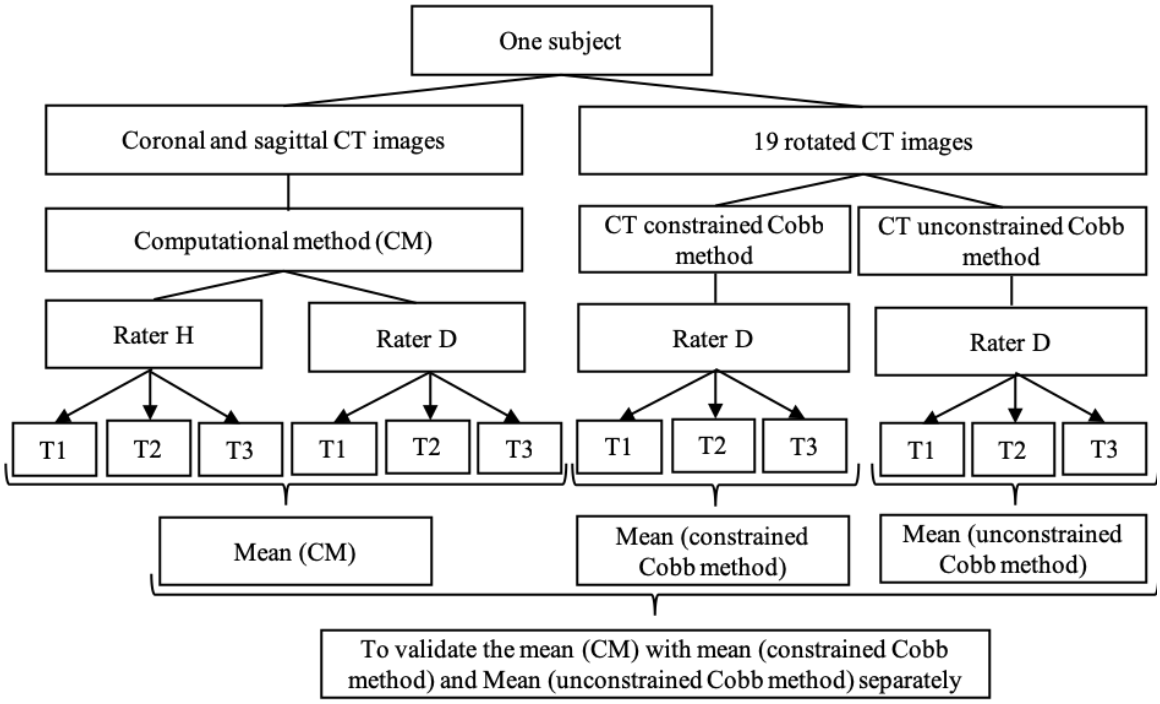

Figure 3.7 Data collection. T1, T2 and T3 represent the 1st, 2nd and 3rd repeated PMC obtained using the CM and CT constrained and unconstrained Cobb methods, respectively

3.2.5 Statistical Analysis

Statistical analysis was performed in SPSS (version 21, IBM, Chicago, IL, USA) with a significant level (p) set at 0.05. The normality of each studied parameter was analysed

using the Shapiro-Wilks test. The PMC obtained from the CM and CT Cobb methods were presented as mean ± standard deviation (SD). Inter- & intra-reliability of PMC acquired from the CM was evaluated using intra-class correlation coefficient (ICC, [2, 1]) (using a two-way random model and absolute agreement) with a confidence interval of 95% (95% CI). The strength of reliability was evaluated using criteria: very reliable (ICC: 0.8–1.0), moderately reliable (ICC: 0.60–0.79) and questionably reliable (ICC: <0.60) [246]. Intra- & inter-rater difference of PMC obtained from CM was compared using one-way repeated ANOVA and paired t-test (2-tailed), respectively. PMC estimated using CM was compared to that acquired using CT using ICC, Bland-Altman method, Pearson correlation (r), linear regression analysis, and mean difference (MD). The strength of correlation was considered as very good to excellent (r: 0.75–1.00), moderate to good (r: 0.50–0.75) and poor correlation (r: 0.25–0.50) [247].

3.3 Results

Fifty curves were selected for this study, including 27 RTs (mean coronal-Cobb: 46.1°±12.4° with a range of 26.2°–71.1°) and 23 LTLs/LLs (30.6°±9.1° with a range of 16.4°–54.2°). For the RTs, there were 10 moderate curves (35.1°±3.2° with a range of 26.3°–39.6°) and 17 severe curves (52.9°±9.7° with a range of 40.5°–71.1°). For the LTLs, there were 8 mild curves (18.6°±4.1° with a range of 16.4°–23.6°), 12 moderate curves (31.8°±6.7° with a range of 26.0°–39.5°), and 3 severe curves.

3.3.1 Mean Trend of Cobb Angle in Each Rotated Plane

As shown in Figure 3.8, the mean trends of Cobb angle in each rotated plane obtained from the CM and CT constrained and unconstrained Cobb methods were generally similar for the overall RTs and LTLs/LLs groups and their subgroups. Compared with the CT unconstrained Cobb method, the CM and CT constrained Cobb method provided closer mean trends for all the groups, and the former tended to give a slightly greater mean Cobb angle than the two latter, especially in rotated planes near to the sagittal plane. Moreover, the mean trends of the three methods in the RTs groups seemed to be generally closer with

each other than those in most of the LTLs/LLs groups except for the mild LTLs/LLs group. Besides, the rotated planes, where maximum Cobb angles were found, were generally closer to the coronal plane in the RTs groups than in most LTLs/LLs groups. By contrast, the rotated plane presenting the maximum mean Cobb angle in the mild LTLs/LLs tended to close to the sagittal plane.

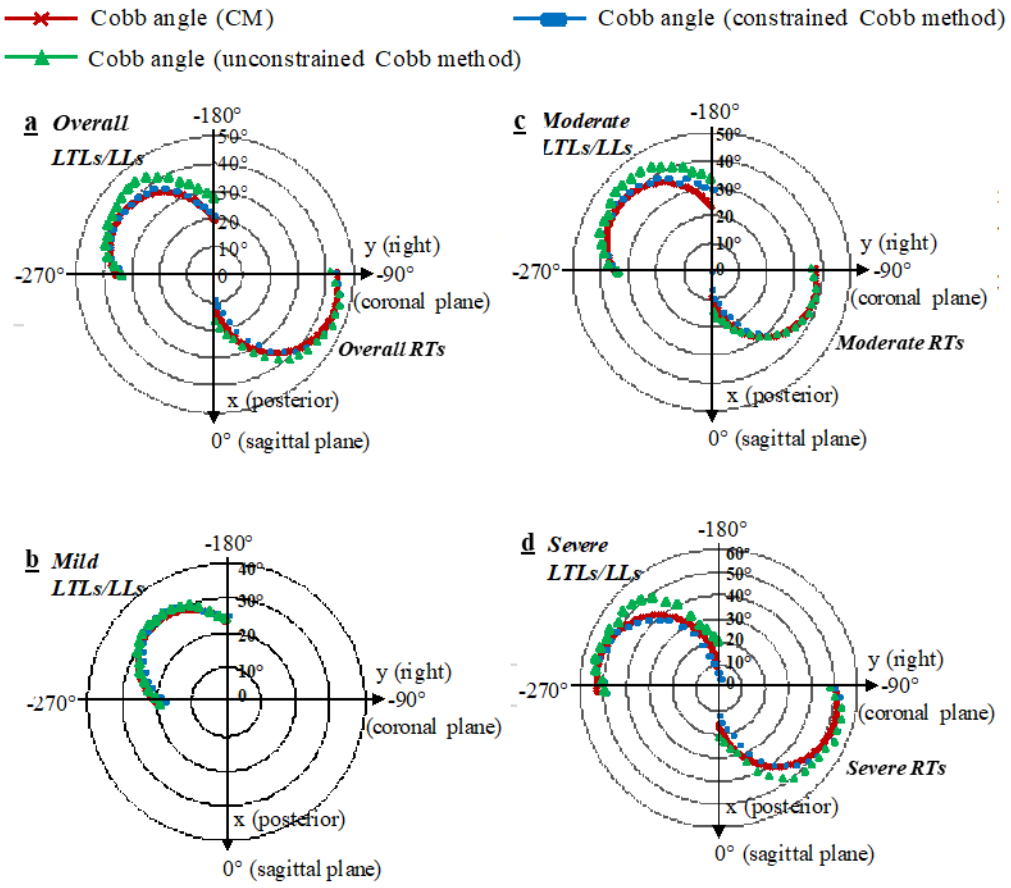

Figure 3.8 Mean Cobb angles in each rotated plane for the different RTs and LTLs/LLs groups. In radars, the x-axis pointing posteriorly represents the sagittal plane (with an orientation of 0°), and the y axis pointing to the right side represents the coronal plane (with an orientation of -90°). The distance from the origin to each circle represents the magnitude of Cobb angle

3.3.2 Reliability of PMC Obtained Using Computational Method

As described in Table 3.1, PMC (PMC-Cobb; PMC-orientation) acquired from the CM showed high intra-rater reliability in all the analysed groups (intra-ICC=0.90–0.98; intra-ICC=0.87–0.98). No significant intra-rater difference was found (p>0.05). Moreover, the PMC-Cobb of CM presented similar strength of intra-rater reliability to the coronal-Cobb (intra-ICC=0.74–0.98)

Table 3.2 showed high inter-ICC values for PMC-Cobb of the CM in all the analysed groups (0.74–0.91) except for the mild LTLs/LLs group (0.68). The strength of inter-rater reliability was similar to that of coronal-Cobb, which had inter-ICC values of 0.90–0.99 for all the groups except for the mild LTLs/LLs group (0.59). Moreover, no significant inter-rater difference was observed in all the analysed groups (p>0.05). Regarding the PMC-orientation, high inter-rater reliability was seen in all the analysed groups (inter-ICC=0.87–0.93) except for the mild LTLs/LLs group (inter-ICC=0.51). A significant inter-rater difference was observed in almost all the analysed groups (p<0.05).

Table 3.1 Intra-rater reliability of PMC acquired using the CM

PMC Parameter	Rater H		Rater D		Coronal parameter	Rater H		Rater D	
	ICC (95%CI)	Sign.*p*	ICC (95%CI)	Sign.*p*		ICC (95%CI)	Sign.*p*	ICC (95%CI)	Sign.*p*
Overall RTs (n=27)									
PMC-Cobb	0.953 (0.913-0.977)	0.196	0.984 (0.970-0.992)	0.059	Coronal-Cobb	0.955 (0.917-0.978)	0.132	0.980 (0.963-0.990)	0.296
PMC-orientation	0.915 (0.847-0.957)	0.171	0.954 (0.914-0.977)	0.046	-	-	-	-	-
Moderate RTs (n=10)									
PMC-Cobb	0.902 (0.745-0.972)	0.906	0.910 (0.763-0.974)	0.107	Coronal-Cobb	0.735 (0.478-0.901)	0.238	0.901 (0.743-0.972)	0.841
PMC-orientation	0.871 (0.675-0.963)	0.227	0.951 (0.866-0.987)	0.215	-	-	-	-	-
Severe RTs (n=17)									
PMC-Cobb	0.944 (0.879-0.977)	0.186	0.975 (0.944-0.990)	0.359	Coronal-Cobb	0.978 (0.952-0.991)	0.164	0.976 (0.946-0.990)	0.162
PMC-orientation	0.942 (0.875-0.977)	0.695	0.957 (0.907-0.983)	0.167	-	-	-	-	-
Overall LTLs/LLs (n=23)									
PMC-Cobb	0.968 (0.935-0.986)	0.065	0.976 (0.953-0.989)	0.970	Coronal-Cobb	0.981 (0.962-0.991)	0.360	0.987 (0.974-0.994)	0.054
PMC-orientation	0.957 (0.914-0.981)	0.473	0.983 (0.966-0.992)	0.101	-	-	-	-	-
Mild LTLs/LLs (n=8)									
PMC-Cobb	0.938 (0.791-0.988)	0.105	0.983 (0.943-0.996)	0.550	Coronal-Cobb	0.903 (0.660-0.984)	0.683	0.902 (0.715-0.978)	0.408
PMC-orientation	0.920 (0.740-0.984)	0.828	0.956 (0.860-0.990)	0.218	-	-	-	-	-
Moderate LTLs/LLs (n=12)									
PMC-Cobb	0.957 (0.881-0.988)	0.204	0.948 (0.864-0.984)	0.734	Coronal-Cobb	0.947 (0.872-0.982)	0.420	0.955 (0.887-0.986)	0.151
PMC-orientation	0.947 (0.854-0.985)	0.986	0.961 (0.897-0.988)	0.126	-	-	-	-	-

Mild: prone corona-Cobb <25°; Moderate: 25°≤ prone coronal-Cobb ≤40°; Severe: prone coronal-Cobb >40°

Table 3.2 Inter-rater reliability of PMC acquired using the CM

PMC parameter	ICC (95%CI)	Sign.*p*	Coronal parameter	ICC (95%CI)	Sign.*p*
Overall RTs (n=27)					
PMC-Cobb	0.905 (0.654-0.917)	0.387	Coronal-Cobb	0.981 (0.958-0.991)	0.054
PMC-orientation	0.929 (0.732-0.938)	0.010	-	-	-
Moderate RTs (n=10)					
PMC-Cobb	0.742 (0.621-0.916)	0.059	Coronal-Cobb	0.900 (0.598-0.975)	0.056
PMC-orientation	0.936 (0.743-0.984)	0.331	-	-	-
Severe RTs (n=17)					
PMC-Cobb	0.872 (0.646-0.954)	0.700	Coronal-Cobb	0.970 (0.916-0.989)	0.053
PMC-orientation	0.927 (0.798-0.974)	0.016	-	-	-
Overall LTLs/LLs (n=23)					
PMC-Cobb	0.884 (0.725-0.951)	0.146	Coronal-Cobb	0.985 (0.963-0.994)	0.051
PMC-orientation	0.873 (0.700-0.946)	0.015	-	-	-
Mild LTLs/LLs (n=8)					
PMC-Cobb	0.684 (0.541-0.907)	0.427	Coronal-Cobb	0.575 (0.432-0.873)	0.437
PMC-orientation	0.510 (0.436-0.859)	0.077	-	-	-
Moderate LTLs/LLs (n=12)					
PMC-Cobb	0.862 (0.486-0.963)	0.069	Coronal-Cobb	0.966 (0.881-0.990)	0.267
PMC-orientation	0.880 (0.554-0.968)	0.003	-	-	-

Mild: prone corona-Cobb <25°; Moderate: 25°≤ prone coronal-Cobb ≤40°; Severe: prone coronal-Cobb >40°

3.3.3 Validity of PMC Obtained Using Computational Method

The mean±SD of PMC acquired from the CM and CT Cobb methods were presented in Table 3.3. The means of PMC-Cobb obtained from the CM were generally smaller than those measured using the two CT Cobb methods in all the analysed groups. Differently, the means of PMC-orientation of the CM were higher than those of the two CT Cobb methods in absolute value in all the analysed groups. Additionally, the CT unconstrained Cobb method gave the largest mean of PMC-Cobb in all the analysed groups; it provided the lowest mean of PMC-orientation in absolute value.

Table 3.3 Mean and standard deviation of PMC obtained using the three methods

PMC parameter	CM (°)	Constrained Cobb method (°)	Unconstrained Cobb method (°)
Overall RTs (n=27)			
PMC-Cobb	48.0±11.4	50.8±12.7	51.1±12.9
PMC-orientation	-74.8±9.1	-72.7±8.9	-71.7±9.9
Moderate RTs (n=10)			
PMC-Cobb	38.6±4.9	40.9±7.0	40.9±7.0
PMC-orientation	-75.7±9.9	-72.3±10.0	-70.5±9.7
Severe RTs (n=17)			
PMC-Cobb	53.5±10.5	56.6±11.7	57.5±11.6
PMC-orientation	-74.3±8.9	-73.0±8.6	-72.4±10.2
Overall LTLs/LLs (n=23)			
PMC-Cobb	39.8±9.9	44.6±9.4	44.9±9.7
PMC-orientation	-234.8±16.1	-232.4±17.1	-230.5±16.9
Mild LTLs/LLs (n=8)			
PMC-Cobb	31.3±6.6	36.9±9.7	36.9±9.7
PMC-orientation	-222.2±10.9	-219.6±13.4	-218.8±14.2
Moderate LTLs/LLs (n=12)			
PMC-Cobb	42.7±7.4	47.4±6.0	48.0±6.4
PMC-orientation	-236.9±12.2	-234.0±14.0	-231.2±13.6
Severe LTLs/LLs (n=3)			
PMC-Cobb	53.6±4.3	55.3±1.8	56.2±2.3
PMC-orientation	-260.8±3.5	-256.1±2.5	-253.9±1.0

Mild: prone corona-Cobb <25°; Moderate: 25°≤ prone coronal-Cobb ≤40°; Severe: prone coronal-Cobb >40°

As shown in Table 3.4, high inter-method ICC values were found between PMC-Cobb of CM and two CT Cobb methods in all the analysed groups (0.84–0.97). The 95% CI was relatively wide in most RTs and LTLs/LLs sub-groups while very narrow in both the overall RTs and LTLs/LLs groups. High inter-method ICC values were also observed between PMC-orientation of the CM and two CT Cobb methods in all the analysed groups (0.85–0.97). Similarly, the 95% CI was narrower in the two overall RTs and LTLS/LLs groups than in their subgroups, especially the mild LTLs/LLs group.

Table 3.4 ICC assessment for PMC taken from the three methods

PMC parameter	CM *vs.* constrained Cobb method	CM *vs.* unconstrained Cobb method
	ICC (95%CI)	ICC (95%CI)
Overall RTs (n=27)		
PMC-Cobb	0.968 (0.930-0.986)	0.968 (0.926-0.986)
PMC-orientation	0.909 (0.801-0.959)	0.905 (0.789-0.957)
Moderate RTs (n=10)		
PMC-Cobb	0.841 (0.361-0.961)	0.842 (0.362-0.961)
PMC-orientation	0.952 (0.807-0.988)	0.960 (0.838-0.990)
Severe RTs (n=17)		
PMC-Cobb	0.963 (0.898-0.987)	0.961 (0.887-0.986)
PMC-orientation	0.882 (0.674-0.957)	0.884 (0.668-0.959)
Overall LTLs/LLs (n=23)		
PMC-Cobb	0.948 (0.877-0.978)	0.933 (0.843-0.972)
PMC-orientation	0.958 (0.901-0.982)	0.952 (0.887-0.980)
Mild LTLs/LLs (n=8)		
PMC-Cobb	0.893 (0.465-0.979)	0.893 (0.466-0.979)
PMC-orientation	0.865 (0.326-0.973)	0.857 (0.284-0.971)
Moderate LTLs/LLs (n=12)		
PMC-Cobb	0.912 (0.674-0.976)	0.835 (0.386-0.956)
PMC-orientation	0.962 (0.858-0.990)	0.967 (0.876-0.991)

Mild: prone corona-Cobb <25°; Moderate: 25°≤ prone coronal-Cobb ≤40°; Severe: prone coronal-Cobb >40°

According to the Bland-Altman method assessment, almost all the PMC (PMC-Cobb; PMC-orientation) measurements were distributed around the central lines in all the analysed groups (Figure 3.9 & 3.10). MD of PMC-Cobb acquired from the CM and two CT Cobb methods were 2.4°–3.1° in all the analysed RTs groups, and 4.7°–5.8° in all the analysed LTLs/LLs groups. For the PMC-orientation, inter-method MD varied from 1.2° to 5.4° and 2.5° to 5.6° for all the analysed RTs and LTLS/LLs groups, respectively.

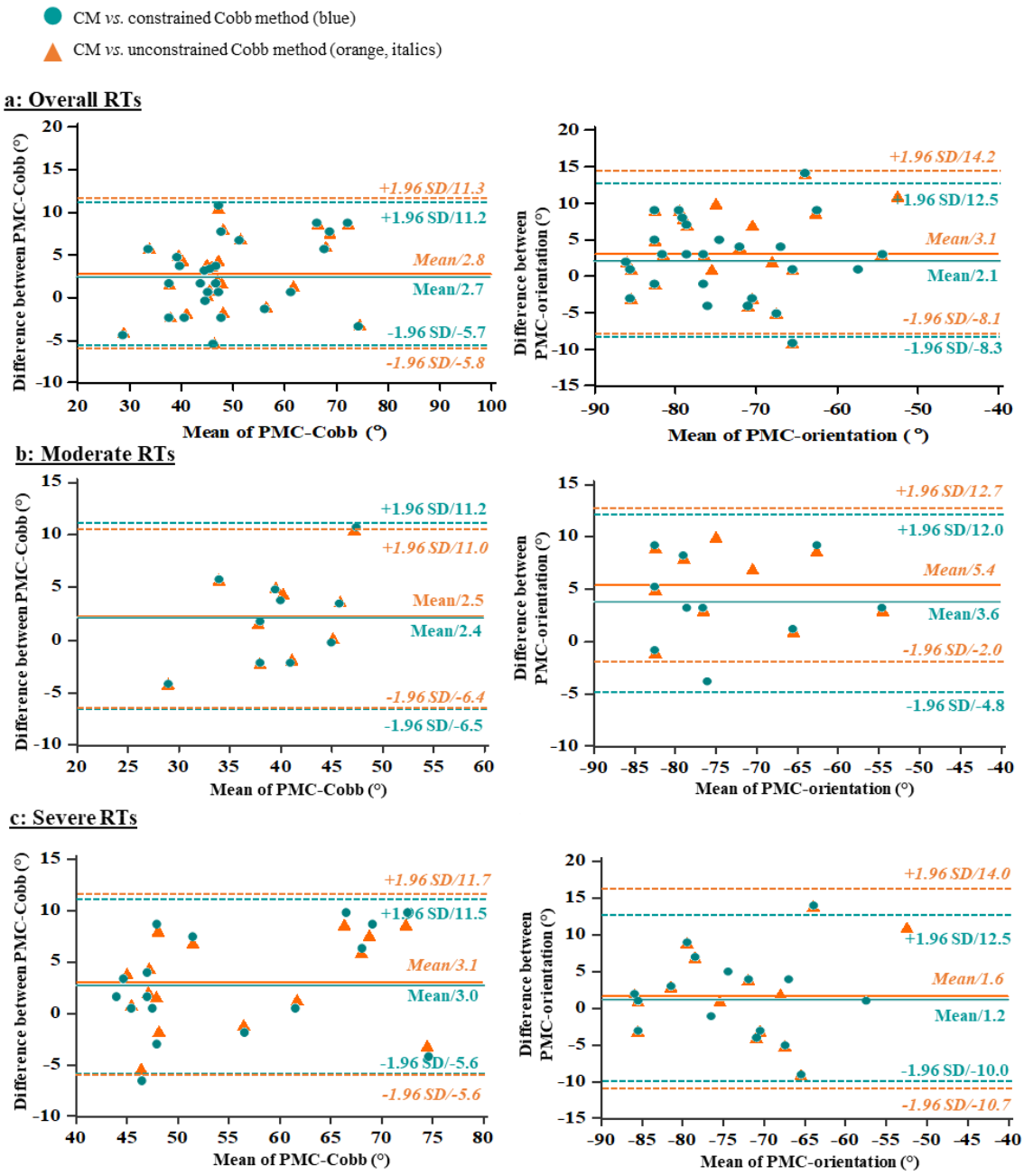

Figure 3.9 Bland-Altman assessment of PMC obtained using the CM and CT constrained and unconstrained Cobb methods for all the analysed RTs groups (mean = (constrained/unconstrained Cobb method + CM) / 2; difference = constrained/unconstrained Cobb method - CM)

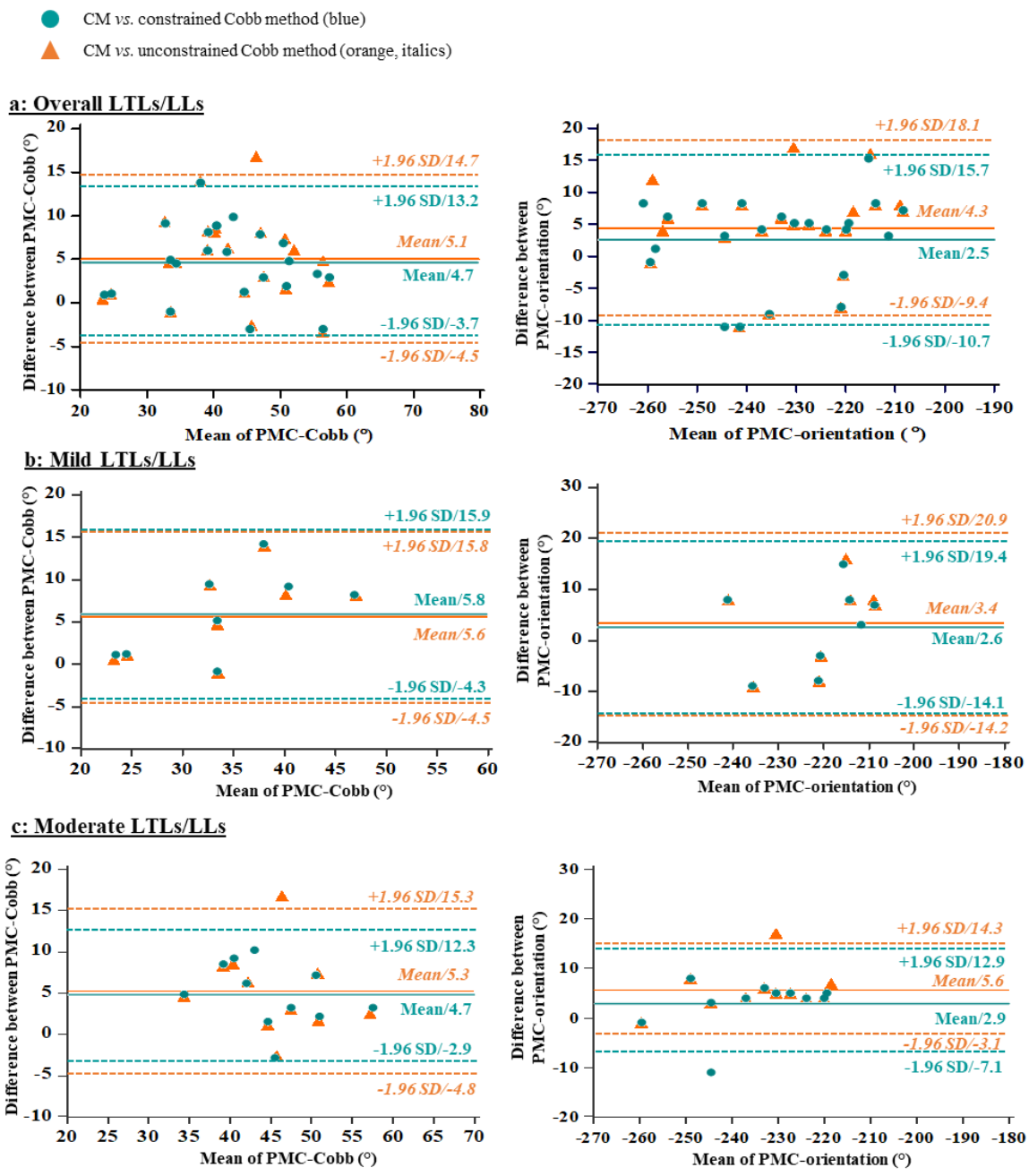

Figure 3.10 Bland-Altman assessment of PMC taken from the CM and CT constrained and unconstrained Cobb methods for all the analysed LTLs/LLs groups (mean = (constrained/unconstrained Cobb method + CM) / 2; difference = constrained/unconstrained Cobb method - CM)

Figures 3.11 & 3.12 showed a good to excellent correlation was observed between PMC-Cobb of the CM and two CT Cobb methods in the overall RTs and LTLs/LLs groups (r=0.88–0.94) as well as in their sub-groups (r=0.72–0.93). Moreover, PMC-orientation of the CM was strongly correlated to that of two CT Cobb methods in the overall RTs and LTLs/LLs groups (r=0.83–0.92) and their sub-groups (r=0.78–0.94).

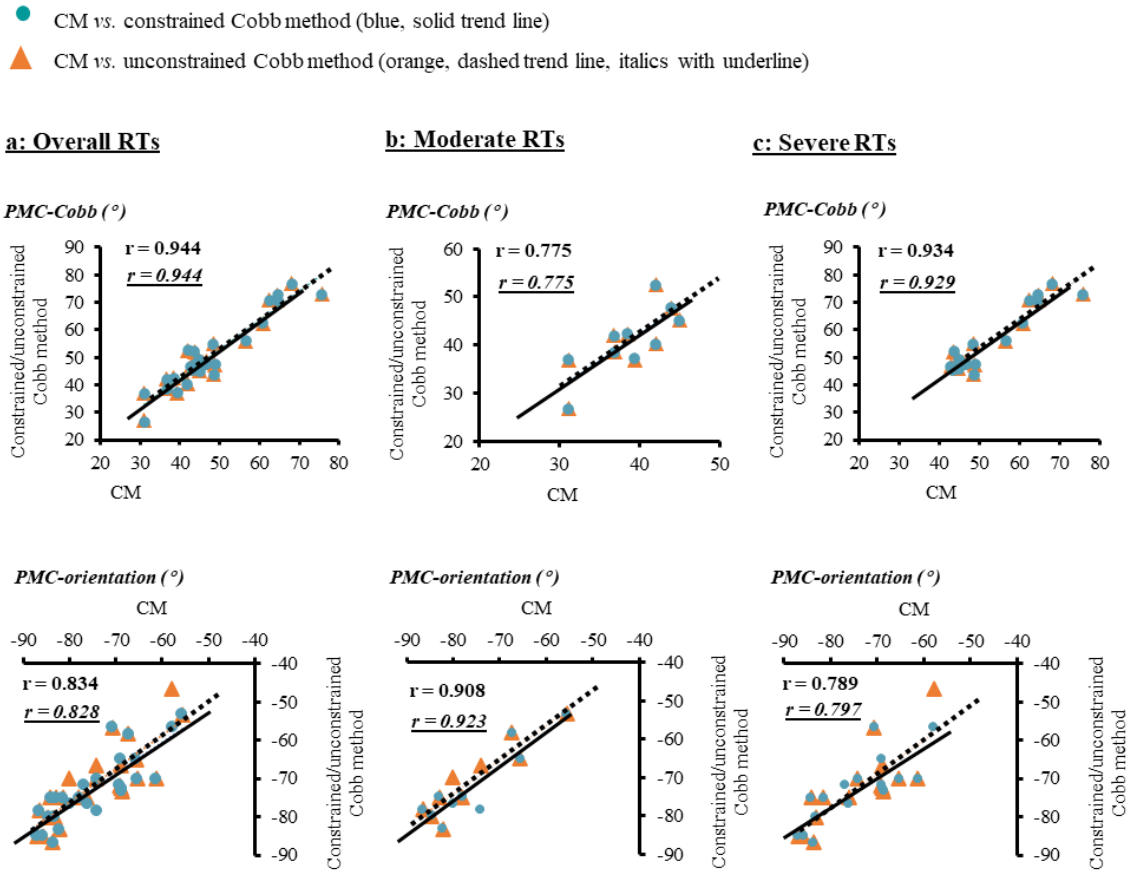

Figure 3.11 Correlation of PMC acquired using the CM and constrained and unconstrained Cobb methods for all the analysed RTs groups (no mild RTs for analysis)

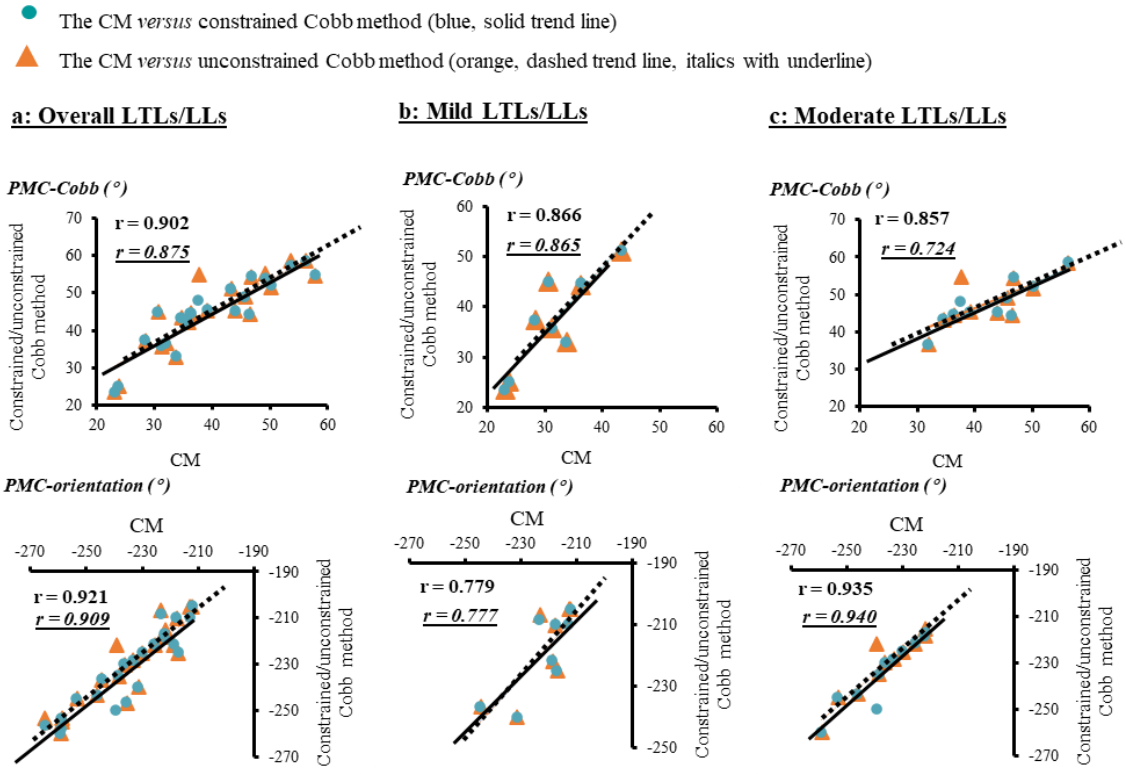

Figure 3.12 Correlation of PMC acquired from the CM and constrained and unconstrained Cobb methods for all the analysed LTLs/LLs groups (no mild RTs for analysis)

According to the linear regression analysis (Table 3.5), good to very good linear correlation was observed between PMC (PMC-Cobb; PMC-orientation) of CM and two CT Cobb methods, with (R^2=0.89; R^2=0.69) and (R^2=0.77; R^2=0.83) in the overall RTs and LTLs/LLs group, respectively. Relevant linear regression equations could be used to transfer the PMC (x) of the CM to the corresponding PMC (y) of the CT constrained/ unconstrained Cobb method.

Table 3.5 Linear regression analyses for PMC of the three methods

PMC parameter	CM (x) to constrained Cobb method (y)		CM (x) to unconstrained Cobb method (y)	
	Linear regression equation (°)	Coefficient of determination (R^2)	Linear regression equation (°)	Coefficient of determination (R^2)
Overall RTs (n=27)				
PMC-Cobb	y = 1.054x + 0.226	0.891	y = 1.053x + 0.330	0.891
PMC-orientation	y = 0.814x – 11.804	0.695	y = 0.877x – 6.168	0.686
Overall LTLs/LLs (n=23)				
PMC-Cobb	y = 0.858x + 10.389	0.814	y = 0.863x + 10.561	0.766
PMC-orientation	y = 0.981x – 2.070	0.848	y = 0.954x – 6.473	0.827

3.3.4 Time Consumption

According to feedback from the two raters, it generally took about 5 and 8 minutes on average to identify the 8 points manually and complete the PMC calculation in excel for each case, respectively, with the use of CM, and spent around 20 minutes to measure the PMC with use of the constrained or unconstrained Cobb method.

3.4 Discussion

This study developed a CM for PMC estimation merely based on the coronal and sagittal images of the spine and verified the results with CT constrained and unconstrained Cobb methods. The main findings were: (1) the mean trends of PMC-Cobb and PMC-orientation obtained from the CM, and CT constrained and unconstrained Cobb methods were generally similar in all the analysed groups; (2) high intra- and inter-rater reliability was observed for the PMC of CM in all the analysed groups; (3) good agreement was found between the PMC of CM and two CT Cobb methods in all the analysed groups; (4) good to excellent correlation was seen between the PMC of the CM and two CT Cobb methods in all the analysed groups.

The mean trends of the Cobb angle in each rotated pane acquired using the three methods were generally similar in all the analysed groups. In most groups, the mean trend of CM was closer to that of the CT constrained Cobb method than to that of the CT unconstrained Cobb method. This may be due to the scoliotic spine's complex regional and local deformities, which probably increases the variation between the Cobb angles in different rotated planes when using the CT unconstrained Cobb method. Besides, the CT unconstrained Cobb method generally provided a greater mean Cobb angle than either the CM or CT constrained Cobb method (Figure 3.8 & Table 3.3). The reason may be related to the selection of end-vertebrae used for the Cobb angle measure. This is because the former's end-vertebrae were most tilted [33] while the two latter's end-vertebrae selected from the coronal plane [23,32] may be or may not be most tilted in that plane (different from the coronal plane), where Cobb angle is measured. Moreover, the mean trends of the three methods were closer to each other in all the analysed RTs groups than in most of the analysed LTLs/LLs groups. This may be due to the increased variation caused by the decreased visibility of certain lumbar vertebrae blocked by the ilia in some rotated planes. Besides, thoracolumbar curves involved in the LTLs/LLs groups cover both the thoracic and lumbar segments, which may also increase the variation. Additionally, the rotated planes presenting the maximum mean Cobb angles in the RTs groups tended to be closer to the coronal plane than those in most LTLs/LLs groups. This phenomenon may be attributed to the rotation of thoracic curve towards the coronal plane more seriously than the (thoraco)lumbar curve segment (most primary curves selected in this study were thoracic curves).

PMC-Cobb of the CM showed high intra-rater reliability in all the analysed RTs and LTLs/LLs groups (intra-ICC=0.90–0.98), of which the strength was similar to that of ultrasound (intra-ICC=0.97) [27]. High inter-rater reliability of PMC-Cobb was observed in all the analysed groups (inter-ICC=0.74–0.91) except the mild LTLs/LLs group (inter-ICC=0.68). The strength of reliability of PMC-Cobb was similar to that of coronal-Cobb, which was also reported earlier [248,249]. Relatively small sample size and/or decreased visibility of some lumbar vertebra may be the reason for the inferior inter-rater reliability of the mild LTLs/LLs group, which may be deserved further investigation. No significant

intra- & inter-rater difference was found (p>0.05). Regarding to PMC-orientation, similar strength of intra- & inter-rater reliability was found in all the analysed groups (intra-ICC=0.87–0.98; inter-ICC=0.87–0.93) except the mild LTLs/LLs group (inter-ICC=0.51). The inferior inter-rater reliability of mild LTLs/LLs group may be related to the relatively small sample size and decreased visibility of certain lumbar vertebrae. A significant inter-rater difference of PMC-orientation was seen in most analysed RTs and LTLs/LLs groups (p<0.05). Reduced accuracy of 8 points identification in the sagittal plane caused by decreased visibility of vertebral endplates may be the reason causing this significant inter-rater difference. Future studies may deserve to further investigate this observation. Nevertheless, high intra- & inter-ICC values demonstrated the high reliability of CM in PMC estimation.

Although the CM tended to slightly underestimate the PMC-Cobb and overestimate the PMC-orientation in absolute value as compared to the two CT Cobb methods, high inter-method ICC values were found between their PMC (PMC-Cobb; PMC-orientation) in all the analysed groups (≥0.84; ≥0.85). The 95% CI was narrow in the overall RTs and LTLs/LLs groups while relatively wider in their subgroups. This may be due to the smaller sample size in these subgroups, and future studies with more cases recruited to these subgroups are suggested. Moreover, the Bland-Altman method assessment showed that all the PMC obtained from the CM and CT methods were almost distributed around the center lines. The inter-method MD of PMC-Cobb was within 3.1° and 5.8° in all the analysed RTs and LTLs/LLs groups, respectively. The inter-method MD was within and close to the clinically accepted threshold (5.0°) [250]. For the PMC-orientation, the inter-method MD was equal to or smaller than 5.4° and 5.6° for RTs and LTLs/LLs groups, respectively. This inter-method MD may be associated with the accuracy of CM (accuracy=1°) and CT constrained and unconstrained Cobb methods (accuracy=5°). This was because the CM calculated the Cobb angle in each rotated plane with an orientation interval of 1º while the two CT Cobb methods measured the Cobb angle in each rotated plane with an orientation interval of 5°. These results suggested a very good agreement between the PMC of CM and two CT Cobb methods. Also, the PMC of the CM and two CT methods showed very good to excellent correlation in the overall RTs and LTLs/LLs groups (r≥0.88; r≥0.83), and good

to excellent correlation in their subgroups (r≥0.72; r≥0.78). The linear regression equations could transfer the PMC of the CM to that of the CT constrained/unconstrained Cobb method for the RTs and LTLs/LLs.

Since the CM was merely based on the coronal and sagittal images, it may be possible to acquire PMC from the coronal and sagittal radiographs (e.g., bi-planar EOS images) without needing 3D reconstruction. After this study, CM has been converted into separate software, named PMC calculator, as shown in Figure 3.13. A preliminary study was conducted among 5 raters (2 with more than 3-year scoliotic image measurement experience and 3 with half-year scoliotic image measurement experience) and the results showed high intra- and inter-reliability of the PMC acquired from this software for patients with AIS based on EOS images (n=10; intra- & inter-ICC=0.95–0.99 & 0.91–0.97). According to the records of time consumption, the 2 raters experienced raters spent 3 minutes on each case and the other 3 raters spent 6.2-10.0 minutes on each case. With future effort, it believes that the CM may potentially serve as a valuable tool for the 3D assessment of AIS in the clinic.

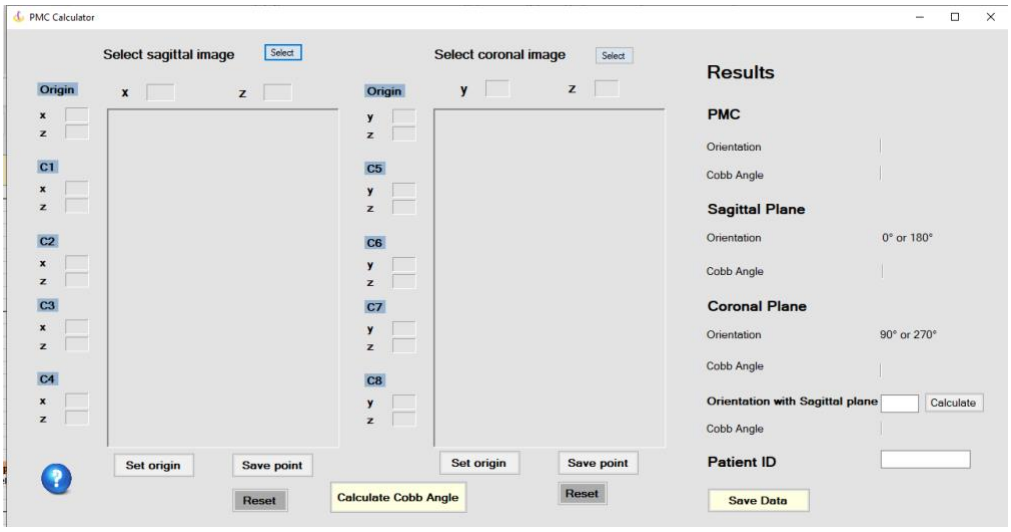

Figure 3.13 Interface of PMC calculator

Additionally, PMC has been applied for 3D assessment [33,57,176] and classification [173,183] of scoliosis as well as correction evaluation of surgical [164,178] and orthotic

[155,179] treatments. Since PMC provides information for both the maximum/"actual" magnitude of a curve (PMC-Cobb) and the degree of the curve rotated towards the coronal plane (PMC-orientation), it may be superior to other clinical indices (e.g., coronal-Cobb) in describing the 3D features of spinal deformities. Labelle, Aubin (170) pointed out that a curve type classified by the Lenke system could be further split into different sub-types based on the PMC. Different curve sub-types may need different surgical/orthotic strategies, which should be considered when making clinical decisions.

Two primary limitations to this study should be noted. The results presented in this study were based on a population with pre-operative CT images, a relatively large age range (10–24 years), and a curve range in the prone position (16°–71°). This study provided evidence supporting the reliability and validity of CM in PMC estimation for thoracic curves and (thoraco)lumbar curves. However, it was worthwhile to recruit more eligible subjects to strengthen the evidence of CM usage for subjects with mild, moderate, and severe AIS. Another limitation is the inherent measurement errors of the CM. The CM estimated the PMC by calculating the Cobb angle in different vertical planes with an interval of rotation at 1°, indicating that the Cobb angle in some vertical planes was not calculated. It may consider decreasing the interval value of rotation between vertical planes if necessary.

3.5 Conclusions

This study proposed a computational method for estimating the plane of maximum curvature based on the coronal and sagittal images and validated its results with CT. The study results revealed the reliability and validity of the computational method in the estimation of the plane of maximum curvature for patients with thoracic curves and (thoraco)lumbar curves. This method has been converted into separate software, which would make it a useful tool for the three-dimensional assessment of AIS. Further studies were in progress to apply the pane of maximum curvature to enhance orthotic management of adolescent idiopathic scoliosis.

CHAPTER 4 ESTIMATION OF PLANE OF MAXIMUM CURVATURE FOR PATIENTS WITH ADOLESCENT IDIOPATHIC SCOLIOSIS VIA COMPUTED TOMOGRAPHY

4.1 Introduction

Computed tomography (CT) is recognized as a standard modality for three-dimensional (3D) assessment of adolescent idiopathic scoliosis (AIS) in clinical practice. It allows the coronal and transverse assessment of deformity with the same dataset [114]. It has been used to evaluate the lateral curvature with a small error of measurement (<2.7°) [114] and the vertebral axial rotation (AVR) with high reliability (intra-class correlation coefficient=0.95) [115,251]. CT has also been applied for the asymmetry evaluation of vertebral bodies and pedicles [29,30] and assessing the anterior-posterior length of the spinal column [31]. However, the feasibility of using CT to assess the plane of maximum curvature (PMC) was not studied. As defined previously, PMC parameters included the maximum Cobb measured in PMC (PMC-Cobb) and orientation of PMC (PMC-orientation, the angle between the PMC and sagittal plane).

Due to the complicated deformities of AIS [23,29-31], as mentioned in Chapter 3, it is unknown if the end-vertebrae most tilted in the coronal plane would always be most tilted in any other vertical planes different from the coronal plane. This indicates that the PMC identified based on the upper and lower end-vertebrae selected from the coronal plane at the beginning may be or may not be the “actual” PMC (presenting the “actual” maximum spinal curvature). The method with end vertebrae constrained to the end vertebral selected from the coronal plane was constrained Cobb method. It was to measure the Cobb angle in any other vertical planes (different from the coronal plane) but with upper and lower end-vertebrae constrained to the upper and lower end-vertebrae selected from the coronal plane at the beginning of the measurement [23,33] (Figure 1.2). Conversely, the method with end vertebrae unconstrained to those selected from the coronal plane was the unconstrained Cobb method. It measured the Cobb angle in any vertical planes with upper and lower end-

vertebrae selected from the plane, where the Cobb angle is measured [32] (Figure 1.2). Although the possible discrepancies between PMC measurements of these two Cobb methods were reported in some studies [32,33], their comparability has not been explicitly investigated.

This study aimed (1) to investigate the feasibility of using CT to obtain the PMC; (2) to evaluate the comparability of PMC acquired from CT constrained and unconstrained Cobb methods.

4.2 Methodology

4.2.1 Study flowchart

This study was retrospective, as described in Chapter 3: 3.2.1

4.2.2 Subjects

Inclusion criteria were detailed in chapter 3: 3.2.2

4.2.3 PMC Estimation using Constrained and Unconstrained Cobb Methods

PMC was identified via rotating a vertical plane, where the spine was projected onto, 90° along a vertical axis with an increment of 5°and measuring the Cobb angle in each rotated plane separately using constrained and unconstrained Cobb methods. The detailed procedures of PMC estimation were described in Chapter 3: 3.2.5.

4.2.4 Data Collection

As described in Chapter 3: 3.2.6, one rater (D) with more than 3-year experience in spinal curvature measurements was arranged for the PMC assessment. She measured the Cobb angle in each rotated plane three times separately using constrained and unconstrained

Cobb methods with one-week interval each time to reduce possible recalling bias. PMC (PMC-Cobb; PMC-orientation) was determined each time (Figure 3.7).

4.2.5 Statistical Analysis

Statistical analysis was performed in IBM SPSS (version 21, IBM, Chicago, IL, USA) with a significance level (*p*) set at 0.05. The normality of each studied parameter was analysed using the Shapiro-Wilks test. Intra-rater reliability of PMC measured using CT (both constrained and unconstrained Cobb methods) was analysed using the intra-class correlation coefficient (ICC [2, 1] using a two-way random model and absolute agreement) with a confidence interval of 95% (95% CI). The strength of reliability was evaluated via the criteria proposed by Currier (246): very reliable (ICC: 0.8–1.0), moderately reliable (ICC: 0.60–0.79), and questionably reliable (ICC: <0.60). The intra-rater variation was analysed through one-way repeated ANOVA, mean absolute difference (MAD), standard deviation (SD), and standard error of measurement (SEM). Also, Paired t-test (2-tailed), MAD, SD, SEM, Pearson correlation coefficient (r), and the Bland-Altman method were used for investigating the comparability of PMC (PMC-Cobb; PMC-orientation) acquired using constrained and unconstrained Cobb methods. The strength of correlation was assessed using the criteria: very good to excellent (r: 0.75–1.00), moderate to good (r: 0.50–0.75), and poor correlation (r: 0.25–0.50) [247].

4.3 Results

As shown in Table 4.1, 50 curves were selected for this study, including 27 right thoracic curves (RTs) and 23 left (thoraco)lumbar curves (LTLs/LLs). For the RTs, there were 10 moderate and 17 severe. For the LTLs/LLs, there were 8 mild, 12 moderate, and 3 severe curves. Since too small sample size involved in the severe LTLs/LLs group, statistical analysis was not performed.

Table 4.1 Characteristics of analysed curves

Curve type	Curves, n	Prone coronal-Cobb mean ± standard deviation (°)	Prone coronal-Cobb range (°)
RTs			
Overall RTs	27	46.1 ± 12.4	26.2 - 71.1
Moderate RTs	10	35.1 ± 3.2	26.3 - 39.6
Severe RTs	17	52.9 ± 9.7	40.5 - 71.1
LTLs/LLs			
Overall LTLs/LLs	23	30.6 ± 11.1	16.4 - 54.2
Mild LTLs/LLs	8	18.6 ± 4.1	16.4 - 2 3.6
Moderate LTLs/LLs	12	31.8 ± 6.7	26.0 - 39.5

Mild: prone corona-Cobb <25°; Moderate: 25°≤ prone coronal-Cobb ≤40°; Severe: prone coronal-Cobb >40°

4.3.1 Mean Trend of Cobb Angle in Each Rotated Plane

As shown in Figure 3.8, the mean trend of the Cobb angle in each rotated plane measured using the CT constrained and unconstrained Cobb methods were similar in all the RTs and LTLs/LLs groups. They separate from the sagittal plane, get closer, and finally almost overlap when approaching the coronal plane. Compared with the constrained Cobb method, the unconstrained Cobb method tended to provide a greater mean Cobb angle in rotated planes, especially in those near the sagittal plane, in all the groups. Moreover, the mean trends of the two methods seemed to be more centralized in RTs groups than in LTLs/LLs groups except for the mild LTLs/LLs group. The maximum mean Cobb angle was generally found in a rotated plane approaching the coronal plane in almost the RTs and LTLs/LLs groups except for the mild LTLs/LLs group. The rotated plane presenting the maximum mean Cobb angle was closer to the coronal plane in RTs groups than in LTLs/LLs groups.

4.3.2 Reliability of PMC Obtained Using CT (constrained & unconstrained Cobb methods)

The CT constrained and unconstrained Cobb methods demonstrated similar intra-rater reliability in PMC (PMC-Cobb; PMC-orientation) estimation in all the groups, with intra-ICC value of (0.94–0.99; 0.85–0.97) and (0.95–0.99; 0.82–0.96), respectively (Table 4.2). The strength of PMC-Cobb was similar to that of coronal-Cobb (0.90–0.99) (Table 3.1). No significant intra-rater difference was found between PMC (PMC-Cobb; PMC-orientation) of either constrained or unconstrained Cobb method in all the groups (p>0.05). Moreover, the PMC (PMC-Cobb; PMC-orientation) of two Cobb methods presented similar intra-rater variation in the two overall RTs and LTLs/LLs groups, with (MAD, SD, SEM) of (=0.3°, ≤1.8°, ≤0.4°) and (≤1.5°, ≤7.3°, ≤1.5°) for the PMC-Cobb and PMC-orientation, respectively.

Table 4.2 Intra-rater reliability of PMC acquired using the two Cobb methods

PMC parameter	Constrained Cobb method		Unconstrained Cobb method	
	ICC (95% CI)	Sign. *p*	ICC (95% CI)	Sign. *p*
Overall RTs (n=27)				
PMC-Cobb	0.993 (0.987-0.997)	0.339	0.992 (0.985-0.996)	0.310
PMC-orientation	0.848 (0.733-0.923)	0.243	0.912 (0.840-0.956)	0.118
Moderate RTs (n=10)				
PMC-Cobb	0.980 (0.943-0.995)	0.121	0.970 (0.916-0.992)	0.381
PMC-orientation	0.866 (0.665-0.961)	0.077	0.819 (0.569-0.946)	0.052
Severe RTs (n=17)				
PMC-Cobb	0.992 (0.981-0.997)	0.143	0.991 (0.980-0.997)	0.153
PMC-orientation	0.857 (0.707-0.943)	0.337	0.947 (0.883-0.979)	0.337
Overall LTLs/LLs (n=23)				
PMC-Cobb	0.982 (0.964-0.992)	0.762	0.979 (0.958-0.990)	0.841
PMC-orientation	0.966 (0.933-0.984)	0.517	0.949 (0.901-0.976)	0.254
Mild LTLs/LLs (n=8)				
PMC-Cobb	0.990 (0.966-0.998)	0.817	0.986 (0.955-0.997)	0.859
PMC-orientation	0.936 (0.804-0.986)	0.765	0.916 (0.751-0.981)	0.775
Moderate LTLs/LLs (n=12)				
PMC-Cobb	0.940 (0.844-0.982)	0.626	0.949 (0.866-0.985)	0.559
PMC-orientation	0.969 (0.918-0.991)	0.437	0.960 (0.895-0.988)	0.735

Mild: prone corona-Cobb <25°; Moderate: 25°≤ prone coronal-Cobb ≤40°; Severe: prone coronal-Cobb >40°

4.3.3 Comparability of PMC Obtained Using Constrained and Unconstrained Cobb Methods

As shown in Figure 4.1, a very good to excellent correlation was found between the PMC (PMC-Cobb; PMC-orientation) of constrained and unconstrained Cobb methods in all the RTs and LTLs/LLs groups (r=0.94–1.00; r=0.81–0.99). According to Bland-Altman method assessment (Figure 4.2), all the PMC (PMC-Cobb; PMC-orientation) obtained from the two methods distributed around the center lines except some outliers in all the RTs and LTLs/LLs groups. Moreover, no significant inter-method difference was observed in all the RTs and LTLs/LLs groups (p>0.05). The (MAD, SD, SEM) between the PMC of two Cobb methods was (≤0.6°, ≤3.0°, ≤0.6°) for PMC-Cobb and (≤0.6°, ≤2.2°, ≤0.4°) for PMC-orientation in the two overall RTs and LTLs/LLs groups.

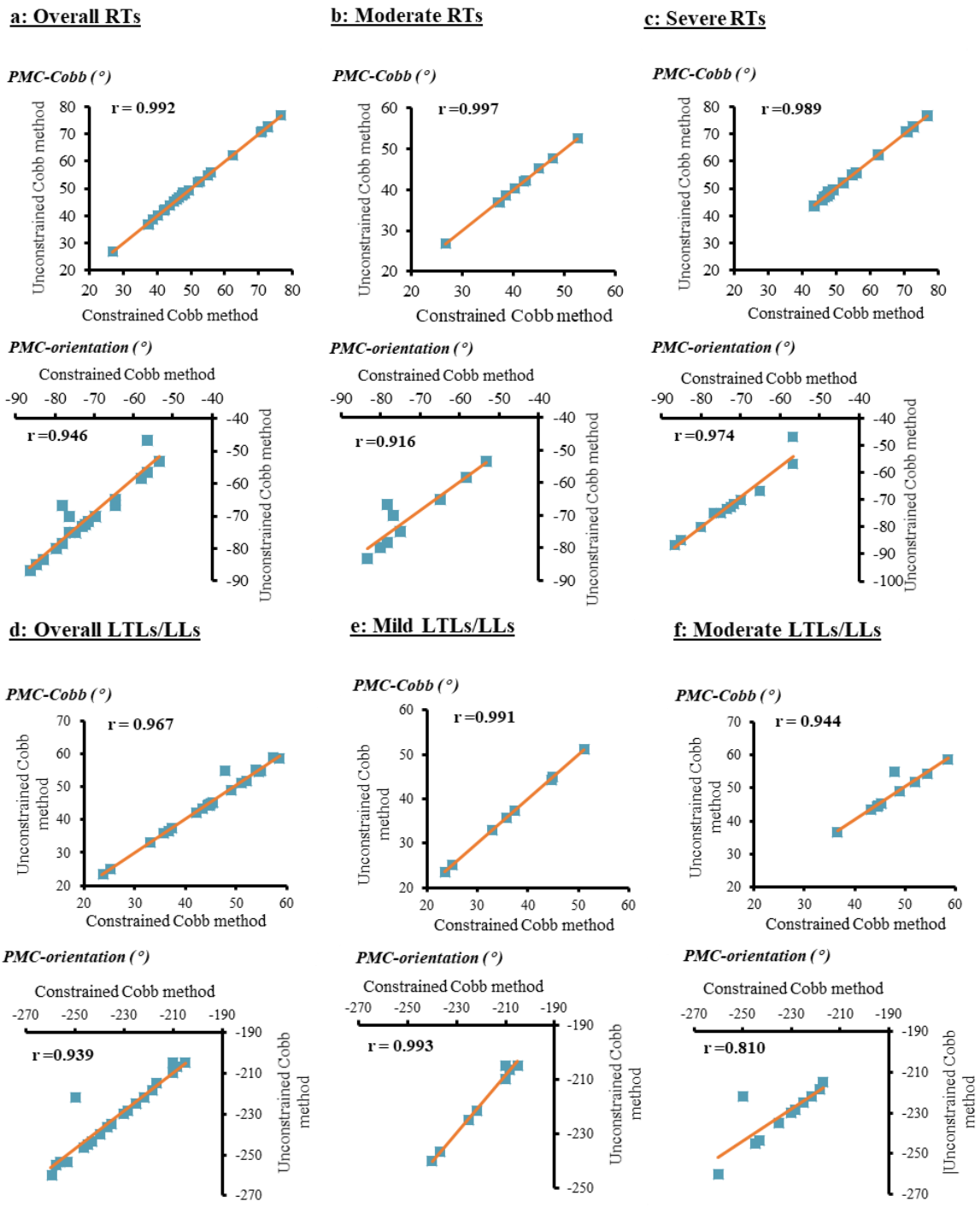

Figure 4.1 Correlation of PMC acquired using the CT constrained and unconstrained Cobb methods for all the analysed RTs and LTLS/LLs groups

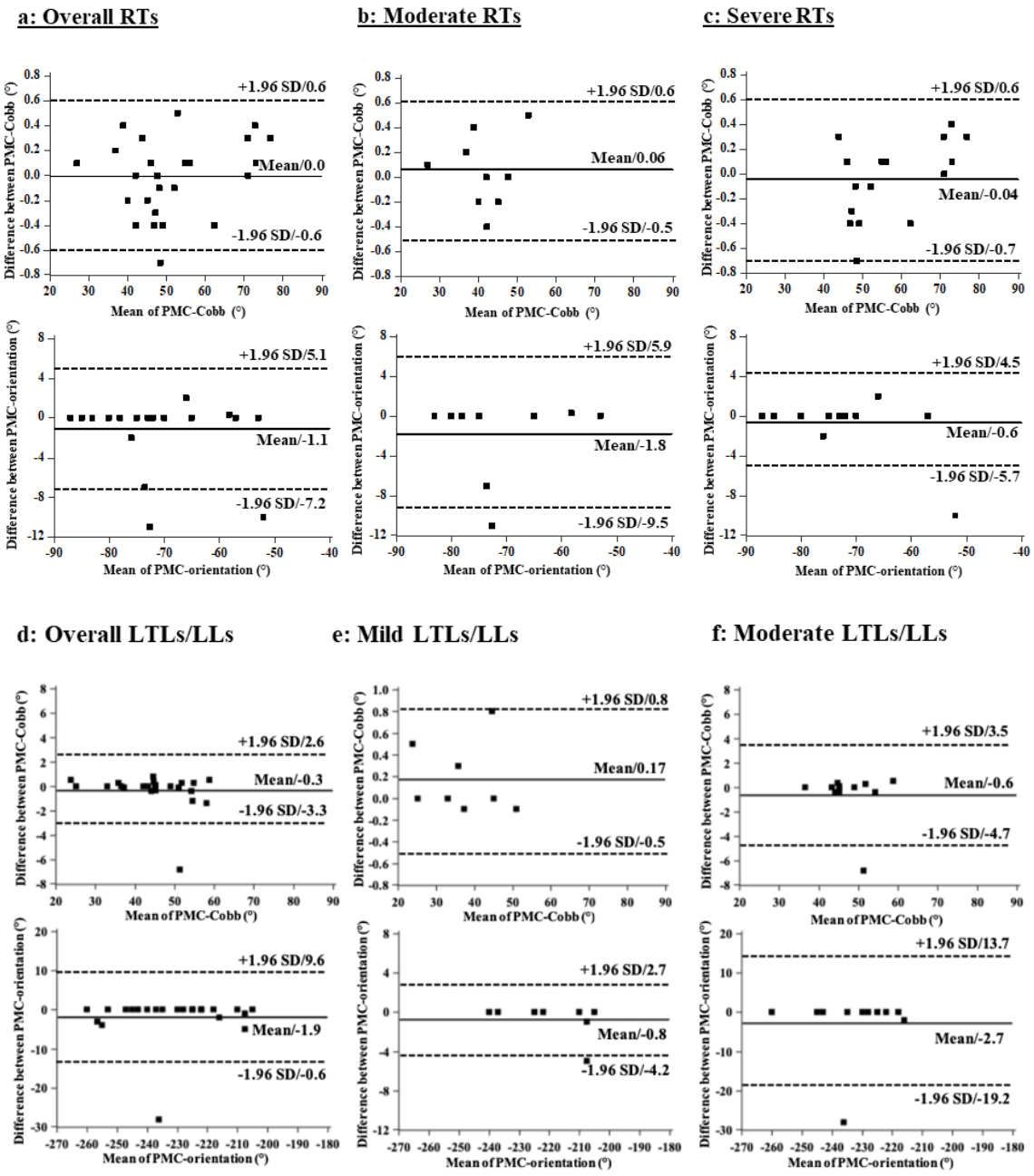

Figure 4.2 Bland-Altman assessment of PMC taken from the CT constrained and unconstrained Cobb methods for all the analysed RTs and LTLs/LLs groups (mean = (constrained Cobb method + unconstrained Cobb method) / 2; difference = constrained Cobb method - unconstrained Cobb method).

4.4 Discussion

This study was the first to use CT to obtain PMC and evaluate the comparability of PMC of constrained and unconstrained Cobb methods. The main findings of this study included: (1) high intra-rater reliability was found for the PMC (PMC-Cobb; PMC-orientation) acquired from either constrained or unconstrained Cobb method; (2) good to excellent correlation and good agreement were observed between the PMC of the two Cobb methods.

Similar mean trends of Cobb angle in each rotated plane were achieved from the two Cobb methods in all the analysed RTs and LTLs/LLs groups. The mean Cobb angle generally increased to a maximum value and then decreased to the coronal-Cobb when rotating the vertical plane, where the scoliotic spine was projected onto, from the sagittal plane towards the coronal plane. Similar mean trends were also reported by Trac, Zheng (27). The mean trends were more centralized in the RTs groups than in the LTLs/LLs groups (except the mild LTLs/LLs group). This may be due to the decreased visibility of lumbar vertebrae. Besides, the thoracolumbar curves involved in the LTLs/LLs groups cover both the thoracic and lumbar segments, which may increase the variation among the Cobb angles measured using constrained and unconstrained Cobb methods in a rotated plane. Additionally, the maximum mean Cobb angle was found in a rotated plane near to the coronal plane in most groups, and that rotated plane was closer to the coronal plane in RTs groups than in LTLs/LLs groups (except the mild LTLs/LLs group). As mentioned in Chapter 3, this indicated that the curve segments seemed to be rotated/twisted towards the coronal plane more seriously in RTs groups than in LTLs/LLs groups in this study. This may be because most of the thoracic curves were primary curves and more severer than the (thoraco)lumbar curves included in LTLs/LLs groups.

The PMC-Cobb of both the two Cobb methods showed high intra-rater reliability (intra-ICC≥0.94), which was similar to that of ultrasound (intra-ICC=0.97) [27]. The strength of intra-rater reliability was also similar to that of coronal-Cobb reported in Chapter 3 and previous studies [248,249]. The intra-rater variation of PMC-Cobb was small (MAD=0.3°) and much smaller than the clinically accepted error (5°) [200]. Regarding the PMC-

orientation, high intra-rater reliability (intra-ICC≥0.82) and small intra-rater variation (MAD≤1.5 °) were also observed for both the two Cobb methods. These results demonstrated the feasibility of using the CT to acquire the PMC for patients scheduled to undergo CT scans during the assessment/treatment of AIS. It may also be useful to validate other techniques (e.g., ultrasound) in PMC assessment in a recumbent position before clinical application.

The PMC of the two Cobb methods were well correlated in all analysed groups (r≥0.94; r≥0.81). The Bland-Altman method assessment showed all the PMC distributed around the center lines. Furthermore, the inter-method MAD was within 0.6° for the PMC-Cobb and PMC-orientation. The inter-method MAD of PMC-Cobb was much less than the clinically accepted bias of two successive curvature measurements (5°) [200]. These results suggested the comparability of constrained and unconstrained Cobb methods in PMC estimation.

As mentioned in Chapter 3, PMC has been applied to 3D assessment [33,176] and classification [21,170] of AIS. Two distinct curves with the same coronal-Cobb could present remarkably disparate maximum spinal curvature and sagittal thoracic kyphosis [21]. In turn, a curve type classified by the Lenke system may be further split into different curve sub-types based on the PMC [170]. This should be considered when making clinical decisions (e.g., surgical/orthotic strategies) since different sub-types may need different treatment strategies. PMC has been also used for evaluating 3D correction of surgical [164,178,180,181] and orthotic [179,212] treatments. Studies showed that surgical treatment provided significant correction for PMC and coronal-Cobb [164,178,180,181]. In the studies of orthotic treatment [164,181], a significant correction was found in the PMC-Cobb and coronal-Cobb. However, the PMC-orientation was significantly increased [179,212], indicating that the curve segment was rotated towards the coronal plane even more, instead of being pushed towards the sagittal plane as expected, after wearing the orthosis. Normally, natural thoracic and lumbar curves exist in the sagittal plane, which is known as sagittal thoracic kyphosis and lumbar lordosis. In a scoliotic spine, the sagittal

thoracic/lumbar curvature could be abnormally rotated towards the coronal plane (surely may combine with increase/decrease in curvature magnitude), generating coronal curvature. If pursuing correction/decrease of coronal-Cobb alone while ignoring the rotation of curve towards the coronal plane (PMC-Cobb), the natural thoracic/lumbar curvature may be reduced (e.g., causing thoracic hypo-kyphosis). In this case, coronal-Cobb alone may not be enough to describe the correction of surgical/orthotic treatment and to reflect the "actual" situation of spinal deformity.

Several limitations to this study should be noted. The spinal curves were relatively severe as the selected CT images were obtained from pre-operative patients. Moreover, the inter-rater reliability of CT in PMC estimation was not investigated in this study, and it was unclear whether the proposed method was reliable for severe curves (>71°) or other spinal deformities. Additionally, the CT was limited to the application in patients suffering from severe AIS or prescribed with surgical treatment because of radiation exposure.

4.5 Conclusions

The PMC taken from CT was found reliable, and hence it could be used as a supplement to the coronal-Cobb in managing AIS. With technological advancement, the radiation dose of CT can be reduced to a safer level for a broader range of patients.

CHAPTER 5 RELATIONSHIP BETWEEN PLANE OF MAXIMUM CURVATURE IN PRONE AND STANDING POSITIONS IN PATIENTS WITH ADOLESCENT IDIOPATHIC SCOLIOSIS

5.1 Introduction

Because of the gravitational effect, spinal deformity could be notably disparate between prone/supine and standing positions. To give an insight into the inter-position relationships of relevant parameters may benefit the understanding of three-dimensional (3D) features of the scoliotic spine.

Spinal deformity can be spontaneously corrected when changing from standing to a recumbent (e.g. supine) position [34,35,37-44,252]. Coronal-Cobb was observed to be significantly smaller in a recumbent position (supine) than in standing in most previous studies (mean difference (MD)= -8.0°– -11°, p<0.05) [34,35,37-40,42]. Apart from some studies, supine and standing coronal-Cobbs were also well correlated (correlation coefficient (r) =0.90–0.97 / intraclass correlation coefficient (ICC) ≥0.96, p<0.05) [37,40,41,43]. The sagittal Cobb (sagittal thoracic kyphosis/lumbar lordosis) significantly increased as well when switching from a recumbent (e.g. supine) to standing position (MD= -4.5° and -6.0°, p<0.05) [39], while strong supine-standing correlation was found (ICC=0.87 and 0.85, p<0.05) [41]. Moreover, vertebral axial rotation (VAR) was significantly smaller in supine position than in standing position (MD=-2.7°– -6.0°, p<0.05) [42,44,252] while there existed strong inter-position correlation (ICC=0.87 / r=0.81, p<0.05) [41,43].

There existed dependent relationships between the coronal-Cobb/sagittal-Cobb (thoracic kyphosis/lumbar lordosis)/VAR and plane of maximum curvature (PMC-Cobb & PMC-orientation) [33,54,56]. PMC-Cobb was generally greater than coronal-Cobb [27,54,56] and sagittal-Cobb [33]. Although no significant correlation existed between the former and two latter [56], PMC-orientation was correlated to the ratio of coronal-Cobb to sagittal-Cobb (coronal thoracic/lumbar curvature to sagittal thoracic kyphosis/lumbar lordosis)

[33,174]. Moreover, PMC-orientation was well correlated with (r=0.64–0.71) but 1.27–1.7 times coronal-Cobb in degree [33,57]. Also, PMC-orientation was greater than the maximum VAR, rotation of rib hump and back surface orderly (r=0.56, 0.48. 0.69) [57], and linked to the geometric torsion [202].

The prone/supine-standing correlation/difference among coronal-Cobb, sagittal-Cobb, and VAR, and between PMC (PMC-Cobb; PMC-orientation) and coronal-/sagittal-Cobb has been investigated. However, the prone/supine-standing correlation/difference was not studied as a comprehensive descriptor. To analyse its prone/supine-standing correlation/difference may deepen the understanding of 3D features of the scoliotic spine, which may further facilitate the management of AIS. Thus, this study aimed to investigate the correlation/difference of PMC acquired in standing and prone positions.

5.2 Methodology

5.2.1 Study flowchart

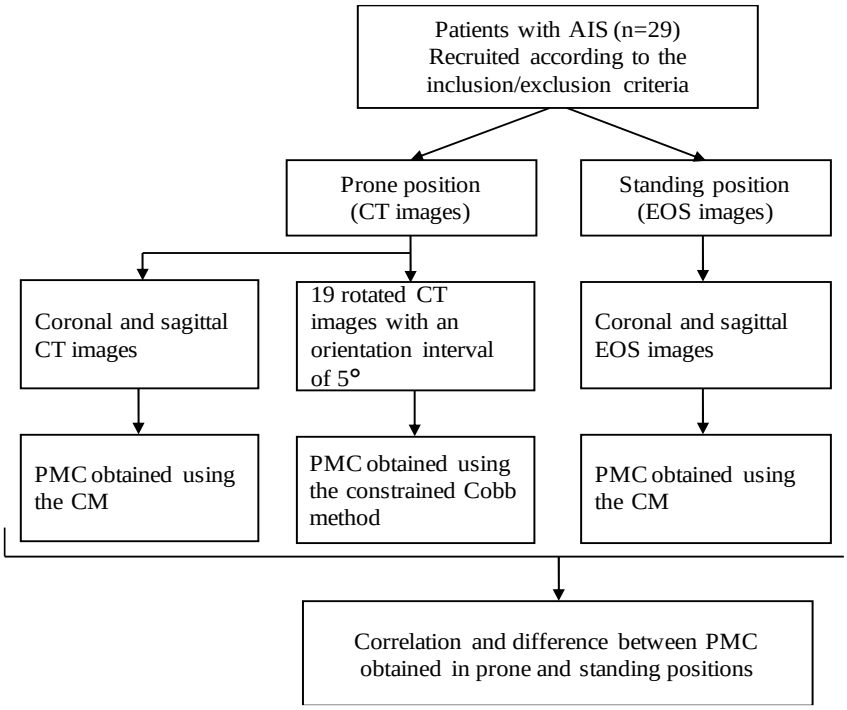

Figure 5.1 Study flowchart

5.2.2 Subjects

Inclusion criteria were detailed in Chapter 3: 3.2.2.

5.2.3 PMC in Prone Position

PMC (PMC-Cobb; PMC-orientation) was acquired using the constrained Cobb method according to the same sets of 19 rotated CT images of the spine with an orientation interval of 5°, as detailed in Chapter 3: 3.2.5. Besides, PMC was also obtained using the CM according to the coronal and sagittal CT images of the spine. The procedures were described in Chapter 3: 3.2.3 & 3.2.4.

5.2.4 PMC in Standing Position

PMC (PMC-Cobb; PMC-orientation) was obtained using the CM developed and verified in Chapter 3 according to the spinal coronal and sagittal EOS images. The procedures were described in Chapter 3: 3.2.3 & 3.2.4.

5.2.5 Other Parameters Different from PMC in Prone and Standing Positions

Based on the coronal and sagittal CT and EOS images of the whole spine, the following parameters were also measured in both the prone and standing positions: coronal-Cobb, sagittal thoracic kyphosis (superior endplate of T4 – inferior endplate of T12), and lumbar lordosis (superior endplate of L1 – superior endplate of S1)

5.2.6 Data Collection

As described in Chapter 3: 3.3, two well-trained raters (H & D) estimated the PMC (PMC-Cobb; PMC-orientation) three times using the CM based on the same sets of the coronal and sagittal CT images of the spine with one-week interval each time to reduce possible recalling bias. With the same protocol, rater D measured the PMC three times separately using the constrained Cobb method based on the same sets of rotated CT images (19 rotated

images with an orientation interval of 5°) and using the CM based on the same sets of coronal and sagittal EOS images. Additionally, coronal-Cobb, sagittal thoracic kyphosis, and lumbar lordosis were also measured three times from the coronal/sagittal CT and EOS images by rater D with the same protocol.

5.2.7 Statistical Analysis

Statistical analysis was performed in SPSS (version 21, IBM, Chicago, IL, USA) with a significant level (Sign. *p*) set at 0.05. The normality of each studied parameter was analysed using the Shapiro-Wilks test. Data were presented as mean ± standard deviation (SD). Prone-standing correlations of parameters were evaluated using the Pearson correlation coefficient (r). The strength of correlation was analysed using criteria: very good to excellent (r: 0.75–1.00), moderate to good (r: 0.50–0.75) and poor correlation (r: 0.25–0.50) [247]. The prone-standing difference of parameters was investigated using MD and paired t-test. The intra-rater reliability of standing PMC of the CM was also investigated using ICC [2, 1] (using a two-way random model and absolute agreement) with a confidence interval of 95% (95% CI). The strength of reliability was analysed using criteria [246]: very reliable (ICC: 0.8–1.0), moderately reliable (ICC: 0.60–0.79), and questionably reliable (ICC: <0.60).

5.3 Results

Forty-eight curves were selected for this study, including 26 right thoracic curves (RTs), and 22 left (thoraco)lumbar curves (LTLs/LLs). The RTs contained 10 moderate (25°–40°) and 16 severe (>40°) curves, and the LTLs/LLs included 8 mild (<25°), 12 moderate (25°–40°) and 2 severe (>40°) curves.

5.3.1 Mean Trend of Cobb Angle in Each Rotated Plane

The mean trends of Cobb angle in each rotated plane obtained from the CM and constrained Cobb method in prone position were remarkably different from those acquired using the CM in standing position in all the analysed groups (Figure 5.2). The mean Cobb angle in

each rotated plane was notably smaller in prone than in standing position; however, the rotated planes presenting the maximum mean Cobb angles in two positions showed similar orientations.

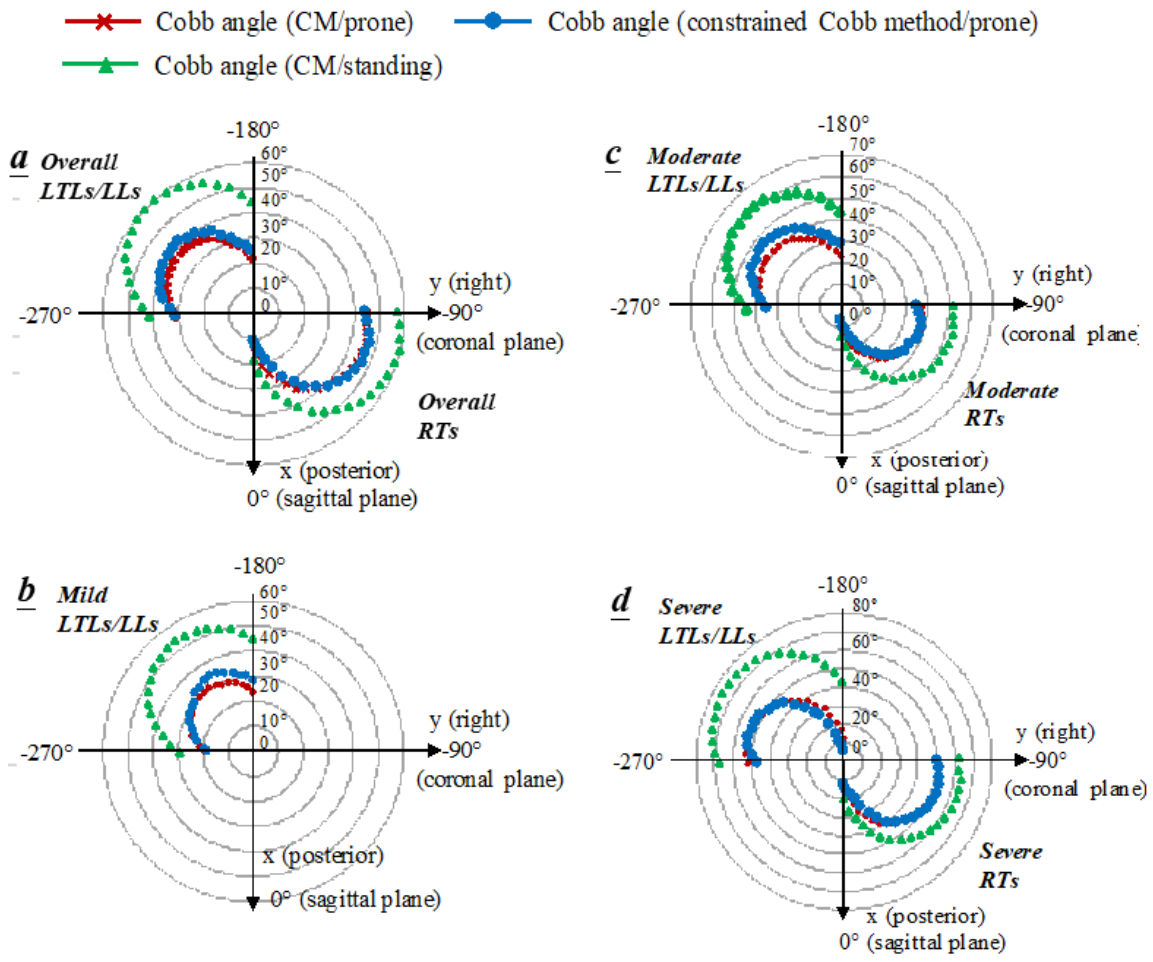

Figure 5.2 Mean Cobb angles acquired using the CM and constrained Cobb method in prone position and using the CM in standing position in each rotated plane for the all the analysed RTs (a, c & d) and LTLs/LLs (a, b, c & d) groups. In the radars, x-axis pointing posteriorly represents the sagittal plane (orientation=0°), and y-axis pointing to the right represents the coronal plane (orientation=-90°). The distance from the origin to each circle represents the magnitude of Cobb angle

5.3.2 Prone-Standing Correlation Assessment

As showed in Figure 5.3, good to excellent prone-standing correlation was found for PMC (PMC-Cobb; PMC-orientation) of CM (r=0.79–0.89; r=0.69–0.78) in all the analysed RTs groups. By contrast, the correlation varied relatively widely between PMC of constrained Cobb method in prone position and CM in standing position among different RTs groups, with (r=0.85; r=0.58), (r=0.42; r=0.69) and (r=0.90; r=0.47) for the overall, moderate and severe RTs group separately.

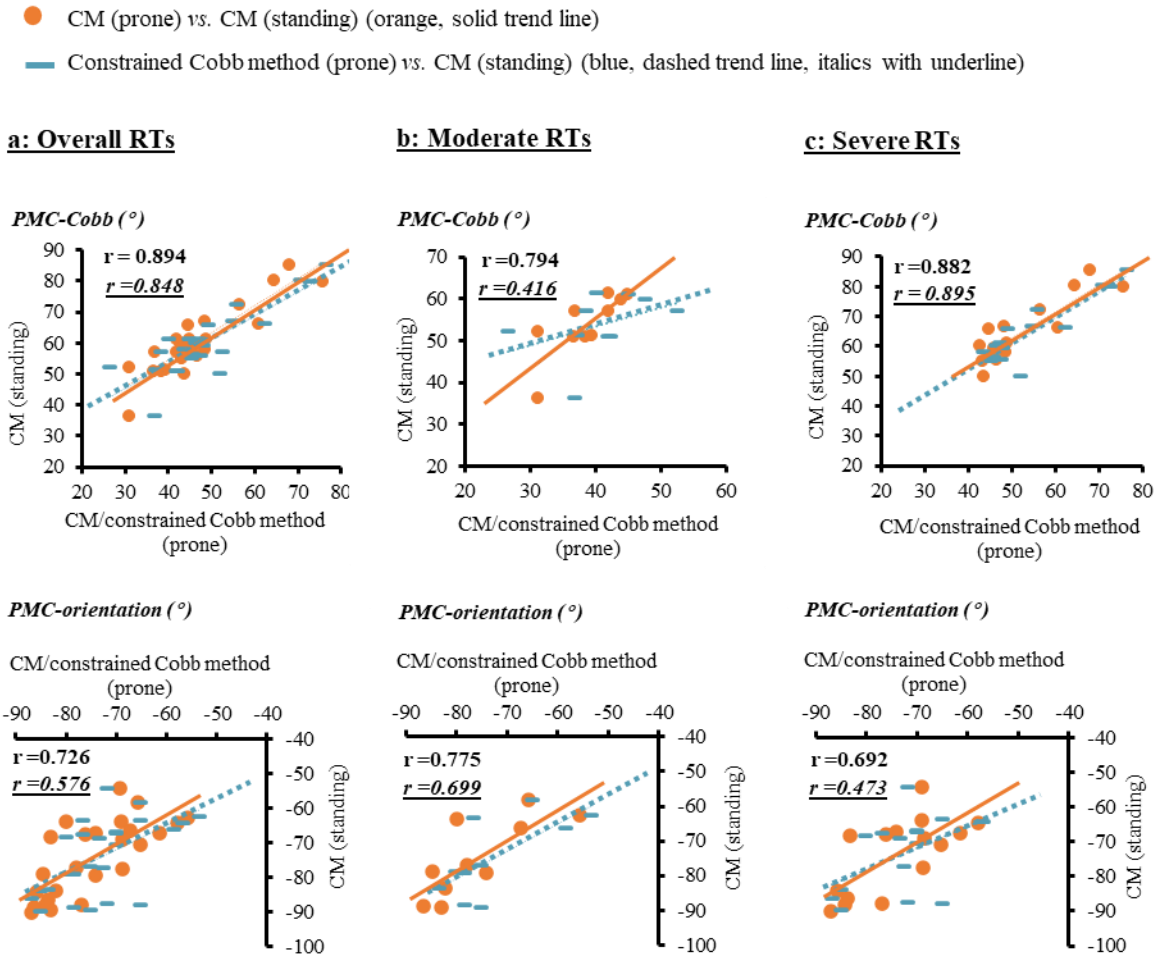

Figure 5.3 Correlation of PMC acquired from the CM and constrained method in prone position and from the CM in standing position for different RTs groups (no mild RTs for analysis here)

For the LTLs/LLs (Figure 5.4), good to excellent correlation was observed between PMC (PMC-Cobb; PMC-orientation) acquired from CM in standing position and either CM or constrained Cobb method in the prone position for the overall and mild LTLs/LLs groups (r=0.69–0.89; r=0.83–0.91). The correlation in the moderate LTLs/LLs group was poor to moderate for PMC-Cobb (r=0.45–0.58) while good to very good for PMC-orientation (r=0.76–0.86).

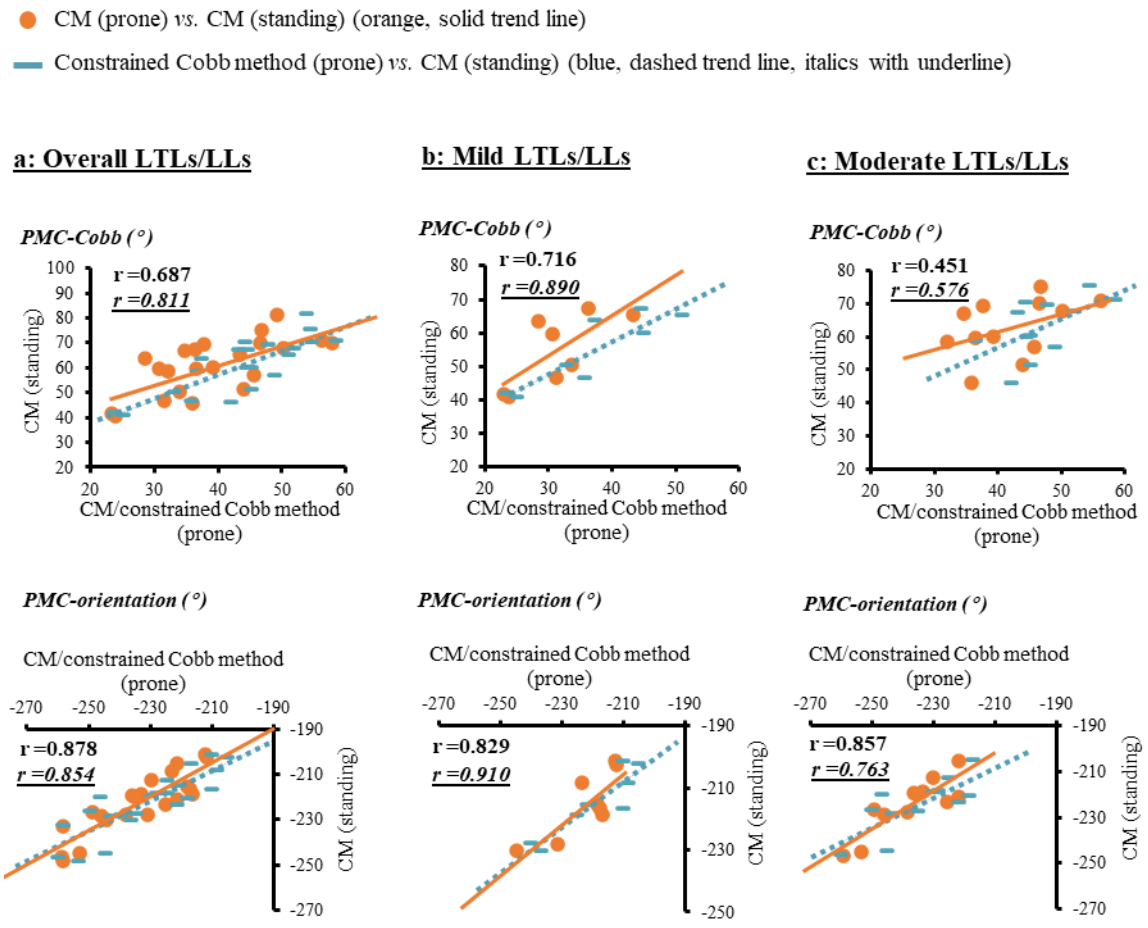

Figure 5.4 Correlation of PMCs obtained using the CM and constrained method in prone position and from the CM in standing position for different LTLs/LLs groups (3 severe LTLs/LLs were not analysed here)

Very good to excellent correlation existed between coronal-Cobbs measured in prone and standing positions in the RTs groups (Figure 5.5), and good to excellent correlation existed

in the LTLs/LLs groups. Moreover, the sagittal thoracic kyphosis in the standing and prone positions was well correlated (r=0.82). A moderate correlation existed between the sagittal lumbar lordosis measured in standing and prone positions (r=0.57).

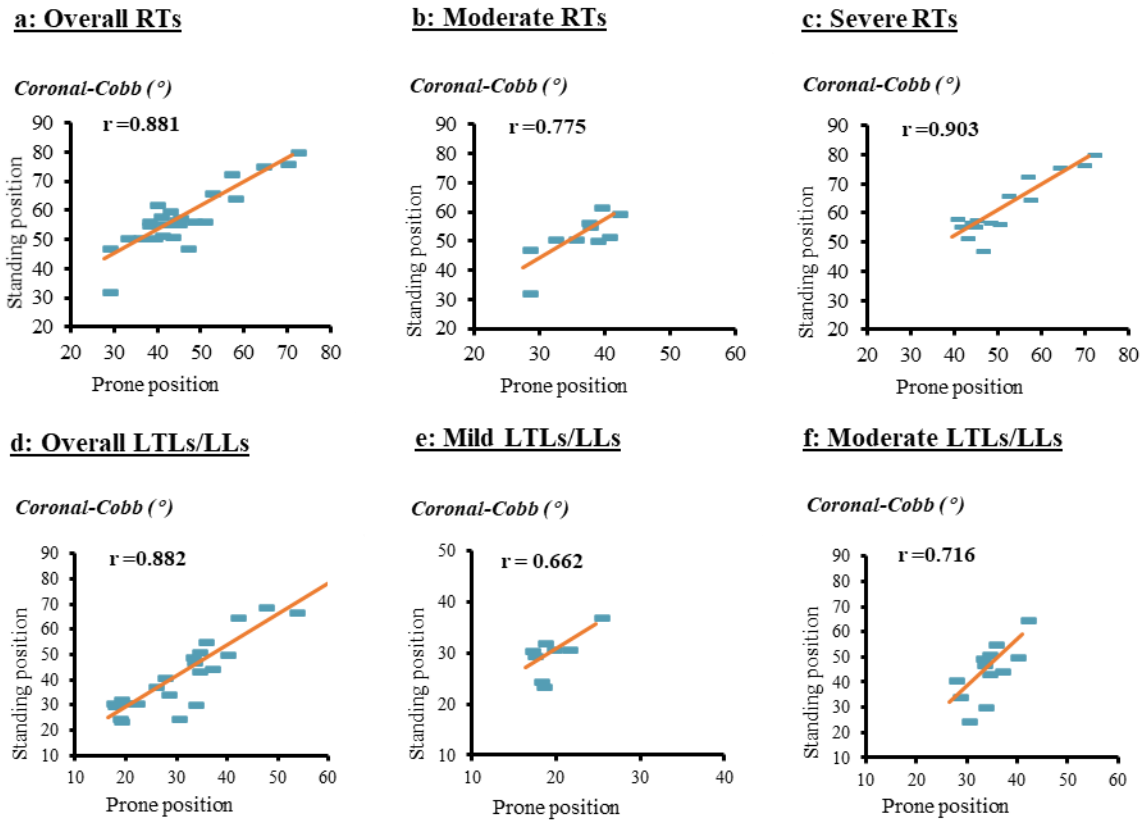

Figure 5.5 Correlation of coronal-Cobb measured in prone and standing positions for different analysed RTs and LTLs/LLs groups

5.3.3 Prone-Standing Difference Assessment

Table 5.1 presented the mean ± SD of PMC (PMC-Cobb; PMC-orientation) obtained from CM and constrained Cobb method in prone position and CM in standing position for different RTs and LTLs/LLs groups. For the RTs (Table 5.1 & Figure 5.6), PMC-Cobb was significantly smaller in the prone position than in the standing position in all the analysed RTs groups (MD= -10.1°– -15.1°, p<0.001) while no significant inter-position difference existed for the PMC-orientation in almost all the analysed RTs groups (MD= -0.9°–2.5°, p>0.05). In comparison with RTs, the inter-position difference of PMC-Cobb

was more significant in all the LTLs/LLs groups (except for the severe LTLs/LLs group) (MD= -15.8– -23.1°, $p<0.001$). The inter-position difference of PMC-orientation was also significant in most of the analysed LTLs/LLs groups (MD= -7.1°– -13.0°, $p<0.05$).

Table 5.1 Comparison of PMC obtained using the CM and constrained Cobb method in the prone position and using the CM in the standing position

PMC parameter	Prone position		Standing position	CM (prone) *vs.* CM (standing)		Constrained Cobb method (prone) *vs.* CM (standing)	
	CM (Mean ± SD) (°)	Constrained Cobb method (Mean ± SD) (°)	CM (Mean ± SD) (°)	Mean difference ± SD (°)	Sign. *p*	Mean difference ± SD (°)	Sign. *p*
Overall RTs (n=27)							
PMC-Cobb	46.8 ± 10.9	49.1 ± 11.6	60.4 ± 10.7	-13.6 ± 5.0	< 0.001	-11.2 ± 6.2	< 0.001
PMC-orientation	-74.7 ± 9.4	-72.9 ± 8.8	-74.1 ± 10.9	-0.6 ± 7.6	0.703	1.2 ± 9.3	0.511
Moderate RTs (n=10)							
PMC-Cobb	38.6 ± 4.9	40.9 ± 7.0	53.7 ± 7.4	-15.1 ± 4.6	< 0.001	-12 ± 7.8	0.001
PMC-orientation	-75.7 ± 9.9	-72.3 ± 10.0	-74.8 ± 11.3	-0.9 ± 7.2	< 0.001	2.5 ± 8.3	0.373
Severe RTs (n=17)							
PMC-Cobb	52.2 ± 10.4	54.6 ± 10.9	64.8 ± 10.5	-12.6 ± 5.1	< 0.001	-10.1 ± 4.9	< 0.001
PMC-orientation	-74.1 ± 9.3	-73.3 ± 8.3	-73.7 ± 11.0	-0.4 ± 8.1	0.863	0.4 ± 10.2	0.871
Overall LTLs/LLs (n=22)							
PMC-Cobb	39.2 ± 9.6	44.0 ± 9.2	60.9 ± 11.0	-21.7 ± 8.3	< 0.001	-16.9 ± 6.4	< 0.001
PMC-orientation	-233.9 ± 15.4	-231.3 ± 16.7	-222.6 ± 13.1	-11.3 ± 7.4	< 0.001	-8.7 ± 8.8	< 0.001
Mild LTLs/LLs (n=8)							
PMC-Cobb	31.3 ± 6.6	36.9 ± 9.7	54.4 ± 10.8	-23.1 ± 2.7	< 0.001	-17.5 ± 4.9	< 0.001
PMC-orientation	-222.2 ± 10.9	-219.6 ± 13.4	-215.1 ± 10.8	-7.1 ± 6.3	0.016	-4.5 ± 5.8	0.065
Moderate LTLs/LLs (n=12)							
PMC-Cobb	42.1±7.3	47.0±5.9	62.7±8.7	-20.6±8.5	<0.001	-15.8 ± 7.2	< 0.001
PMC-orientation	-237.6±12.2	-235.0±13.8	-224.6±11.9	-13.0±6.5	<0.001	-10.4 ± 9.0	0.002
Severe LTLs/LLs (n=3)							
PMC-Cobb	53.5±6.1	54.3±0.6	75.7±8.0	-22.1±14.1	-	-21.3 ± 8.6	-
PMC-orientation	-258.8±0.1	-255.8±3.5	-240.5±11.1	-18.3±11.2	-	-15.3 ± 14.6	-

Mean difference = prone – standing

Note: paired t-test was not performed for severe LTLs/LLs group because of its small sample size

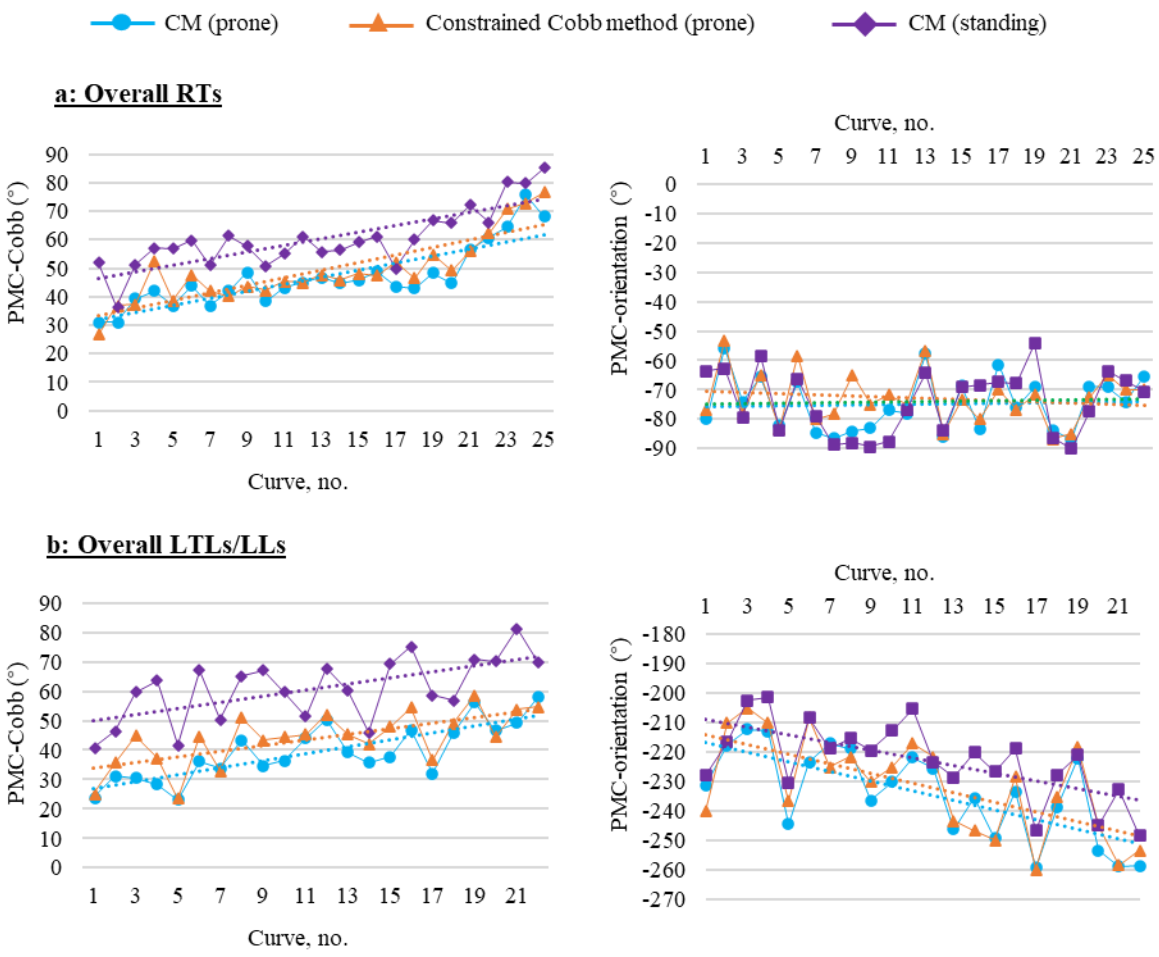

Figure 5.6 Comparison of PMC taken in prone and standing positions for the Overall RTs and LTLs/LLs groups

As shown in Table 5.2 & Figure 5.7, the coronal-Cobb was significantly smaller in the prone position than in the standing position for all the analysed RTs and LTLs/LLs groups (except for the severe LTLs/LLs group) (MD=-10.8°– -16.0°, $p \leq 0.001$). In the sagittal plane (Table 5.3 & Figure 5.7), both the thoracic kyphosis and lumbar lordosis were significantly smaller in the prone position than in the standing position ($p<0.05$). The inter-position difference of thoracic kyphosis was notably smaller than that of lumbar lordosis (MD: -3.4° *vs.* -10.9°).

Table 5.2 Comparison of coronal-Cobb in prone/supine and standing positions

Reference	**Curve type**	**Curves, n**	**Prone/supine coronal-Cobb (Mean ± SD) (°)**	**Standing coronal-Cobb (Mean ± SD) (°)**	**Prone/supine *vs.* standing**	
					Mean difference ± SD (°)	**Sign. *p***
Present study	RTs	25	44.0 ± 11.4	57.4 ± 10.5	-12.9 ± 5.4	< 0.001
Harmouche, Cheriet (253)	Primary Ts	14	35.4	46.0	-10.6	-
Vavruch and Tropp (40)	Primary Ts	82	50.2± 12.1*	61.5 ±12.4	11.3*	-
Brink, Colo (41)	Ts	62	53.9 ± 14.8 56.7 ± 13.5*	68.2 ± 15.4	-14.3 -11.5*	< 0.05
Present study	**LTLs/LLs**	**22**	**30.6 ± 11.1**	**41.1 ± 13.9**	**-11.8 ± 6.9**	**< 0.001**
Harmouche, Cheriet (253)	Ls	14	33.9	44.5	-10.6	-
Brink, Colo (41)	Ls	62	33.1 ± 15.0 35.2 ± 15.9*	44.3 ± 16.8	-11.2 -9.1*	< 0.05
Wessberg, Danielson (35)	Mixed	30	23.1*	30.8	-7.7*	-
Torell, Nachemson (34)	Mixed	280	-	10.0 ~ 70.0	-7.1 ~ -11.8*	-
Lee, Solomito (37)	Mixed	70	48.0 ± 14.0*	58.0 ± 14.0	-10.0*	-
Keenan, Izatt (38)	Mixed	52	40.5 ± 6.6*	51.9 ± 6.7	-11.4*	-
Shi, Mao (39)	Mixed	80	22.4 ± 14.3*	29.4 ± 13.7	-7.0*	-
Vavruch and Tropp (40)	Primary Ls	46	44.4*	55.1	-10.7*	-
Hasegawa, Okamoto (42)	Mixed	24	31.0*	39.5	-8.5*	-
Yang, Li (43)	Mixed	94	21.0 ± 12.0*	26.0 ± 12.0	5.0*	-
Yazici, Acaroglu (44)	Mixed	25	39.4*	55.7	-16.3*	-

Ts or Ls: thoracic curves or lumbar curves

Mixed: may involve both the thoracic and (thoraco)lumbar curves

Mean difference = prone/supine – standing

*: supine position

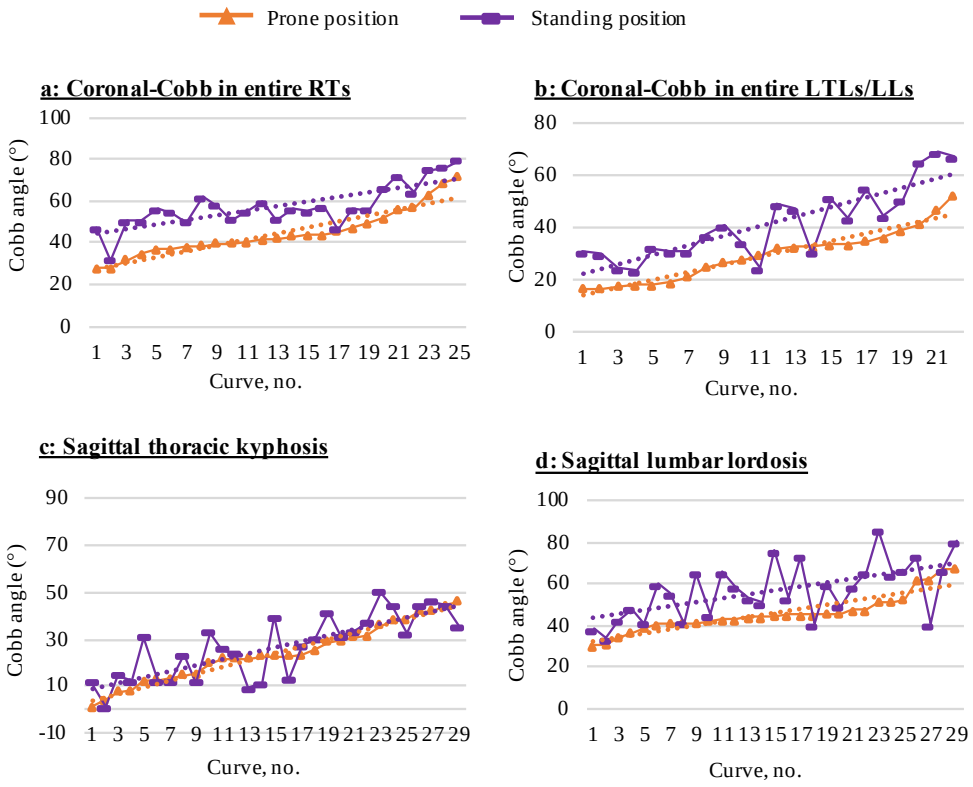

Figure 5.7 Comparison of coronal-Cobb, sagittal thoracic kyphosis, and lumbar lordosis measured in prone and standing positions

Table 5.3 Comparison of thoracic kyphosis and lumbar lordosis acquired in prone/supine and standing positions

Reference	Measure limits	Curves, n	Prone/supine Mean (± SD) (°)	Standing Mean (± SD) (°)	Prone/supine *vs.* standing	
					Mean difference (± SD) (°)	Sign. p
Sagittal thoracic kyphosis						
Present study	**T4-T12**	**29**	**24.0±12.5**	**26.8±13.7**	**-3.4±8.7**	**0.040**
Shi, Mao (39)	T5-T12	80	11.8±6.1*	16.3±9.1	-4.5*	-
Brink, Colo (41)	T4-T12	62	22.4 ± 11.6 17.3 ± 9.8*	25.8 ± 11.4	-3.4 -8.5*	<0.05
Hasegawa, Okamoto (42)	T4-T12	24	15.3*	17.8	-2.5*	-
Sagittal lumbar lordosis						
Present study	**L1-S1**	**29**	**45.9±9.2**	**56.9±13.6**	**-10.9±11.1**	**<0.001**
Shi, Mao (39)	T12-S1	80	39.5±10.5*	45.5±12.2	-6.0*	-
Brink, Colo (41)	L1-S1	62	45.4 ± 10.8 43.7 ± 12.4*	48.8 ± 12.0	-3.4 -5.1*	<0.05
Hasegawa, Okamoto (42)	L1-S1	24	21.8*	33.1	-11.3*	-

Mean difference = prone/supine – standing

*: supine position

5.4 Discussion

This study was the first to investigate the prone-standing relationship for PMC (PMC-Cobb; PMC-orientation). A prone-standing relationship was also analysed between coronal-Cobb, sagittal thoracic kyphosis, and lumbar lordosis. The main findings were: (1) for the RTs groups, good to excellent correlation was observed between PMC of CM in prone and standing positions, however, poor to excellent correlation was found between those of constrained Cobb method in prone position and CM in standing position; (2) regarding the LTLs/LLs groups, good to excellent correlation was seen between PMC of CM/constrained Cobb method in prone position and CM in standing position for the overall and mild groups (that in the moderate group varied widely); (3) PMC-Cobb was significantly smaller in prone position than in standing position, and the inter-position differences were smaller in the RTs groups than in the LTLs/LLs groups; (4) the inter-position difference of PMC-orientation was not significant in RTs groups while significant in LTLs/LLs groups; (5) the prone-standing correlation was good to excellent for coronal-Cobb and sagittal thoracic kyphosis while was moderate for sagittal lumbar lordosis; (6) coronal-Cobb, sagittal thoracic kyphosis and lumbar lordosis were significantly smaller in prone position than in standing position, and the inter-position difference of lumbar lordosis was notably greater than that of thoracic kyphosis.

Because of the gravitational effect, the mean trends of Cobb angle in each rotated plane in prone position were notably different from those in the standing position. The mean Cobb angle in each rotated plane was remarkably smaller in the prone position than in the standing position, while the rotated plane showing the maximum mean Cobb angle in two positions had a similar orientation. This indicated that the curve magnitude changed while the degree of the curve rotated towards the coronal plane tended to not change.

For the RTs groups, good to excellent correlation was observed between PMC (PMC-Cobb; PMC-orientation) of CM in prone and standing positions ($r \geq 0.79$; $r \geq 0.69$). By contrast, the correlation between PMC of constrained Cobb method in prone position and CM in standing position varied relatively widely. This may be due to there was a discrepancy between the accuracy of the constrained Cobb method and CM (constrained Cobb method: accuracy=5° in

PMC-orientation since the orientation interval of each rotated plane was 5°; CM: accuracy=1° since the orientation of each rotated plane was 1°). The discrepancy may increase the variation between the PMC acquired using these two methods. Additionally, because decreased visibility of thoracic vertebrae blocked by ribs could also increase the variation of PMC, which may further enlarge the discrepancy of PMC of the two methods in prone and standing positions. Regarding the LTLs/LLs, the correlation between PMC of CM/constrained Cobb method in prone position and CM in standing position was good to excellent in the overall and mild groups while poor to very good in the moderate group. The correlation in the moderate group varied relatively widely compared to the overall and mild groups. The possible reasons may be that its sample size was smaller than the overall group, and its curves were severer than those in the mild group (severer curves may increase the variation of PMC assessment). Smaller sample size and severer curves may negatively affect the correlation in the moderate LTLs/LLs group.

A good to excellent correlation existed between coronal-Cobb in prone and standing positions in the overall RTs and LTLs/LLs groups (r=0.88), which was similar but slightly inferior to that between supine and standing positions reported previously (r=0.90–0.97 / ICC≥0.96) [37,39-41,43]. The inter-position correlation was very good for sagittal thoracic kyphosis (r=0.82) while moderate for the sagittal lumbar lordosis (r=0.57). This may be because the lumbar region has a more flexible structure compared to that of the thoracic region.

Because of gravitational effect, the PMC-Cobb, coronal-Cobb and sagittal thoracic kyphosis and lumbar lordosis were significantly smaller in the prone position than in the standing position (except for the severe LTLs/LLs group) (MD=-10.1°– -23.1°, -10.8°– -16.0°, -3.4°, -10.9°; p<0.05). As shown in Table 5.2, similar recumbent (supine)-standing difference was reported earlier for coronal-Cobb (MD=-7.0°– -16.3°) [34-44], and for thoracic kyphosis [39,41,42] and lumbar lordosis [42]. By contrast, PMC-orientation was greater in the prone position than in the standing position in the LTLs/LLs groups (MD= -7.1°– -13.0°, p<0.05), while tended to do not change in RTs groups (p>0.05). This indicated that the rotation of the curve segment towards the coronal plane was not significantly affected by gravity. Additionally, the prone-standing differences tended to be greater in LTLS/LLs groups than in RTs groups (PMC-Cobb: -15.8°– -23.1° *vs.* -10.1°– -15.1°; PMC-orientation: -7.1°– -13.0° *vs.* -0.9°–2.5°;

coronal-Cobb: 10.8°–11.8° *vs.* 10.9°–16.0°). The prone-standing difference of lumbar lordosis was also notably greater than that of thoracic kyphosis (MD: 10.9° *vs.* 3.4°). Besides, the inter-position difference of lumbar lordosis between prone/supine and standing positions varied relatively widely compared to the thoracic kyphosis [39,41,42]. This may be due to the anatomical structure of the lumbar segment being more flexible than that of the thoracic segment. The lumbar segment allows lateral, forward/backward bending, and axial rotation, making it more changeable; by contrast, besides the inter-vertebral structures, the thoracic segment is also stabilized by ribs and soft tissue around ribs, which make the thoracic segment more stable.

A limitation of this study should be noted. the curves involved in this study were selected from subjects with AIS and prone coronal-Cobb of 16–71°, so it is unknown whether the prone-standing relationships found in this study would be changed in larger curves or other spinal deformities. Nevertheless, although standing position was an golden standard in assessing AIS, this study gave an insight into 3D characteristics of AIS in prone position because of a teenager may spend a third of his/her time in lying position. Besides, it provided information regarding the changes and correlations between 3D deformities of AIS in prone and standing positions.

5.5 Conclusions

A prone-standing correlation was observed for PMC and coronal-Cobb, sagittal thoracic kyphosis and lumbar lordosis in all the analysed RTs and LTLs/LLs groups. Moreover, these analysed parameters were significantly smaller in the prone position than in the standing position except PMC-orientation in RTs groups. Additionally, the prone-standing differences of the analysed parameters tended to be greater in LTLs/LLs groups than in RTs groups, which may be attributed to the segment's anatomical structure being more flexible than that of the thoracic segment. These findings may benefit the understanding of 3D features of AIS and should be considered when assessing AIS in a recumbent position. Future studies with more subjects are suggested to further investigate the inter-position relationship of relevant parameters, especially the PMC, for patients with different curve magnitudes.

CHAPTER 6 BIOMECHANICAL INVESTIGATION OF TLSO: SHAPE OF PRESSURE PAD, DIRECTION OF CORRECTING FORCE, AND CONCEPT OF PLANE OF MAXIMUM CURVATURE – A PILOT STUDY

6.1 Introduction

Orthotic intervention is the most popular conservative treatment for adolescent idiopathic scoliosis (AIS) with a primary curve of 20°–40° in the growth stage, alone or in association with exercises. Except for some negative reports [46,47], the orthotic treatment positively affected curve progression and incidence of surgery [48-52].

'Three-point system' is essential principle for the spinal orthosis design. However, no consistent documents are available for explicitly guiding the orthotic design. Orthosis is designed empirically, and pressure-pad shapes inside the orthosis and correcting-force directions provided via the orthosis remarkably differ among orthoses designed by different orthotists. According to an investigation conducted by the Society on Scoliosis Orthopaedic and Rehabilitation Treatment (SOSORT) [53]: (1) for the thoracic curve, there were 5 pressure-pad shapes used most frequently in the clinical practice (Figure 6.1) and shapes C and D were the most common with a preference of 42% and 33% specialists, respectively; the responses were almost evenly divided about placing the pressure-pad at the apex level or below apex level but at apical rib; three directions of correcting force were proposed (Figure 6.2), and a 'dorsolateral to ventromedial' direction (B) was the most preferred by specialists (85%). (2) for the lumbar curve, no specific pressure-pad shape was proposed while an overwhelming percentage of specialists (76%) agreed to place it at the apex level; and 66% of specialists recommended a 'dorsolateral to ventromedial' correcting force (Figure 6.2). The importance of 3D correction was stressed strongly, but correction mechanisms remained inconsistent [53]. It was unknown what pressure-pad shape and correcting-force direction would provide superior clinical efficacy for patients with AIS.

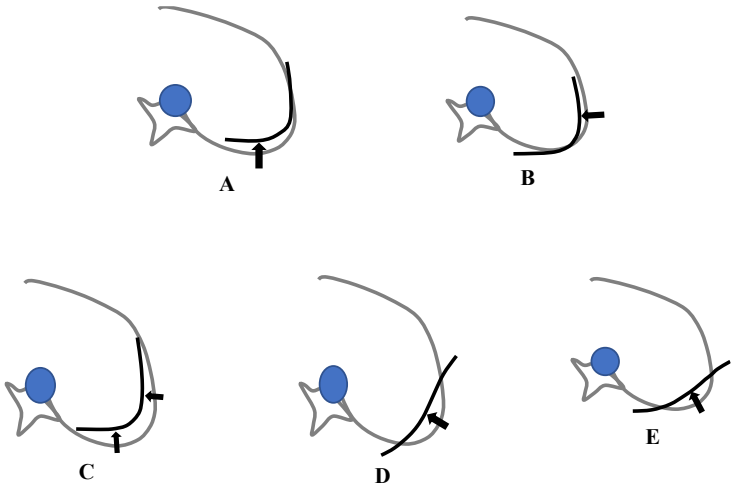

Figure 6.1 Five pressure-pad shapes applied inside orthoses (shape A, B, C, D & E) [53]

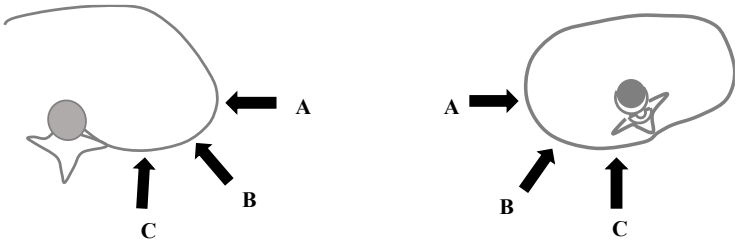

Figure 6.2 Correcting-froce direction applied on the convex side of the thoracic (the left) and lumbar (the right) curves [53]

The correction mechanism of orthoses was designed mainly based on the Cobb and curve type of AIS identified from the coronal plane during the clinical practice, which, however, may not always fully reflect the "actual" Cobb and curve type [21,56,170,172-174,183]. The plane of maximum curvature (PMC, including PMC-Cobb & PMC-orientation) was a promising descriptor in assessing three-dimensional (3D) spinal deformity [23]. The PMC has been applied to assess [33,54-57] and classify [173,183] AIS, and evaluate surgical [164,178,180,181] and orthotic [155,179] treatments' effectiveness. However, PMC was barely considered during orthotic strategy-making.

This study aimed to enhance the orthotic management of AIS by investigating:

(1) What pressure-pad shape would provide superior clinical efficacy to other shapes among the 5 pressure-pad shapes used most frequently in the clinical practice;

(2) What correcting-force direction would produce superior clinical efficacy to other directions;

(3) Whether the PMC concept would improve the clinical efficacy of orthosis.

6.2 Methodology

6.2.1 Study Flowchart

As shown below, this study included substudies I, II, and III. Subjects were grouped according to their spinal orthoses designs regarding pressure-pad shape, correcting-force direction, and whether the orthosis designed with PMC concept or not accordingly.

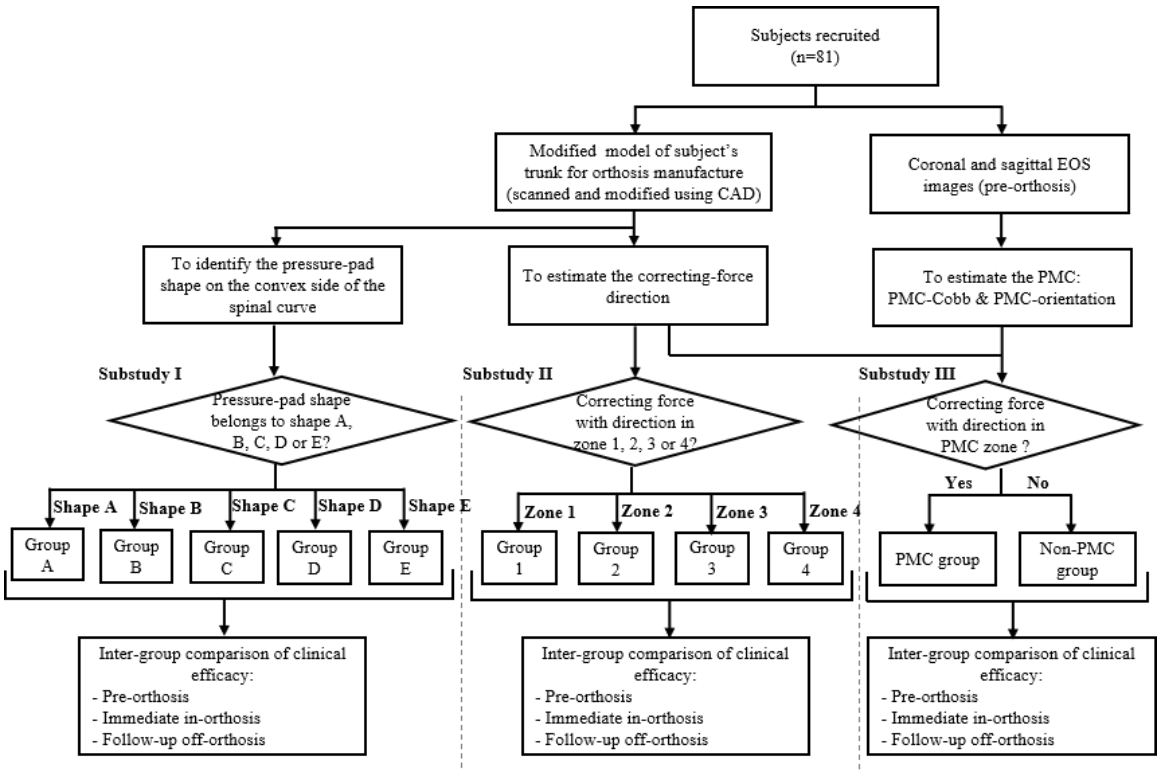

Figure 6.3 Study flowchart

6.2.2 Subjects

According to SRS's criteria, the inclusion criteria were: (1) diagnosed with progressive AIS; (2) primary curve was 25°–40° and apical vertebra was at or below T6; (3) aged 10–16; (4) received orthotic intervention (full-time rigid under-arm spinal orthosis); (5) existed modified model of the trunk inthe Computer-Aided Design /Computer-Aided Manufacturing system (CAD/CAM) (the modified model was used for orthosis manufacture); (6) existed bi-planar EOS images of the spine taken at pre-orthosis, immediate in-orthosis (within one month after orthosis fitting) and/or follow-up off-orthosis (6–12 months after immediate in-orthosis images). Subjects who received prior surgery or were diagnosed with other diseases that might affect the spinal profile were excluded from this study. Human subject ethical approval was granted from the author's Institutional Review Board (Ref.HSEARS20170807003).

The sample sizes of sub-study I, II, and III were calculated in G*power3.1.9.7 software using a priori power analysis with type 1 error rate of 0.05, power of 0.8, effect size f of 0.4, and effect size d of 0.8 estimated based on the Cobb angle of study of Zheng, et al.[256] and Gao, et al.[257], respectively. The total sample size was 80 subjects with 16 for each group for sub-study I, 76 subjects with 19 for each group for sub-study II, and 52 subjects with 26 for each group for sub-study III.

Based on the inclusion & exclusion criteria, 81 consecutive subjects (27males/54females with an average age of 13.7±1.7 (10.0–18.0) years) were selected from the database of a local hospital in 2016-2017. Sixty-six out of 81 subjects were eligible for the follow-up analysis since the images of follow-up off-orthosis were not available for the rest. The follow-up period averaged 7.5±2.1 (5.0–18.0) months.

6.2.3 Procedures of Substudies I, II, and III

Substudy I

The pressure-pad shape on the convex side of the thoracic or (thoraco)lumbar curve was involved for analysis in substudy I. Based on the modified model of the subject's trunk in the

CAD/CAM system, the pressure-pad shape was identified via making a transverse plane across the middle level of the pressure area, where the pressure pad was located inside the orthosis (Figure 6.4: a & b.). The profile of the pressure area in the transverse plane was considered the pressure-pad shape. A rater with more than 3 years of experience in spinal orthosis design identified the pressure-pad shape three times with at least one-week interval each time to reduce recalling bias. If the identified shapes of the 3 times were the same, the shape of the pressure-pad was then determined; otherwise, a senior would be consulted. According to the determined shape, the corresponding subject/curve was assigned to group A (shape A), B (shape B), C (shape C), D (shape D), or E (shape E).

Substudy II

Two assumptions were made: (1) the pressure produced by the pressure pad was comparable to the hydrostatic pressure. The resultant correcting-force direction in the transverse plane across the middle level of the pressure pad would be perpendicular to the connecting line between the two ends of the pressure pad in the transverse plane (Figure 6.4: b) [254]. (2) the directions of the estimated correcting force and the actual correcting force applied on the subject's body were analogous.

As shown in Figure 6.4: c, the x-axis pointing to the posterior represents the sagittal plane (orientation=0°), and the y-axis pointing to the right represents the coronal plane (orientation=-90°). The quadrant of 0° to 90° was the location where correcting force was applied for controlling the right spinal curve and the quadrant of 0° to -90° was the location where correcting force applied for controlling the left spinal curve. Each quadrant was evenly divided into 4 zones, including zone 1 (0° to -22.5° or 0° to +22.5°), zone 2 (-22.5° to -45° or +22.5° to +45°), zone 3 (-45° to -67.5° or +45° to +67.5°), and zone 4 (-67.5° to -90° or +67.5° to +90°). According to which zone the estimated correcting-force direction located in, the corresponding subject/curve was assigned to group 1 (zone 1), group 2 (zone 2), group 3 (zone 3), or group 4 (zone 4).

Substudy III

Similar to the substudy II, the two assumptions were also made in this substudy, and the correcting force was estimated using the same method detailed in substudy II. PMC was estimated from the coronal and sagittal EOS images of the spine using the computational method developed and verified in Chapter 3.

The PMC concept in orthotic design referred to whether the estimated correcting force was located in the PMC zone (Figure 6.4: d: PMC-orientation ±15°) for the thoracic curve or perpendicular to the plane situated in the PMC zone for the (thoraco)lumbar curve. Subjects whose spinal orthosis was designed with PMC concept would be sent to the PMC group, otherwise, to the non-PMC group.

The (thoraco)lumbar curve is convex towards the anterolateral, and its PMC is located in the left/right anterolateral quadrant (Figure 6.5). Applying a “ventromedial to dorsolateral” correcting force in the lumbar region seems inappropriate.. Therefore, the (thoraco)lumbar curve is commonly corrected via a "dorsolateral to ventromedial" correcting force. Since coronal-Cobb of a (thoraco)lumbar curve could be reduced by diminishing the rotation of the curve towards the coronal plane (PMC-orientation). Thus, theoretically, an external force perpendicular to the plane where the maximum curvature lies (PMC) could be considered effective in pushing the curve segment towards the sagittal plane. Thus, the (thoraco)lumbar curves were grouped upon whether the estimated correcting-force direction was perpendicular to a plane positioned in the PMC zone.

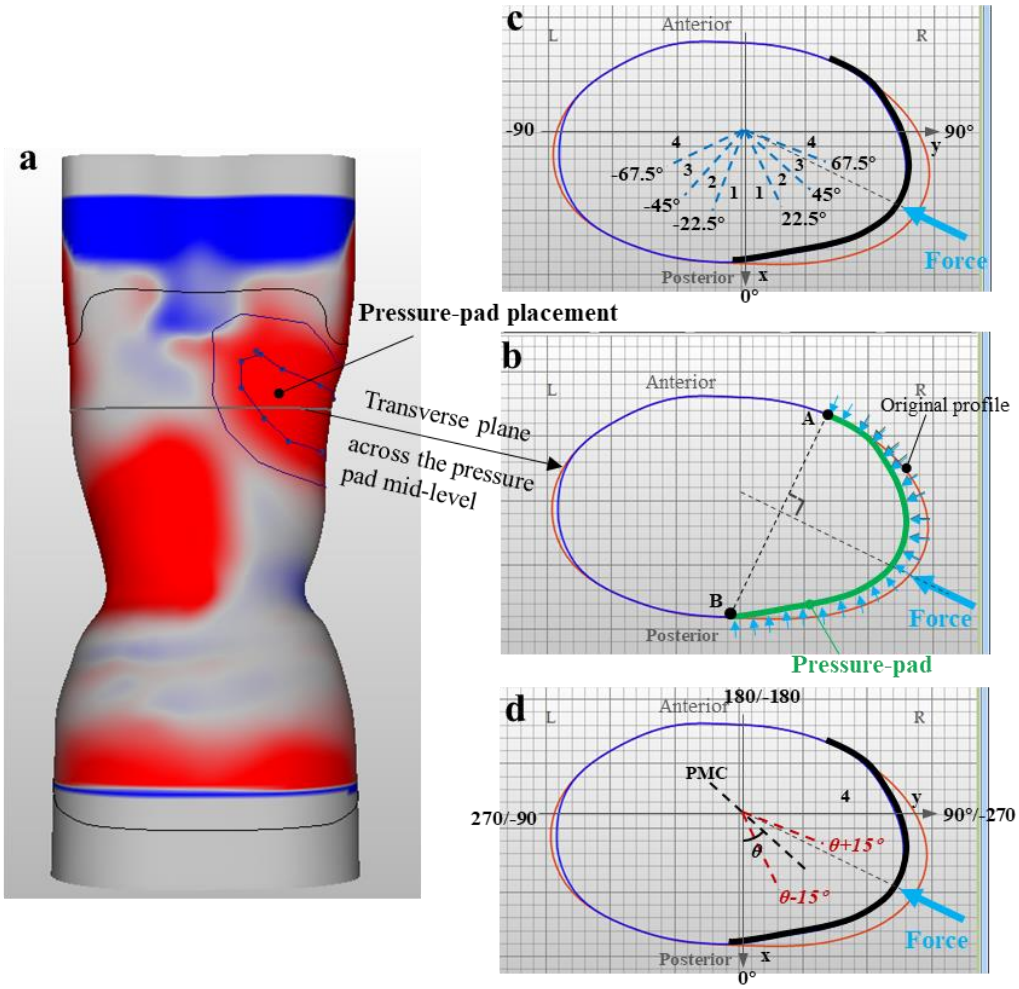

Figure 6.4 Identification of direction of correcting force and shape of pressure-pad, and definitions of correcting force zones and PMC zone. (a) a modified model of subject's trunk scanned and modified using the CAD/CAM system. The b, c & d are transverse plane taken across the middle level of "pressure pad". In the axis system, x-axis pointing to the posterior represents the sagittal plane (orientation=0°), and y-axis pointing to the right represents the coronal plane (orientation=90°/-270°). Clockwise and counter-clockwise rotation are recorded as positive (-) and negative (+) separately. As shown in b, the pressure-pad shape can be identified in the transverse plane. (b) when assuming the pressure produced by pressure pad to be hydrostatic pressure, the direction of resultant correcting force would be perpendicular to the connecting line between the two ends (A, B) of the pressure pad in the transverse plane. (c) the left and right posterolateral quadrants are separately divided into 4 zones evenly, including zone 1, zone 2, zone 3 and zone 4. (d) PMC zone: PMC-orientation ±15° (θ±15°)

6.2.4 Outcome Measurements

The outcome measurements included PMC (PMC-Cobb; PMC-orientation), coronal-Cobb, sagittal thoracic kyphosis (T4 –T12), and sagittal lumbar lordosis (L1–S1) at pre-orthosis, immediate in-orthosis, and follow-up off-orthosis visits. For easier understanding of correction in PMC-orientation, all the PMC-orientation (θ) was recorded as an absolute value in clinical efficacy analysis (differing from the records for grouping in 6.2.3), reflecting the rotation of the spinal curve towards the coronal plane (Figure 6.5). Correction in PMC-orientation suggested the correction in the rotation of the spinal curve towards the coronal plane. PMC-Cobb represented the "actual" curvature. Coronal-Cobb was a projected Cobb in the coronal plane and hence was a component of the actual curve Cobb angle. It could be affected by the actual curve Cobb angle and rotation of the spinal curve. For instance, a decrease in the actual curve Cobb would result in a decreased coronal-Cobb, and an increase in the rotation of the curve could result in an increased coronal-Cobb.

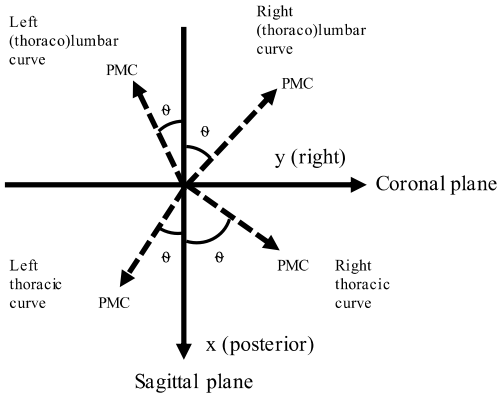

Figure 6.5 PMC-orientation (θ) regarding the sagittal plane for different curve types was presented as an absolute value

6.2.5 Data Analyses

Statistical analyses were performed in SPSS (version 21, IBM, Chicago, IL, USA) with a significant level (*p*) set at 0.05. The normality of each studied parameter was analysed using the Shapiro-Wilks test. Statistical data analysis was performed for the primary curves (1st way), primary & secondary curves (2nd way), thoracic curves and (thoraco)lumbar curves (3rd way) in each of substudies (Figure 6.6). If the results of data anlyses were inconsistent among the 1st, 2nd, and 3rd ways, the results of the 1st way would be considered a priority. All the data were presented as mean ± standard deviation (SD). The clinical efficacy was evaluated using: (1)

correction at immediate in-orthosis and follow-up off-orthosis: mean difference (MD) = pre-orthosis – immediate in-orthosis/follow-up off-orthosis, respectively; (2) success/failure rate at follow-up off-orthosis visit. Success rate referred to the percentage of subjects/curves with curvature/PMC-orientation progression ≤5° or percentage of subjects/curves with curvature ≤45° at follow-up off-orthosis. Conversely, the failure rate was the percentage of subjects/curves with curvature/PMC-orientation progression ≥6° or curvature ≥45° at the follow-up off-orthosis. The intra-group difference was analysed using the paired t-test (2-tailed) for 2 datasets or one-way repeated ANOVA for ≥3 datasets. The inter-group difference was assessed using the independent t-test (2-tailed) for 2 independent sample groups or one-way ANOVA for ≥3 independent sample groups. Also, inter-group comparisons of success and failure rates were performed using the Pearson Chi-square (frequency, n>5) or Fisher's exact test (frequency, n≤5).

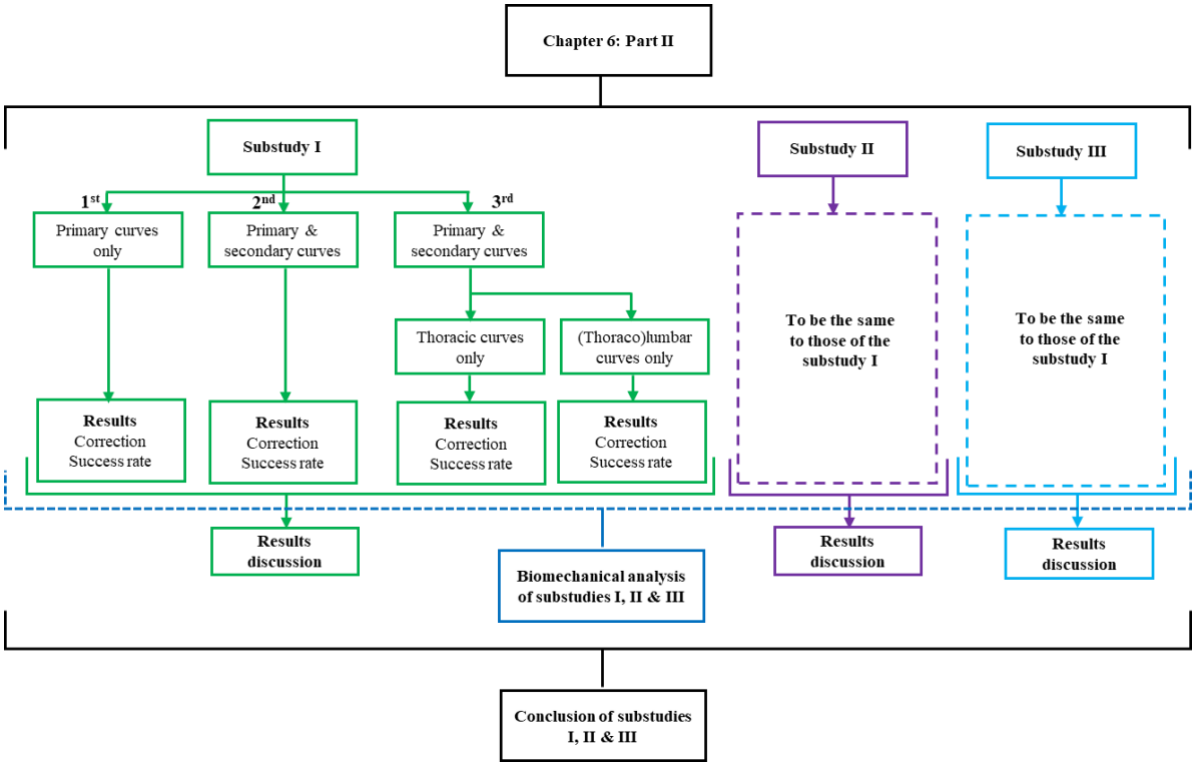

Figure 6.6 Data analyses

6.3 Results

6.3.1 Substudy I

Primary Curves Only

Subjects

Table 6.1 showed that 25, 2, 23, 7, and 24 subjects were separately sent to groups A, B, C, D, and E. As sample size of group B was too small, data analysis was not performed for it. The groups demonstrated a comparable baseline ($p>0.05$) except for the coronal-Cobb and sagittal lumbar lordosis in group C ($p<0.05$). Additionally, the mean±SD of coronal-Cobb, PMC-Cobb, PMC-orientation, thoracic kyphosis, and lumbar lordosis at pre-orthosis, immediate in-orthosis, and follow-up off-orthosis were presented in Table 6.2.

Table 6.1 Characteristics of subjects selected into groups A, C, D and E (substudy I – primary curves only)

	Group A	**Group C**	**Group D**	**Group E**
Subjects, n	25	23	7	24
Gender, male/female	8/17	8/15	0/7	9/15
Age, mean ± SD (range) (yrs)	14.2 ± 1.8 (10.0–18.0)	13.6 ± 1.7 (10.5–17.0)	12.7 ± 1.8 (10.4–15.5)	13.5 ± 1.4 (11.0–16.0)
Primary curves, n	25	23	7	24
Coronal-Cobb, mean ± SD (range) (°)	22.6 ± 6.4 (13.0–40.4)	**26.1 ± 5.8**[#] (15.8–38.7)	19.1 ± 7.9 (15.3 – 27.6)	20.6 ± 5.2 (12.6–30.7)

#: inter-group difference was significant ($p<0.05$).

Note: since only 2 subjects were selected for group B, data analysis was not performed for this group.

Clinical Efficacy (correction and success/failure rate)

Table 6.2 and Figure 6.7 presented correction in most parameters at immediate in-orthosis and/or follow-up off-orthosis in all the analysed groups. A significant correction in coronal-Cobb was only found at immediate in-orthosis in all the groups (MD=4.0°–5.9°, $p<0.05$). PMC-Cobb was significantly decreased at the immediate in-orthosis and follow-up off-orthosis in group A (MD=7.0°/4.4°, $p<0.05$), however, only at immediate in-orthosis in groups C and E (MD=4.2°/5.1°, $p<0.05$). PMC-orientation was significantly reduced only at immediate in-orthosis in group D (MD=10.7°, $p<0.05$). A significant decrease in thoracic kyphosis was only found at immediate in-orthosis and follow-up off-orthosis in group A (MD=3.1°/6.6°, $p<0.05$).

Lumbar lordosis demonstrated a significant reduction at immediate in-orthosis and follow-up off-orthosis in all the groups except group C (MD=4.8°–11.5°, $p<0.05$).

Table 6.3 presented a high success rate in all the groups based on the coronal-Cobb and PMC-Cobb (≥75%). Group A showed the highest success rate, followed by groups E, D, and C according to coronal-Cobb and PMC-Cobb. By contrast, based on the PMC-orientation, the success and failure rates tended to be similar in all the groups.

Table 6.2 Mean and standard deviation of different parameters in different groups (substudy I – primary curves only)

	Curves, n	Coronal-Cobb (°)	PMC-Cobb (°)	PMC-orientation (°)	Thoracic kyphosis (°)	Lumber-lordosis (°)
Group A						
Pre-orthosis	25	22.6 ± 6.4	32.9 ±12.4^	51.0 ± 21.5	24.3 ±12.4	56.3 ± 9.1^, # (*vs.* C)
In-orthosis	25	17.6 ± 7.4^	25.9 ± 10.8	48.6 ± 20.0^	21.1 ± 10.7	46.8 ± 8.7
Off-orthosis	22	22.0 ± 9.7	29.5 ± 11.1	52.7 ± 19.4^	18.0 ± 9.5^	45.5 ± 10.9
Group C						
Pre-orthosis	23	26.1 ± 5.8^, # (*vs.* A, D or E)	35.4 ± 8.4^	52.2 ± 18.0	22.3 ± 8.0	50.4 ± 8.3# (*vs.* A)
In-orthosis	23	22.0 ± 8.6^, # (*vs.* A, D or E)	31.2 ± 7.1^	49.7 ± 23.1	21.3 ± 9.0	45.4 ± 8.4
Off-orthosis	16	24.3 ± 9.3# (*vs.* D or E)	33.0 ± 10.0	52.4 ± 20.9	21.6 ± 8.4	47.4 ± 11.5
Group D						
Pre-orthosis	7	19.1 ± 7.9^	36.7 ± 12.0	45.3 ± 32.2^	23.7 ± 22.4	56.4 ± 15.3^
In-orthosis	7	13.1 ± 8.8^	30.4 ±12.2	34.6 ± 30.1^	25.1 ± 21.0	48.4 ± 12.6
Off-orthosis	6	13.7 ± 13.9	29.7 ± 14.7	41.7 ± 37.1	24.3 ± 26.5	47.6 ± 10.4
Group E						
Pre-orthosis	24	20.6 ± 5.2	31.3 ± 12.2^	50.1 ± 21.5	19.6 ± 9.8	51.5 ± 8.6^
In-orthosis	24	15.5 ± 5.4^	26.5 ± 11.1^	45.0 ± 24.5	20.6 ± 9.3	46.6 ± 6.8
Off-orthosis	20	17.6 ± 7.9	29.2 ± 11.9	46.2 ± 23.8	22.0 ± 9.2	45.8 ± 9.4

^: in a group, the marked value significantly differs from the other two values ($p<0.05$).

^^ or ^^^: in a group, these marked values significantly differ from each other($p<0.05$).

#: inter-group difference was significant ($p<0.05$).

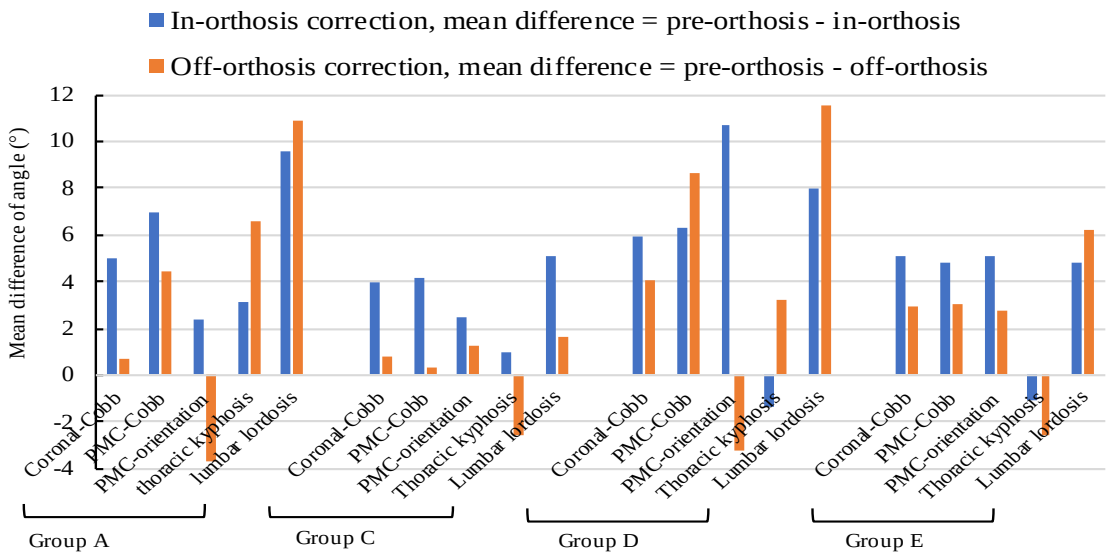

Figure 6.7 Correction at immediate in-orthosis and follow-up off-orthosis in groups A, C, D and E (substudy I – primary curves only)

Table 6.3 Success and failure rates based on different parameters in different groups (substudy I – primary curves only)

	Subjects, n	Coronal-Cobb	PMC-Cobb	PMC-orientation
Group A				
Success rate (n)	22	**95.5% (21)**	**95.5% (21)**	59.1% (13)
Failure rate (n)		4.5% (1)	4.5% (1)	40.9% (9)
Group C				
Success rate (n)	16	81.3% (13)	75.0% (12)	62.5% (10)
Failure rate (n)		18.7% (3)	25.0% (4)	37.5% (6)
Group D				
Success rate (n)	6	83.3% (5)	83.3% (5)	50.0% (3)
Failure rate (n)		16.7% (1)	16.7% (1)	50.0% (3)
Group E				
Success rate (n)	20	**90.0% (18)**	**85.0% (17)**	55.0% (11)
Failure rate (n)		10.0 % (2)	15.0% (3)	45.0% (9)

Curve progression = pre-orthosis – follow-up off-orthosis

Success rate: the percentage of subjects/curves with curvature/PMC-orientation progression ≤5°

Failure rate: the percentage of subjects/curves with curvature/PMC-orientation progression ≥6° or curve ≥45°

[#]: inter-group difference was significant (p<0.05).

Primary and Secondary Curves

Clinical Efficacy (correction and success/failure rate)

Table 6.4 and Figure 6.8 showed a significant correction in coronal-Cobb at immediate in-orthosis in all the groups (MD=3.7°–6.9°, $p<0.05$). PMC-Cobb was significantly diminished at immediate in-orthosis and follow-up off-orthosis in group A (MD=7.5°/4.5°, $p<0.05$), while only at immediate in-orthosis in groups C, D, and E (MD=4.5°–7.0°, $p<0.05$). For PMC-orientation, a significant decrease was only found at immediate in-orthosis in group D (MD=6.6°, $p<0.05$). Additionally, a significantly reduced thoracic kyphosis was seen at immediate in-orthosis and follow-up off-orthosis in group A (MD=5.0°/9.0°, $p<0.05$), while a a significantly reduced lumbar lordosis was observed at immediate in-orthosis and/or follow-up off-orthosis in groups A, D, and E (MD=5.8°–9.2°, $p<0.05$).

As detailed in Table 6.5, group A had the highest success rate based on coronal-Cobb and PMC-Cobb, followed by groups D, E, and C. However, success and failure rates were similar in all groups based on PMC-orientation. No significant difference existed between the success rate of the groups A, C, and E ($p>0.05$).

Table 6.4 Mean and standard deviation of different parameters in different groups (substudy I – primary and secondary curves)

	curves, n	Coronal-Cobb (°)	PMC-Cobb (°)	PMC-orientation (°)	Thoracic kyphosis (°)	Lumbar lordosis (°)
Group A					(n=16, 16,14)	(n=22, 22, 19)
Pre-orthosis	39	21.3 ± 7.0	35.0 ± 12.4^	43.6 ± 21.0	26.5 ± 11.8^	53.9 ± 8.5^
In-orthosis	39	15.9 ± 6.8^, # (*vs.* C)	27.5 ± 10.2^	42.2 ± 21.4^	21.5 ± 9.3^	47.7 ± 7.5
Off-orthosis	34	19.2 ± 9.0	30.9 ± 12.0^	45.8 ± 21.8^	19.1 ± 9.0^	47.1 ± 9.4
Group C					(n=21, 21,14)	(n=9, 9, 6)
Pre-orthosis	30	24.6 ± 6.8#	35.1 ± 8.8^	49.0 ± 19.1	22.3 ± 7.8	51.9 ± 5.9
In-orthosis	30	20.9 ± 8.4^, #	30.6 ± 6.8^	47.2 ± 22.5	22.0 ± 9.9	44.9 ± 7.5
Off-orthosis	20	22.4 ± 9.4	33.1 ± 9.7	48.1 ± 21.3	21.1 ± 7.8	51.5 ± 11.1
Group D					(n=7, 7, 4)	(n=6, 6, 5)
Pre-orthosis	13	23.6 ± 9.4^	39.5 ± 12.1^	48.0 ± 28.6^	24.2± 24.6	57.2 ± 11.5^
In-orthosis	13	16.7 ± 8.4^	32.5 ± 11.5^	41.4 ± 30.2^	23.8 ± 23.5	49.0 ± 8.8^
Off-orthosis	9	20.4 ±15.2	33.2 ± 12.8	48.0 ± 32.5	24.5 ± 34.1	46.7 ± 4.9
Group E					(n=13, 13, 10)	(n=26, 26, 20)
Pre-orthosis	39	20.0 ± 5.5#	31.2 ± 12.2	48.5 ± 20.6	21.4 ± 9.7	51.8 ± 9.2^
In-orthosis	39	15.4 ± 6.4^, # (*vs.* C)	25.3 ± 11.2^	45.6 ± 23.5	21.5 ± 8.8	46.0 ± 8.9
Off-orthosis	32	17.9 ± 9.2	29.1 ± 12.7	44.2 ± 23.4	21.5 ± 8.4	46.3 ± 11.4

^: in a group, the marked value significantly differs from the other two values (p<0.05).

^^ or ^^^: in a group, these marked values significantly differ from each other(p<0.05).

#: inter-group difference was significant (p<0.05).

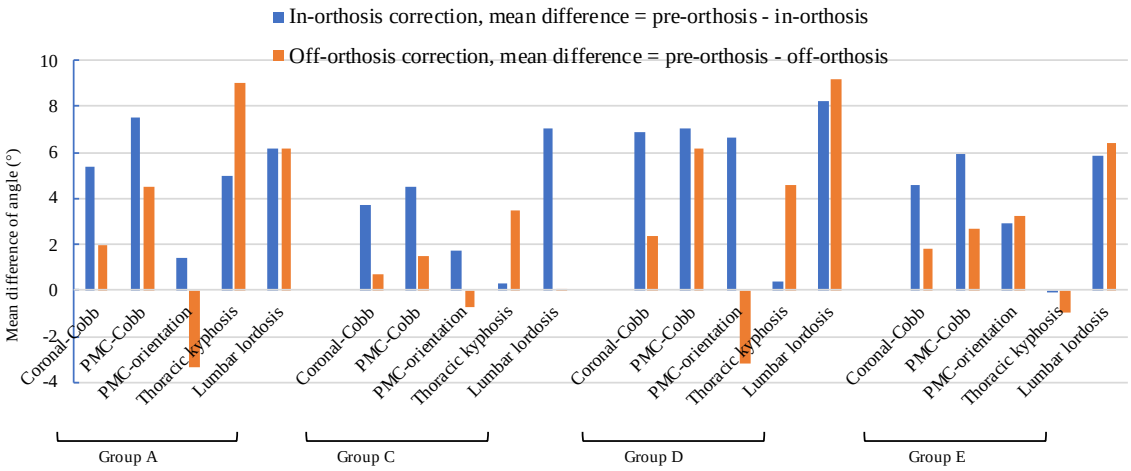

Figure 6.8 Correction at immediate in-orthosis and follow-up off-orthosis in groups A, C, D, and E (substudy I – primary and secondary curves)

Table 6.5 Success and failure rates based on different parameters in different groups (substudy I – primary and secondary curves)

	Curves, n	Coronal-Cobb	PMC-Cobb	PMC-orientation
Group A				
Success rate (n)	34	**97.1% (33)**	**94.1% (32)**	64.7% (22)
Failure rate (n)		2.9% (1)	5.9% (2)	35.3% (12)
Group C				
Success rate (n)	20	80.0% (16)	80.0% (16)	65.0% (13)
Failure rate (n)		20.0% (4)	20.0% (4)	35.0% (7)
Group D				
Success rate (n)	9	88.9% (8)	88.9% (8)	44.4% (4)
Failure rate (n)		11.1% (1)	11.1% (1)	55.6% (5)
Group E				
Success rate (n)	32	81.3% (26)	84.4% (27)	62.5% (20)
Failure rate (n)		18.8% (6)	15.6% (5)	37.5% (12)

Curve progression = pre-orthosis – follow-up off-orthosis

Success rate: the percentage of subjects/curves with curvature/PMC-orientation progression ≤5°

Failure rate: the percentage of subjects/curves with curvature/PMC-orientation progression ≥6° or curve ≥45°

#: inter-group difference was significant ($p<0.05$).

Primary and Secondary Curves (with subgroups of thoracic and (thoraco)lumbar curves)

Clinical Efficacy (correction and success/failure rate)

For the thoracic curves (Table 6.6 & Figure 6.9), a significantly decreased coronal-Cobb was found at immediate in-orthosis in all the groups (MD=2.3°–8.2°, $p<0.05$). PMC-Cobb was significantly diminished at immediate in-orthosis in groups A, C, and E (MD=1.9°–5.1°, $p<0.05$); however, no significant reduction was observed at follow-up off-orthosis ($p>0.05$). Only a fluctuated PMC-orientation was seen in all the groups ($p>0.05$). Additionally, significantly decreased thoracic kyphosis was found in group A at immediate in-orthosis and follow-up off-orthosis (MD=4.0°/9.0°, $p<0.05$). Apart from group D (small sample size, n=4), group A showed the highest value based on coronal-Cobb and PMC-Cobb, followed by groups E and C (Table 6.7). Based on PMC-orientation, group E presented the highest success rate while group D had the lowest.

Table 6.6 and Figure 6.9 showed significant correction in coronal-Cobb for the (thoraco)lumbar curves at immediate in-orthosis in all the analysed groups (MD=5.0°–9.3°, $p<0.05$). Significantly decreased PMC-Cobb was found at immediate in-orthosis and follow-up off-orthosis in group A (MD=9.2°/5.4°, $p<0.05$), while only at immediate in-orthosis in groups C, D, and E (MD=7.6°–10.9°, $p<0.05$). PMC-orientation only fluctuated after orthosis fitting in all the groups ($p>0.05$). In all the groups, sagittal lumbar lordosis was significantly diminished at immediate in-orthosis and/or follow-up off-orthosis (MD=5.8°–9.2°, $p<0.05$). Apart from groups D and C (too small sample size, n=5, 6), success rate was higher in group A than in group E (coronal-Cobb: 100% *vs.* 81.8%, PMC-Cobb: 90.0% *vs.* 85.7%, PMC-orientation: 70.0% *vs.* 52.4%) (Table 6.7). However, no significant difference was observed among the success rates of the two groups ($p>0.05$).

Table 6.6 Mean and standard deviation of different parameters in different groups (substudy I – primary and secondary curves with subgroups of thoracic and (thoraco)lumbar curves)

	Thoracic curves					(Thoraco)lumbar curves				
	curves, n	Coronal-Cobb (°)	PMC-Cobb (°)	PMC-orientation (°)	Thoracic kyphosis (°)	curves, n	Coronal-Cobb (°)	PMC-Cobb (°)	PMC-orientation (°)	Lumbar lordosis (°)
Group A										
Pre-orthosis	16	22.4 ± 8.7	31.4 ± 9.4^	50.1 ± 21.5	26.5 ± 11.8^	23	20.5 ± 5.6^	37.6 ± 13.8^	39.1 ± 19.9	52.3 ± 11.2^
In-orthosis	16	18.5 ± 8.1^	26.3 ± 9.2^	50.8 ± 20.4	21.5 ± 9.3^	23	14.2 ± 5.3	28.4 ± 10.9	36.2 ± 20.4	47.7 ± 7.5
Off-orthosis	14	23.5 ± 12.2	29.6 ± 11.6	55.4 ± 19.9^	19.1± 9.0^	20	16.2 ± 4.2	31.8 ± 12.5	39.1 ± 20.9	47.1 ± 9.4
Group C										
Pre-orthosis	21	25.6 ± 7.1^,#	32.2 ± 6.1^	54.9 ± 15.1	22.3 ± 7.8	9	22.2 ± 5.7^	41.9 ± 10.7	35.1 ± 21.1	51.9 ± 5.9^
In-orthosis	21	23.3 ± 8.0^#	30.3 ± 5.9^,#	53.6 ± 21.0	22.0 ± 9.9	9	15.1 ± 6.3^	31.3 ± 8.9^	32.2 ± 19.3	44.9 ± 7.5^
Off-orthosis	14	24.3 ± 10.5	30.4 ± 9.6	56.5 ± 19.1	21.1 ± 7.8	6	18.0 ± 3.5	39.4 ± 7.1	28.3 ± 10.9	51.5 ± 11.1
Group D										
Pre-orthosis	7	21.2 ± 7.7^	32.8 ± 10.1	55.3 ± 29.8	25.8 ± 26.5	6	26.3 ± 11.2^	47.3 ± 9.7^	39.5 ± 27.3^	57.2 ± 11.5^
In-orthosis	7	16.4 ± 8.0^	29.1 ± 12.9	47.7 ± 32.0	23.8 ± 23.5	6	17.1 ± 9.6^	36.5 ± 9.1^	34.0 ± 28.9^	49.0 ± 8.8^
Off-orthosis	4	18.0 ± 17.5	33.0 ± 17.5	56.0 ± 38.4	24.5 ± 34.1	5	22.2 ± 16.4	33.2 ± 9.9	41.6 ± 29.9	46.7 ± 4.9
Group E										
Pre-orthosis	13	17.7 ± 5.1^,#	22.4 ± 6.6^,#	57.9 ± 17.0	21.4 ± 9.7	26	21.1 ± 5.4	35.6 ± 12.0	43.8 ± 20.9	51.8 ± 9.2^
In-orthosis	13	13.9 ± 6.6^,#	19.8 ± 6.9^,#	46.7 ± 23.7	21.5 ± 8.8	26	16.1 ± 6.4^	28.1 ± 12.0^	45.0 ± 23.9	45.6 ± 8.7
Off-orthosis	11	15.5 ± 9.9	20.9 ± 9.4	46.5 ± 24.5	21.5 ± 8.4	21	19.1 ± 8.9	33.3 ± 12.2	58.6 ± 69.0	46.3 ± 11.4

^: in a group, the marked value significantly differs from the other two values (p<0.05).

^^ or ^^^: in a group, these marked values significantly differ from each other(p<0.05).

#: inter-group difference was significant (p<0.05).

Note: no curve was selected for group B.

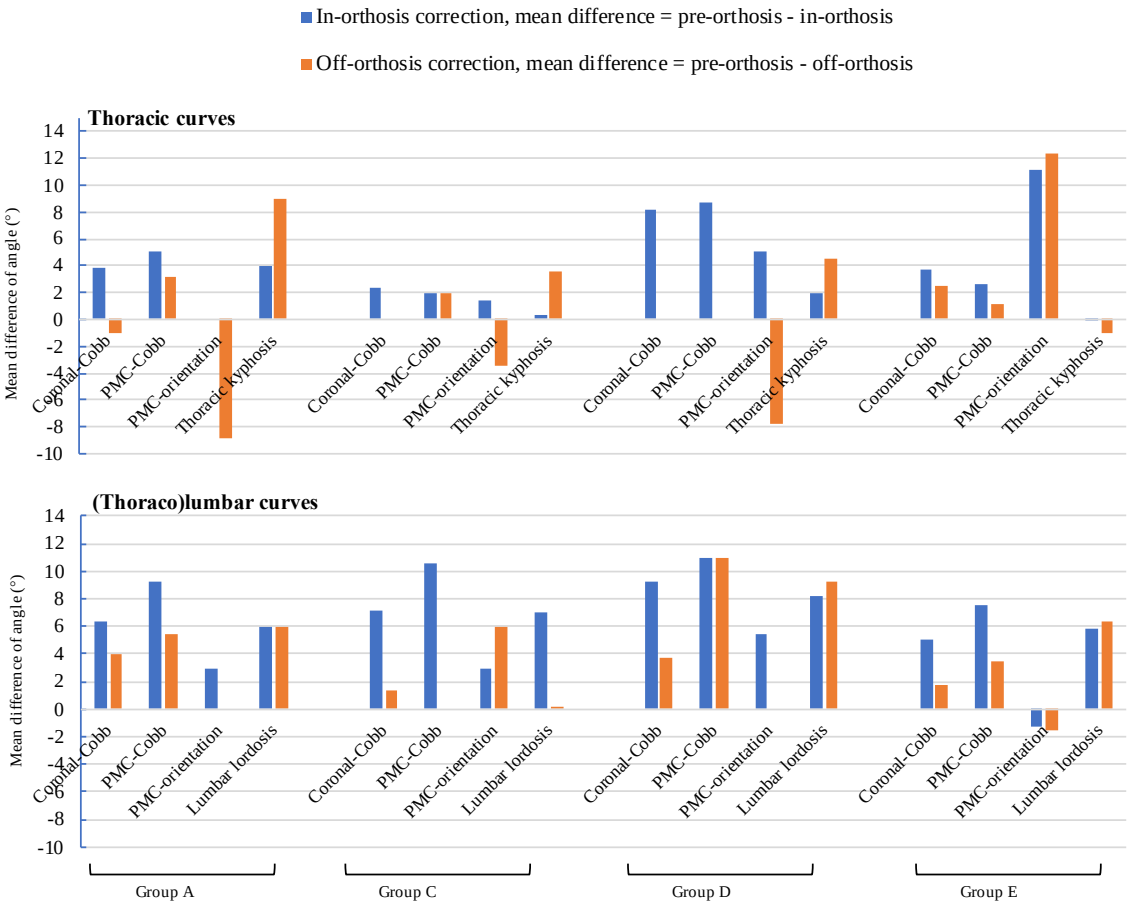

Figure 6.9 Correction at immediate in-orthosis and follow-up off-orthosis in groups A, C, D and E (substudy I – primary and secondary curves with subgroups of thoracic and (thoraco)lumbar curves)

Table 6.7 Success and failure rates based on different parameters in different groups (substudy I – primary and secondary curves with subgroups of thoracic and (thoraco)lumbar curves)

	Thoracic curves				(Thoraco)lumbar curves			
	Curves, n	**Coronal-Cobb**	**PMC-Cobb**	**PMC-orientation**	**Curves, n**	**Coronal-Cobb**	**PMC-Cobb**	**PMC-orientation**
Group A								
Success rate (n)	14	**92.9% (13)**	**100% (14)**	57.1% (8)	20	**100 % (20)**	**90.0% (18)**	**70.0 % (14)**
Failure rate (n)		7.1% (1)	0% (0)	42.9 % (6)		0 % (0)	10.0 % (2)	30.0 % (6)
Group C								
Success rate (n)	14	71.4% (10)	78.6% (11)	50% (7)	6	100 % (6)	83.3% (5)	83.3% (5)
Failure rate (n)		28.6% (4)	21.4% (3)	50% (7)		0 % (0)	16.7% (1)	16.7% (1)
Group D								
Success rate (n)	4	75.0% (3)	75.0% (3)	25.0% (1)	5	100% (5)	100% (5)	60.0% (3)
Failure rate (n)		25.0% (1)	25.0% (1)	75.0% (3)		0% (0)	0% (0)	40.0% (2)
Group E								
Success rate (n)	11	**90.9% (10)**	**81.8% (9)**	**81.8% (9)**	21	76.2% (16)	85.7% (18)	52.4% (11)
Failure rate (n)		9.1% (1)	18.2% (2)	18.2% (2)		23.8% (5)	14.3% (3)	47.6% (10)

Curve progression = pre-orthosis – follow-up off-orthosis

Success rate: the percentage of subjects/curves with curvature/PMC-orientation progression ≤5°

Failure rate: the percentage of subjects/curves with curvature/PMC-orientation progression ≥6° or curve ≥45°

#: inter-group difference was significant ($p<0.05$).

6.3.2 Substudy II

Primary Curves Only

Subjects

Table 6.8 showed 3, 17, 56, and 5 subjects eligible for groups 1, 2, 3, and 4, respectively. Because of small sample size, data analyse was not performed for group 1. Baseline data of.groups 2, 3, and 4 were comparable. Table 6.9 presented the mean ± SD of coronal-Cobb, PMC-Cobb, PMC-orientation, thoracic kyphosis, and lumbar lordosis at pre-orthosis, immediate in-orthosis, and follow-up off-orthosis.

Table 6.8 Characteristics of subjects selected into groups 2, 3 and 4 (substudy II – primary curves only)

	Group 2	**Group 3**	**Group 4**
Subjects, n	17	56	5
Gender, male/female	5/12	19/37	1/4
Age, mean± SD (range) (yrs)	14.0 ± 1.7	13.5 ± 1.6	13.8 ± 0.6
	(10.0–16.7)	(10.4–17.0)	(12.8–14.8)
Primary curves, n	17	56	5
Coronal-Cobb, mean ± SD (range) (°)	24.7 ± 7.1	21.7 ± 6.3	23.5 ± 8.1
	(15.3–40.4)	(15.6–38.7)	(12.7–31.8)

Note: since only 3 subjects were selected into group 1, data analysis was not performed for it.

Clinical Efficacy (correction and success/failure rate)

No significant alterations were found in group 4 due to its small sample size (n=4). Significantly decreased coronal-Cobb was observed at immediate in-orthosis in groups 2 and 3 (MD=4.8°/4.4°, $p<0.05$) (Table 6.9 & Figure 6.10). PMC-Cobb was significantly lessened at immediate in-orthosis in groups 2 and 3 (MD=6.6°/4.6°, $p<0.05$). Moreover, there was no significant decrease in PMC-orientation after orthosis fitting in groups 2 and 3 ($p>0.05$). Thoracic kyphosis was significantly decreased at immediate in-orthosis and follow-up off-orthosis in group 2 (MD=4.2°/7.6°, $p<0.05$), while not significantly changed in group 3 ($p>0.05$). By contrast, groups 2 and 3 showed significantly decreased in lumbar lordosis at immediate in-orthosis and follow-up off-orthosis (MD=6.3°–13.9°, $p<0.05$).

Based on coronal-Cobb and PMC-Cobb, the success rate was generally high in all the analysed groups (≥75.0%) (Table 6.10). Group 2 demonstrated the highest success rate, followed by groups 3 and 4. Based on PMC-orientation, success and failure rates were at a similar level. No significant difference was seen among the success rates of the 2 groups (p>0.05).

Table 6.9 Mean and standard deviation of different parameters in different groups (substudy II – primary curves only)

	Curves, n	Coronal-Cobb (°)	PMC-Cobb (°)	PMC-orientation (°)	Thoracic kyphosis (°)	Lumbar lordosis (°)
Group 2						
Pre-orthosis	17	24.7 ± 7.1	32.5 ± 11.0^	57.5 ± 21.5	23.1 ± 12.5^	57.0 ± 9.3^, # (*vs.* 4)
In-orthosis	17	19.9 ± 7.6^	25.9 ± 9.9^	58.1 ± 19.6# (*vs.* 3)	18.9 ± 11.1	45.2 ±9.4 # (*vs.* 4)
Off-orthosis	15	25.4 ± 11.3# (*vs.* 3)	29.7 ± 11.6	60.9 ± 16.2# (*vs.* 3)	17.0 ± 8.8	44.1 ± 12.6
Group 3						
Pre-orthosis	56	21.7 ± 6.3	32.9 ± 11.4	47.8 ± 20.6	22.7 ± 11.6	52.9 ± 10.0^
In-orthosis	56	17.3 ± 7.5^	28.3 ± 10.8^	44.4 ± 22.6# (*vs.* 2)	23.0 ± 10.9	47.8 ± 7.7 # (*vs.* 4)
Off-orthosis	44	18.8 ± 9.3# (*vs.* 2)	30.5 ± 11.4	46.4 ± 24.5# (*vs.* 2)	23.0 ± 12.5	48.3 ± 10.1
Group 4						
Pre-orthosis	5	23.5 ± 8.1	29.2 ± 3.6	61.0 ± 25.7	18.5± 10.8	45.4 ± 5.0^
In-orthosis	5	19.9 ± 9.9	28.5 ± 6.8	49.4 ± 31.0	18.0 ± 12.8	34.6 ± 4.8^, # (*vs.* 2, 3)
Off-orthosis	4	18.4 ± 6.8	25.6 ± 11.5	51.8 ± 18.8	18.7 ± 12.5	38.6 ± 8.2

^: in a group, the marked value significantly differs from the other two values (p<0.05).

^^ or ^^^: in a group, these marked values significantly differ from each other(p<0.05).

#: inter-group difference was significant (p<0.05).

Note: too small sample size in group 1, so the data analysis was not performed.

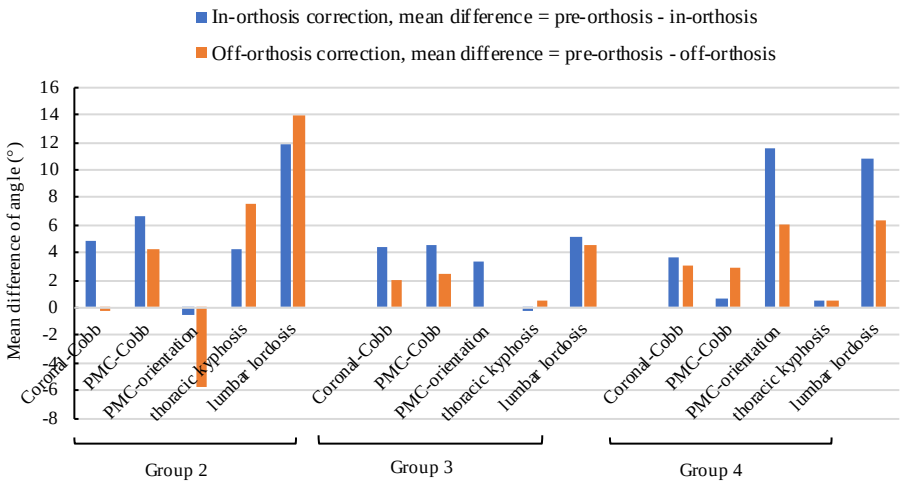

Figure 6.10 Correction at immediate in-orthosis and follow-up off-orthosis in groups 2, 3 and 4 (substudy II – primary curves only)

Table 6.10 Success and failure rates based on different parameters in different groups (substudy II – primary curves only)

	Subjects, n	Coronal-Cobb	PMC-Cobb	PMC-orientation
Group 2				
Success rate (n)	15	**93.3% (14)**	**93.3% (14)**	60.0% (9)
Failure rate (n)		6.7% (1)	6.7% (1)	40.0% (6)
Group 3				
Success rate (n)	44	81.8% (36)	81.8% (36)	56.8% (25)
Failure rate (n)		18.2% (8)	18.2% (8)	43.2% (19)
Group 4				
Success rate (n)	4	75.0% (3)	75.0% (3)	50.0% (2)
Failure rate (n)		25.0% (1)	25.0% (1)	50.0% (2)

Curve progression = pre-orthosis – follow-up off-orthosis

Success rate: the percentage of subjects/curves with curvature/PMC-orientation progression ≤5°

Failure rate: the percentage of subjects/curves with curvature/PMC-orientation progression ≥6° or curve ≥45°

[#]: inter-group difference was significant (p<0.05).

Primary and Secondary Curves

Clinical Efficacy (correction and success/failure rate)

As detailed in Table 6.11 and Figure 6.11, coronal-Cobb (MD=4.8°, $p<0.05$) and PMC-Cobb (MD=6.3°/6.0°, $p<0.05$) were significantly decreased at immediate in-orthosis in groups 2 and 3. No significant changes in PMC-orientation was observed after orthosis fitting in the two groups ($p>0.05$). Also, a significant decrease in thoracic kyphosis was found at immediate in-orthosis in group 2 (MD=2.7°, $p<0.05$) while at follow-up off-orthosis in group 3 (MD=4.1°, $p<0.05$). Significantly diminished lumbar lordosis was only seen at immediate in-orthosis and follow-up off-orthosis in group 3 (MD=6.2°/5.5°, $p<0.05$).

Group 2 showed a higher success rate than group 3 based on coronal-Cobb (90.5% *vs.* 83.3%), PMC-Cobb (85.7% *vs.*84.8%), and PMC-orientation (71.4% *vs.* 57.6%) (Table 6.12). No significant difference was observed between the success rates of the 2 groups ($p>0.05$).

Table 6.11 Mean and standard deviation of different parameters in different groups (substudy II – primary and secondary curves)

	Curves, n	Coronal-Cobb (°)	PMC-Cobb (°)	PMC-orientation (°)	Thoracic kyphosis (°)	Lumbar lordosis (°)
Group 2					(n=21, 21, 17)	(n=5, 5, 3)
Pre-orthosis	26	21.9 ± 7.4	31.7 ± 11.0	53.2 ± 22.5	23.4 ± 12.8^	54.0 ± 3.7
In-orthosis	26	17.1 ± 8.0^	25.3 ± 9.6^	51.1 ± 25.7	20.7 ± 11.0^	43.6 ± 8.4
Off-orthosis	21	21.3 ± 12.2	29.5 ± 12.6	52.5 ± 23.2	19.1 ± 8.8	48.6 ± 20.0
Group 3					(n= 31, 31, 22)	(n= 53, 53, 43)
Pre-orthosis	84	21.9 ± 6.9^	34.8 ± 12.0^	45.0 ± 20.5	25.3 ± 12.2^	53.0 ± 9.3^
In-orthosis	84	17.1 ± 7.4^	28.8 ± 10.7^	43.4 ± 22.3	24.2 ± 12.0	46.8 ± 8.3
Off-orthosis	66	19.3 ± 9.4^	31.7 ± 11.5^	44.3 ± 23.8	24.0 ± 14.8^	47.4 ± 9.7

^: in a group, the marked value significantly differs from the other two values ($p<0.05$).

^^ or ^^^: in a group, these marked values significantly differ from each other($p<0.05$).

#: inter-group difference was significant ($p<0.05$).

Note: too small sample size in groups 1 and 4, so data analysis was not performed for these 2 groups.

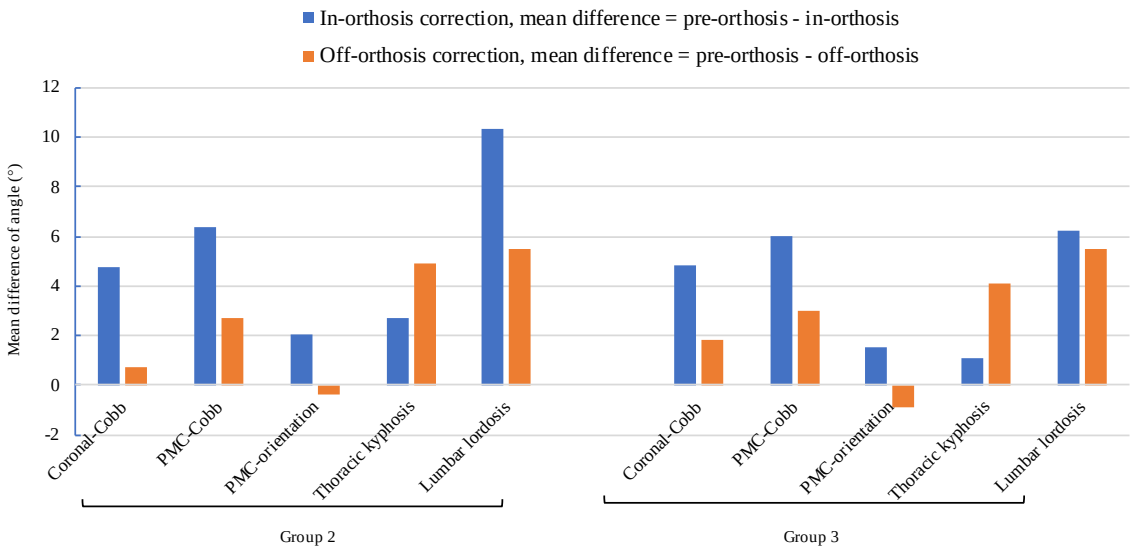

Figure 6.11 Correction at immediate in-orthosis and follow-up off-orthosis in groups 2 and 3 (substudy II – primary and secondary curves)

Table 6.12 Success and failure rates based on different parameters in different groups (substudy II – primary and secondary curves)

	Curves, n	Coronal-Cobb	PMC-Cobb	PMC-orientation
Group 2				
Success rate (n)	21	**90.5% (19)**	**85.7% (18)**	71.4% (15)
Failure rate (n)		9.5% (3)	14.3% (4)	28.6% (6)
Group 3				
Success rate (n)	66	83.3% (55)	84.8% (56)	57.6% (38)
Failure rate (n)		16.7% (11)	15.2% (10)	42.4% (28)

Curve progression = pre-orthosis – follow-up off-orthosis

Success rate: the percentage of subjects/curves with curvature/PMC-orientation progression ≤5°

Failure rate: the percentage of subjects/curves with curvature/PMC-orientation progression ≥6° or curve ≥45°

#: inter-group difference was significant ($p<0.05$).

Note: too small sample size in groups 1 and 4, so data analysis was not performed for these two groups.

Primary and Secondary Curves (with subgroups of thoracic and (thoraco)lumbar curves)

Clinical Efficacy (correction and success/failure rate)

For the thoracic curves, Table 6.13 and Figure 6.12 showed significantly diminished coronal-Cobb (MD=4.6°/2.3°, $p<0.05$) and PMC-Cobb (MD=5.3°/2.1°, $p<0.05$) at immediate in-orthosis in groups 2 and 3. By contrast, there was no significant reduction in PMC-orientation at either immediate in-orthosis or follow-up off-orthosis in the two groups ($p>0.05$). Besides, significantly reduced thoracic kyphosis was seen at immediate in-orthosis in group 2 (MD=2.7°, $p<0.05$), but at follow-up off-orthosis in group 3 (MD=4.1°, $p<0.05$). Table 6.14 presented higher success rate in group 2 as compared to group 3 according to coronal-Cobb (88.2% *vs.* 73.9%, $p>0.05$), PMC-Cobb (88.3% *vs.* 78.3%, $p>0.05$), and PMC-orientation (70.6% *vs.* 43.5%, $p>0.05$).

Regarding the (thoraco)lumbar curves, a significant reduction in coronal-Cobb (MD=5.8°/6.3°, $p<0.05$) and PMC-Cobb (MD=10.7°/8.3°, $p<0.05$) was observed at immediate in-orthosis in groups 2 and 3. PMC-orientation did not significantly alter after orthosis fitting ($p>0.05$). Moreover, significantly decreased lumbar lordosis was only found at immediate in-orthosis and follow-up off-orthosis in group 3 (MD=5.8°/5.5°, $p<0.05$). In comparison with group 3, group 2 demonstrated a higher success rate according to coronal-Cobb (100% *vs.* 88.4%) and PMC-orientation (75.0% *vs.* 65.1%), but a lower success rate based on PMC-Cobb (75.0% *vs.* 88.4%).

Table 6.13 Mean and standard deviation of different parameters in different groups (substudy II – primary and secondary curves with subgroups of thoracic and (thoraco)lumbar curves)

	Thoracic curves					(Thoraco)lumbar curves				
	Curves, n	**Coronal-Cobb (°)**	**PMC-Cobb (°)**	**PMC-orientation (°)**	**Thoracic kyphosis (°)**	**Curves, n**	**Coronal-Cobb (°)**	**PMC-Cobb (°)**	**PMC-orientation (°)**	**Lumbar lordosis (°)**
Group 2										
Pre-orthosis	21	23.0 ± 7.5	29.9 ± 9.8^	57.0 ± 19.6	23.4 ± 12.8^	5	17.5 ± 5.4^	39.2 ± 13.4^	37.2 ± 29.4	54.0 ± 3.7
In-orthosis	21	18.4 ± 8.2^	24.6 ± 9.4^	54.8 ± 23.9	20.7 ± 11.0^	5	11.7 ±5.8^	28.5 ± 10.9^	35.8 ± 30.0	43.6 ± 8.4
Off-orthosis	17	23.2 ± 12.4	27.6 ± 11.7	57.0 ± 20.0	19.1 ± 8.8	4	13.0 ± 7.2	37.3 ± 15.5	33.3 ± 28.8	48.6 ± 20.0
Group 3										
Pre-orthosis	31	21.4 ± 8.3^	29.8 ± 8.9^	49.3 ± 19.7	25.3 ± 12.2^	53	22.2 ± 6.0^	37.8 ± 12.7^	42.4 ± 20.7	53.0 ± 9.3^
In-orthosis	31	19.1 ±8.8^	27.7 ± 9.5^	48.6 ± 20.9	24.2 ± 12.0	53	15.9 ± 6.2^	29.5 ± 11.5^	40.4 ± 22.8	46.8 ± 8.3
Off-orthosis	23	20.3 ± 11.5	29.1 ± 11.7	51.0 ± 25.3	24.0 ± 14.8^	43	18.7 ± 8.1^	33.1 ± 11.3^	40.7 ± 22.4	47.4 ± 9.7

^: in a group, the marked value significantly differs from the other two values (p<0.05).

^^ or ^^^: in a group, these marked values significantly differ from each other(p<0.05).

#: inter-group difference was significant (p<0.05).

Note: too small sample size in group 1 and 4, so data analysis was not performed for these two groups.

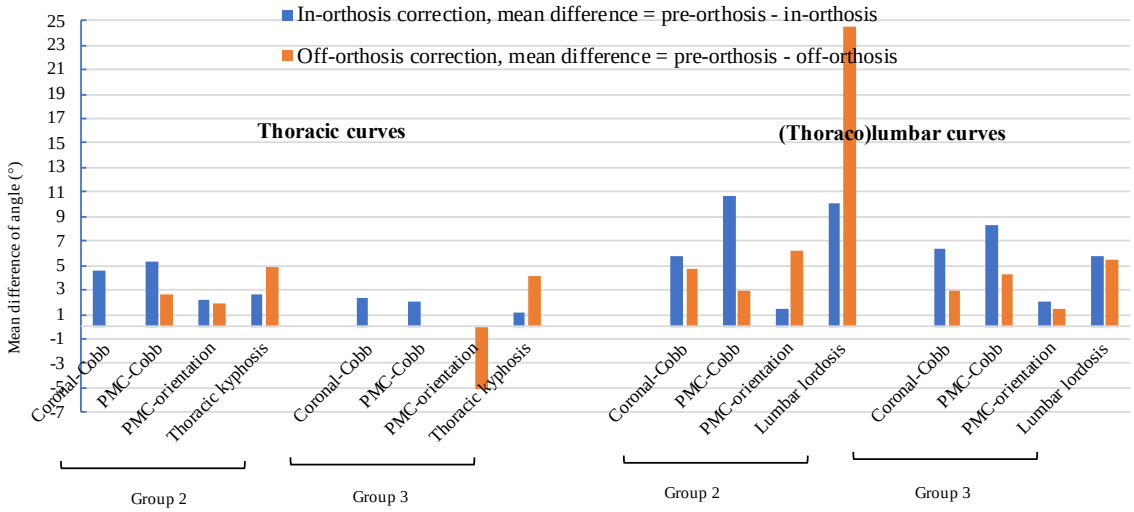

Figure 6.12 Correction at immediate in-orthosis and follow-up off-orthosis in groups 2 and 3 (substudy II – primary and secondary curves with subgroups of thoracic and (thoraco)lumbar curves)

Table 6.14 Success and failure rates based on different parameters in different groups (substudy II – primary and secondary curves with subgroups of thoracic and (thoraco)lumbar curves)

	Thoracic curves				(Thoraco)lumbar curves			
	Curves, n	**Coronal-Cobb**	**PMC-Cobb**	**PMC-orientation**	**Curves, n**	**Coronal-Cobb**	**PMC-Cobb**	**PMC-orientation**
Group 2								
Success rate (n)	17	**88.2% (15)**	**88.2% (15)**	**70.6% (12)**	4	**100% (4)**	75.0% (3)	**75.0% (3)**
Failure rate (n)		11.8% (2)	11.8% (2)	29.4% (5)		0%	25.0% (1)	25.0% (1)
Group 3								
Success rate (n)	23	73.9% (17)	78.3% (18)	43.5% (10)	43	88.4% (38)	**88.4% (38)**	65.1% (28)
Failure rate (n)		26.1 % (6)	21.7% (5)	56.5% (13)		11.6% (5)	11.6% (5)	34.9% (15)

Curve progression = pre-orthosis – follow-up off-orthosis

Success rate: the percentage of subjects/curves with curvature/PMC-orientation progression ≤5°

Failure rate: the percentage of subjects/curves with curvature/PMC-orientation progression ≥6° or curve ≥45°

#: inter-group difference was significant (p<0.05).

Note: too small a sample size in groups 1 and 4, so data analysis was not performed for these two groups.

6.3.3 Substudy III

Primary Curves Only

Subjects

According to grouping criteria, 44 and 37 subjects were assigned into PMC and non-PMC groups, respectively (Table 6.15). The 2 groups had comparable baselines. Table 6.16 presented the mean ± standard deviation of coronal-Cobb, PMC-Cobb, PMC-orientation, thoracic kyphosis, and lordosis at pre-orthosis, immediate in-orthosis, and follow-up off-orthosis visits.

Clinical Efficacy (correction and success/failure rate)

Table 6.16 and Figure 6.13 showed significantly diminished coronal-Cobb was observed at immediate in-orthosis in PMC and non-PMC groups (MD=4.4°/5.0°, $p<0.05$). A PMC-Cobb was significantly decreased at the immediate in-orthosis and follow-up off-orthosis in the 2 groups (MD=5.1°–5.5° / 3.1°–3.5°, $p<0.05$). However, PMC-orientation was not significantly changed after orthosis fitting ($p > 0.05$). Thoracic kyphosis was significantly reduced at immediate in-orthosis and follow-up off-orthosis in the PMC group (MD=0.7°/3.1°, $p<0.05$), however, only slightly faltered in the non-PMC group. A significant reduction in lumbar lordosis was seen at immediate in-orthosis and follow-up off-orthosis in the 2 groups (MD=5.1°–8.7° / 4.6°–9.0°, $p<0.05$). Based on coronal-Cobb and PMC-Cobb (Table 6.17), a high success rate was found in the 2 groups (87.8%–81.8%). By contrast, success and failure rates based on PMC-orientation,were similar in the 2 groups. Additionally, no significant difference was observed between the success rates of the 2 groups ($p>0.05$).

Table 6.15 Characteristics of subjects selected into PMC and non-PMC groups (substudy III – primary curves only)

	PMC group	Non-PMC group
Subjects, n	44	37
Gender, male/female	15/29	11/26
Age, mean ± SD (range) (yrs)	13.7 ± 1.7 （10.5–17.0）	13.6 ± 1.6 （10.0–18.0）
Primary curves, n	44	44
Coronal-Cobb, mean ± SD (range) (°)	23.3 ± 6.0 (16.6–38.7)	21.5 ± 7.0 (15.3–40.4)

Table 6.16 Mean and standard deviation of different parameters in different groups (substudy III – primary curves only)

	Primary curves, n	Coronal-Cobb (°)	PMC-Cobb (°)	PMC-orientation (°)	Thoracic kyphosis (°)	Lumber-lordosis (°)
PMC group						
Pre-orthosis	44	23.3 ± 6.0	34.3 ± 9.5^	46.3 ± 15.4	22.3 ± 9.9	51.3 ± 9.4^
In-orthosis	44	18.9 ± 7.7^	29.2 ± 7.2	43.5 ± 19.6^	21.6 ± 9.3^	46.2 ± 7.6
Off-orthosis	33	21.5 ± 8.8	31.1 ± 10.0	51.6 ± 30.0^	20.3 ± 8.4^	46.2 ± 10.0
Non-PMC group						
Pre-orthosis	37	21.5 ± 7.0	31.9 ± 13.1^	54.0 ± 26.7	22.3 ± 13.5	55.6 ± 9.7^
In-orthosis	37	16.5 ± 7.8^	26.4 ± 13.1	50.5 ± 26.5	21.7 ± 12.7	46.9 ± 9.5
Off-orthosis	33	19.2 ± 10.6	29.5 ± 12.5	51.3 ± 25.6	22.1 ± 14.3	47.2 ± 11.3

^: in a group, the marked value significantly differs from the other two values (p<0.05).

^^ or ^^^: in a group, these marked values significantly differ from each other(p<0.05).

#: inter-group difference was significant (p<0.05).

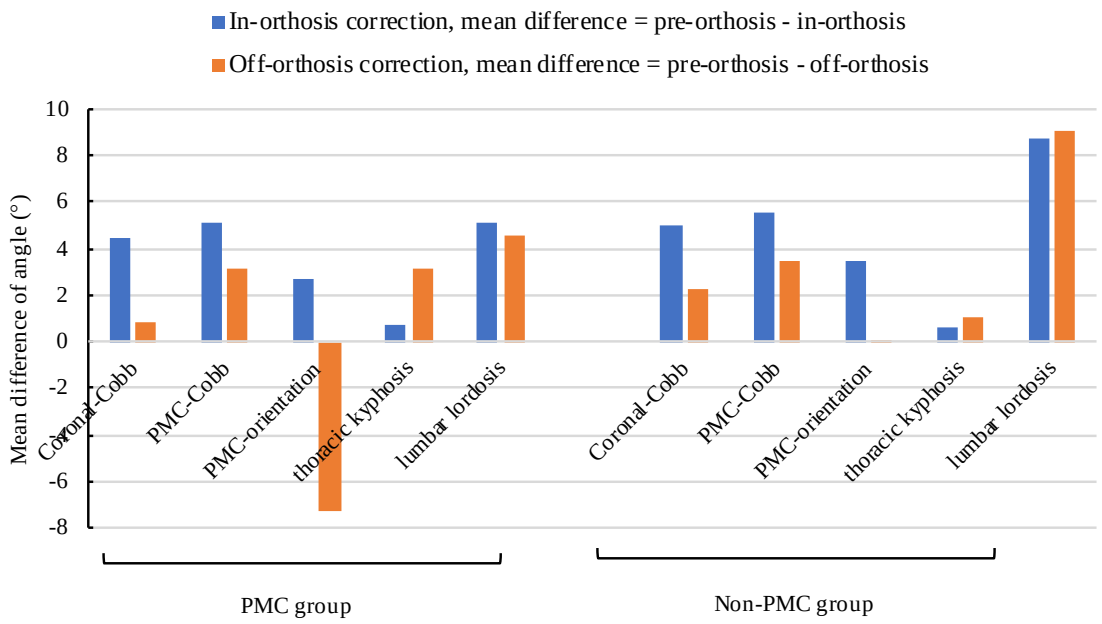

Figure 6.13 Correction at immediate in-orthosis and follow-up off-orthosis in PMC and non-PMC groups (substudy III – primary curves only)

Table 6.17 Success and failure rates based on different parameters in different groups (substudy III – primary curves only)

	Subjects, n	Coronal-Cobb	PMC-Cobb	PMC-orientation
PMC group				
Success rate (n)	33	81.8% (27)	84.8% (28)	51.5% (17)
Failure rate (n)		18.2% (6)	15.2% (5)	48.5% (16)
Non-PMC group				
Success rate (n)	33	87.8% (29)	84.8% (28)	60.6% (20)
Failure rate (n)		12.2% (4)	15.2% (5)	39.4% (13)

Curve progression = pre-orthosis – follow-up off-orthosis

Success rate: percentage of subjects with curve/PMC-orientation progression ≤5°

Failure rate: percentage of subjects with curve/PMC-orientation progression ≥6° or curve ≥45°

Primary and Secondary Curves

Clinical Efficacy (correction and success/failure rate)

Table 6.18 and Figure 6.14 presented a significantly reduced coronal-Cobb was observed at immediate in-orthosis in the PMC and non-PMC groups (MD=4.5°/5.0°, $p<0.05$). PMC-Cobb was significantly decreased at immediate in-orthosis and follow-up off-orthosis in the 2 groups (MD=6.0°–6.2° / 2.4°–4.2°, $p<0.05$); differently, no significant alterations were found in PMC-orientation ($p>0.05$). Additionally, a significant decrease in thoracic kyphosis was only observed at follow-up off-orthosis in the PMC group (MD=6.1°, $p<0.05$). By contrast, lumbar lordosis was significantly decreased at immediate in-orthosis and follow-up off-orthosis in the 2 groups (MD=5.7°–7.4° / 5.2°–6.7°, $p<0.05$).

Based on coronal-Cobb and PMC-Cobb (Table 6.19), a similar success rate was seen in the 2 groups (83.7%–87.0%). However, the success and failure rates were similar according to PMC-orientation. No significant difference between the success rates was found between the 2 groups ($p>0.05$).

Table 6.18 Mean and standard deviation of different parameters in different groups (substudy III – primary and secondary curves)

	Curves, n	Coronal-Cobb (°)	PMC-Cobb (°)	PMC-orientation (°)	Thoracic kyphosis (°)	Lumbar lordosis (°)
PMC group					(n=31, 31, 21)	(n=29, 29, 22)
Pre-orthosis	60	23.0 ± 5.8	35.1 ± 10.7^	44.8 ± 15.3	24.6 ± 9.2	52.3 ± 10.3^
In-orthosis	60	18.5 ± 7.4^,#	28.9 ± 8.6	44.2 ± 19.8^	22.5 ± 9.0	44.9 ± 9.1
Off-orthosis	43	20.9 ± 8.6	30.4 ± 10.0	47.7 ± 19.9^	20.6 ± 7.0^	45.1 ± 10.5
Non-PMC group					(n=28, 28, 23)	(n=34, 34, 28)
Pre-orthosis	63	20.6 ± 7.8	33.2 ± 12.6^	48.2 ± 25.8	23.1 ± 14.9	53.8 ± 7.3^
In-orthosis	63	15.6 ± 7.4^,#	27.2 ± 11.6^	44.9 ± 26.2	22.1 ± 14.0	48.0 ± 6.9
Off-orthosis	54	18.4 ± 10.5	31.3 ± 13.1^	44.6 ± 25.3	22.4 ± 15.9	48.9 ± 9.4

^: in a group, the marked value significantly differs from the other two values ($p<0.05$).

^^ or ^^^: in a group, these marked values significantly differ from each other($p<0.05$).

#: inter-group difference was significant ($p<0.05$).

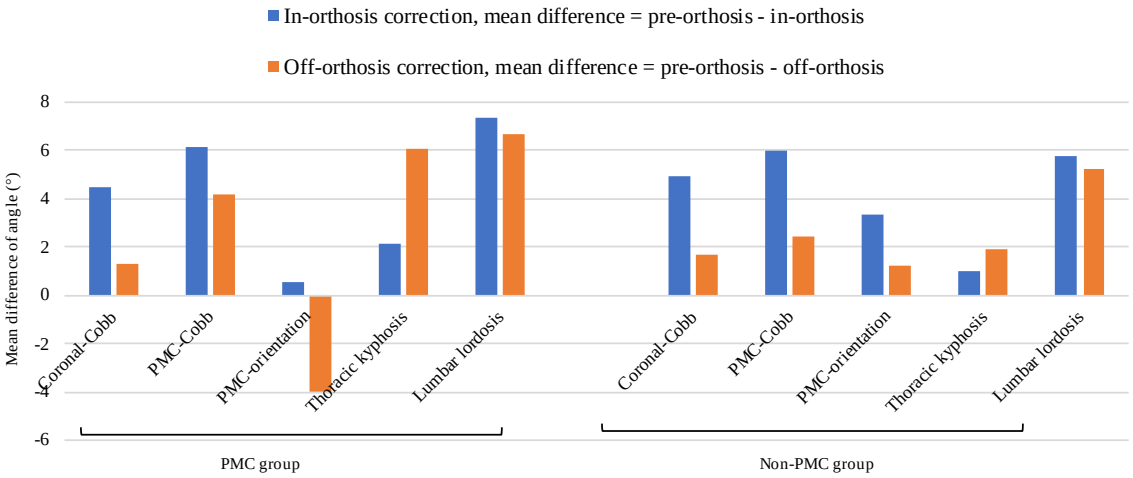

Figure 6.14 Correction at immediate in-orthosis and follow-up off-orthosis in PMC and non-PMC groups (substudy III – primary and secondary curves)

Table 6.19 Success and failure rates based on different parameters in different groups (substudy III – primary and secondary curves)

	Curves, n	Coronal-Cobb	PMC-Cobb	PMC-orientation
PMC group				
Success rate (n)	43	83.7% (36)	**88.4% (38)**	48.8% (21)
Failure rate (n)		16.3% (7)	11.6% (5)	51.2% (22)
Non-PMC group				
Success rate (n)	54	**87.0% (47)**	83.3% (45)	68.5% (37)
Failure rate (n)		13.0% (7)	16.7% (9)	31.5% (17)

Curve progression = pre-orthosis – follow-up off-orthosis

Success rate: the percentage of subjects/curves with curvature/PMC-orientation progression ≤5°

Failure rate: the percentage of subjects/curves with curvature/PMC-orientation progression ≥6° or curve ≥45°

#: inter-group difference was significant (p<0.05).

Primary and Secondary Curves (with subgroups of thoracic and (thoraco)lumbar curves)

Clinical Efficacy (correction and success/failure rate)

For the thoracic curves, Table 6.20 and Figure 6.15 significantly diminished coronal-Cobb was observed at immediate in-orthosis in PMC and non-PMC groups (MD=2.9°/3.5°, $p<0.05$). A significant decrease PMC-Cobb was found at immediate in-orthosis and follow-up off-orthosis in the 2 groups (MD=2.9°–3.2° / 0.2°–3.1°, $p<0.05$). PMC-orientation was not significantly changed after orthosis fitting ($p>0.05$). Significantly reduced thoracic kyphosis was only seen at follow-up off-orthosis in the PMC group (MD=6.1°, $p<0.05$). Table 6.21 demonstrated a higher success rate in the PMC group compared to non-PMC group according to coronal-Cobb (81.0% *vs.* 79.2%, $p>0.05$) and PMC-Cobb (90.5% *vs.* 75.0%, $p>0.05$). PMC-orientation-based success and failure rates were similar between the 2 groups.

For (thoraco)lumbar curves, a significantly reduced coronal-Cobb was seen at immediate in-orthosis in the 2 groups (MD=6.2°–6.1°, $p<0.05$). A significant decrease PMC-Cobb was noted at immediate in-orthosis and follow-up off-orthosis (MD=8.2°–9.7° / 4.2°–5.2°, $p<0.05$). By contrast, only some fluctuations were found in PMC-orientation in the 2 groups ($p>0.05$). Additionally, lumbar lordosis was significantly diminished at immediate in-orthosis and follow-up off-orthosis in the 2 groups (MD=5.7°–7.4° / 5.2°–6.7°, $p<0.05$). Non-PMC group tended to have a higher success rate than PMC group according to coronal-Cobb (93.3% *vs.* 86.4%, $p>0.05$), PMC-Cobb (90.0% *vs.* 86.4%, $p>0.05$) and PMC-orientation (73.3% *vs.* 50.0%, $p>0.05$). Success and failure rates were the same in the PMC group.

Table 6.20 Mean and standard deviation of different parameters in different groups (substudy III – primary and secondary curves with subgroups of thoracic and (thoraco)lumbar curves)

	Thoracic curves					(Thoraco)lumbar curves				
	Curves, n	**Coronal-Cobb (°)**	**PMC-Cobb (°)**	**PMC-orientation (°)**	**Thoracic kyphosis (°)**	**Curves, n**	**Coronal-Cobb (°)**	**PMC-Cobb (°)**	**PMC-orientation (°)**	**Lumbar lordosis (°)**
PMC group										
Pre-orthosis	31	24.2 ± 6.2$^{\#}$	31.6 ± 7.8$^{\wedge}$	52.6 ± 13.8	24.6 ± 9.2	29	21.8 ±5.3	38.8 ± 12.2$^{\wedge}$	36.4 ± 12.2	52.3 ± 10.3$^{\wedge}$
In-orthosis	31	21.3 ± 7.1$^{\wedge,\#}$	28.8 ± 6.6	51.2 ± 18.2$^{\wedge}$	22.5 ± 9.0	29	15.6 ± 6.6$^{\wedge}$	29.1 ± 10.4$^{\wedge}$	36.8 ± 19.1	44.9 ± 9.1
Off-orthosis	21	23.5 ± 9.1	28.5 ± 9.5	57.8 ± 15.6$^{\wedge}$	20.6 ± 7.0$^{\wedge}$	22	18.4 ± 7.5	32.3 ± 10.3$^{\wedge}$	38.0 ± 19.0	45.1 ± 10.5
Non-PMC group										
Pre-orthosis	28	19.7 ± 8.7$^{\#}$	27.4 ± 9.2	53.7 ± 25.3	23.1 ± 14.9	35	21.3 ± 7.1$^{\wedge}$	37.9 ± 13.0$^{\wedge}$	43.8 ± 25.7	53.8 ± 7.3$^{\wedge}$
In-orthosis	28	16.1 ± 8.9$^{\wedge,\#}$	24.1 ± 11.1$^{\wedge}$	50.0 ± 26.7	22.1 ± 14.0	35	15.2 ± 6.0$^{\wedge}$	29.7 ± 11.7$^{\wedge}$	40.9 ± 25.3	48.0 ± 6.8
Off-orthosis	24	19.0 ± 12.9	27.7 ± 13.0	49.3 ± 26.6	22.4 ± 15.9	30	18.0 ± 8.3$^{\wedge}$	34.2 ± 12.6$^{\wedge}$	41.0 ± 24.0	48.9 ± 9.4

^: in a group, the marked value significantly differs from the other two values (p<0.05).

^^ or ^^^: in a group, these marked values significantly differ from each other(p<0.05).

#: inter-group difference was significant (p<0.05).

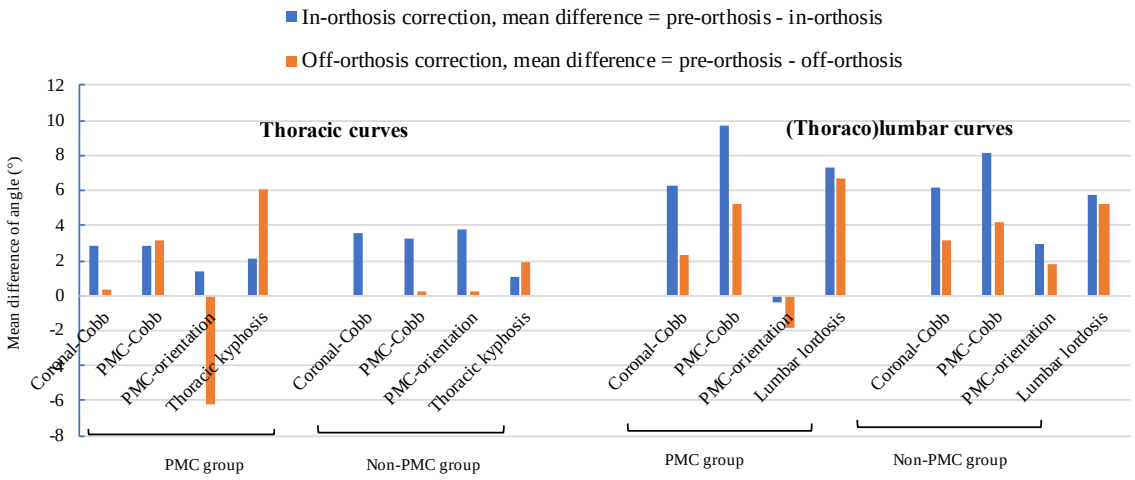

Figure 6.15 Correction at immediate in-orthosis and follow-up off-orthosis in PMC and non-PMC groups (substudy III – primary and secondary curves with subgroups of thoracic and (thoraco)lumbar curves)

Table 6.21 Success and failure rates based on different parameters in different groups (substudy III – primary and secondary curves with subgroups of thoracic and (thoraco)lumbar curves)

	Thoracic curves				(Thoraco)lumbar curves			
	Curves, n	**Coronal-Cobb**	**PMC-Cobb**	**PMC-orientation**	**Curves, n**	**Coronal-Cobb**	**PMC-Cobb**	**PMC-orientation**
PMC group								
Success rate (n)	21	81.0% (17)	90.5% (19)	47.6% (10)	22	86.4% (19)	86.4% (19)	50.0% (11)
Failure rate (n)		19.0% (4)	9.5% (2)	52.4% (11)		13.6% (3)	13.6% (3)	50.0% (11)
Non-PMC group								
Success rate (n)	24	79.2% (19)	75.0% (18)	62.5% (15)	30	93.3% (28)	90.0% (27)	73.3% (22)
Failure rate (n)		20.8% (5)	25.0% (6)	37.5% (9)		6.7% (2)	10.0% (3)	26.7% (8)

Curve progression = pre-orthosis – follow-up off-orthosis

Success rate: the percentage of subjects/curves with curvature/PMC-orientation progression ≤5°

Failure rate: the percentage of subjects/curves with curvature/PMC-orientation progression ≥6° or curve ≥45°

#: the inter-group difference was significant (p<0.05).

6.4 Discussion

Spinal orthosis was basically designed empirically and mainly corrected coronal-Cobb, which may not meet the expectations of 3D correction of AIS. This study investigated the optimal biomechanical design of spinal orthosis to enhance the orthotic management of AIS. Substudies I, II, and III separately focused on the correcting-force direction generated by the pressure pad inside orthosis, pressure-pad shapes inside the spinal orthosis, and the PMC concept applied to orthosis design. Data were statistically analysed for the primary curves (1st way), primary and secondary curves (2nd way), and thoracic and (thoraco)lumbar curves (3rd way) of each substudy. The results of the 1st way served as a priority, to which the results of the 2nd and 3rd ways were employed as supplement.

6.4.1 Substudy I

According to the 1st and 2nd ways results, coronal-Cobb was significantly reduced at immediate in-orthosis in groups A, C, D, and E (p<0.05). Group A presented significantly decreased PMC-Cobb at the immediate in-orthosis and follow-up off-orthosis; however, groups C and E (and D) showed significant correction only at immediate in-orthosis. These results suggested a positive effect of orthoses on the correcting spinal curvature, which was consistent with earlier reports [226,255]. Furthermore, group A had the highest success rates according to coronal-Cobb and PMC-Cobb, followed by groups E and C (group D was not considered as its sample size was too small, n=6/9). Considering correction and success rate, group A demonstrated superior clinical efficacy to other analysed groups in correcting coronal-Cobb and PMC-Cobb. Changes in sagittal curves were also noted. Group A presented significantly decreased thoracic kyphosis (p<0.05). By comparison, a significant reduced lumbar lordosis was observed in all the analysed groups (p<0.05), suggesting all the studied pressure-pad could effectively correct the lumbar lordosis. Musculoskeletal structure of thoracic spine and rib cage was complex and stable, which make it more difficult to be re-aligned. By comparison, lumbar spine's structure seems relatively simple and flexible, making it easier be re-aligned. Combining correction of coronal and sagittal curvature, shape A appeared more effectve in controlling curves acompanied by thoracic hyper-kyphosis (>40° [97]) comapred to shapes C and E. By

comtrast, shape E seemed to be more helpful for curves combined with thoracic hypo/normal-kyphosis (≤40° [97]).

6.4.2 Substudy II

No significant results were found in group 4 (p>0.05), which may attribute to its small sample size (n=5/4). Regarding the results of groups 2 and 3, significantly decreased coronal-Cobb and PMC-Cobb was found at immediate in-orthosis (p<0.05). Group 2 presented a slightly higher success rate than group 3 based on the coronal-Cobb and PMC-Cobb separately. Combining curve correction and success rate, correcting force in zone 2 seemed more effective on correcting the spinal curvature compared to that in zone 3 (p>0.05). Regarding the sagittal profile, thoracic kyphosis was significantly diminished at immediate in-orthosis and follow-up off-orthosis in group 2 (p<0.05) but only not significantly wobbled in group 3 (p>0.05). This suggested that correcting force in zone 2 may worsen thoracic hypo-kyphosis (<10° [97]), but may be helpful for controlling hyper-kyphosis (>40° [97]). By comparison, correcting force in zone 3 had less effect on thoracic kyphosis. Additionally, a significant decrease in the sagittal lumbar lordosis was found at immediate in-orthosis and follow-up off-orthosis in groups 2 and 3. This suggested that correcting force in either zone 2 or zone 3 could efficiently control the lumbar lordosis. Considering the correction in spine's coronal and sagittal profiles, correcting force in zone 2 may be more effective for controlling curves combined with thoracic hyper-kyphosis (>40° [97]); and correcting force in zone 3 may be more helpful for those accompanied with thoracic hypo-/normal-kyphosis (<40° [97]).

6.4.3 Substudy III

Significant decreases in coronal-Cobb and PMC-Cobb were observed in all the PMC and non-PMC groups (p<0.05). This finding was in line with the results of substudies I&II. Unexpectedly, the non-PMC group tended to have higher success rates compared to the PMC group based on the coronal-Cobb and PMC-Cobb (p>0.05). But thi may not mean that the PMC concept was usless in spinal orthosis design. The PMC was estimated from the subjects' EOS images, which may be somewhat different from the PMC in the posture used for the CAD/CAM scan. Besides, this substudy only involved the correcting-force

direction on the convex side of the spinal curves in analysis while ignoring some confounding factors, sch as correcting-force level and counter-forces as well as subjects' spinl flexibility and compliance. The continuous prospective study with those confounding factors controlled and parameters in the coronal, sagittal, and transverse planes analysed will be conducted to better understanding PMC's application in spinal orthosis design. For the sagittal profile, thoracic kyphosis was significantly diminished at immediate in-orthosis in the PMC group (p<0.05). This indicated that correcting force in the PMC zone may worsen thoracic hypo-kyphosis (<10°); however, it may effectively control the thoracic hyper-kyphosis. The lumbar lordosis was significantly lessened in the two groups (p<0.05), which was similar to the reports of substudies I&II.

PMC-orientation was not significantly cerrected after orthosis fitting in all the substudies, which was similar to the earlier reports [48,49]. This may be because of the spine's complexed musculoskeletal structure and orthotic biomechanical design. For instance, a posterolateral correcting force was usually applied on the rib, through which the force was transferred to the scoliotic spine. The correcting force could be changed during the transferring process and did not produce a correction as expected. It was thereby necessary to have a deeper investigation for this. Additionally, coronal-Cobb measured from the coronal plane was a component of the actual curvature. It could be affected by the actual curvature and rotation of the curve. Hence, it could not tell whether a correction in coronal-Cobb results from the decrease in the actual curvature or the rotation of the curve towards the coronal plane. With the supplement of PMC, it could be known that the significantly corrected coronal-Cobb mainly resulted from the significantly decreased PMC-Cobb other than the PMC-orientation. During correction evaluation of treatment, if only the coronal-Cobb was applied, the spinal curvature may be changed abnormally. For instance, if a case's lateral curvature only results from the rotation of the spinal segment towards the coronal plane other than the spinal curvature. In this case, it may be necessary to correcting the rotation of the spinal curve, pushing the spinal segnment back to the sagittal plane, instead of decreasing the spinal curvature. Therefore, it should employ the PMC-Cobb and PMC-orientation as the supplements to the coronal-Cobb to better understand the

deformities (spinal curvature & rotation of spinal curve) and make an appropiate clinical decision during managing AIS.

6.4.4 Biomechanical Analysis for Substudies I, II & III

This section gave some possible explanations for the findings of the three substudies from the biomechanical view: (1) shape A and correcting force in zone 2 provided superior clinical efficacy, but a significant decrease in the sagittal thoracic kyphosis as compared to shape E and correcting force in zone 3; (2) the sagittal thoracic kyphosis was significantly reduced only in some analysis groups, but lumbar lordosis was diminished in all the analysed groups (except some groups involving with too small sample size); (3) the degree of the curve rotated towards the coronal plane (PMC-orientation) was not significantly altered after fitting orthosis; (4) whether the PMC concept could improve the clinical efficacy. To better understand its rationales, this section first introduced the possible biomechanical mechanism of correction.

A “dorsolateral to ventromedial” force combined with other counter-forces is commonly used to control spinal deformities. A “dorsolateral to ventromedial” force is composed of dorsoventral and lateromedial components. The dorsoventral force was considered to control the VAR and rib hump; however, it could also be used to reduce the curve magnitude when working with relevant ventrodorsal forces. A greater dorsoventral force could better decrease the curve magnitude (PMC-Cobb), resulting in decreased coronal-Cobb and sagittal-Cobb (thoracic kyphosis & lumbar lordosis). The lateromedial force may push the curve segment towards the sagittal plane, reducing the PMC-orientation. A greater lateromedial force may reduce PMC-orientation, generating smaller coronal-Cobb, but greater sagittal-Cobb (thoracic kyphosis/lumbar lordosis).

(1) Shape A and correcting force in zone 2 provided superior clinical efficacy but a significant decrease in the sagittal thoracic kyphosis in comparison with shape E and correcting force in zone 3.

According to the superiority of clinical efficacy, different analysed groups could be ordered as follows: group A > E > C & D in substudy I, and group 2 > 3 in substudy II. As shown

in Table 6.22, those showing superior clinical efficacy tended to have correcting forces closer to the sagittal plane (group A *vs.* E *vs.* C/D = 36.9° *vs.* 51.1° *vs.* 57.3°/57.0° in substudy I; group 2 *vs.* 3 = 33.0° *vs.* 52.4° in substudy II). A more medial correcting force could generate a greater dorsoventral component, better reducing the curve magnitude. This could also be why sagittal thoracic kyphosis was significantly diminished in these groups. By contrast, those providing slightly inferior clinical efficacy had correcting force closer to the coronal plane, and it may produce a smaller dorsoventral component, resulting in a relatively inferior reduction/correction in curve magnitude.

Table 6.22 Mean and standard deviation of direction of correcting force and of PMC-orientation at pre-orthosis in different analysed groups of the three substudies (substudies I, II & III – primary curves only)

	Curves, n	Direction of correcting force (°)	PMC-orientation (°)
Substudy I			
Shape A (group A)	25	**36.9 ± 10.8**	51.0 ± 21.5
Shape C (group C)	23	57.3 ± 7.6	52.2 ± 18.0
Shape D (group D)	7	57.0 ± 6.1	45.3 ± 32.2
Shape E (group E)	24	**51.1 ± 4.7**	50.1 ± 21.5
Substudy II			
Zone 2 (group 2)	17	**33.0 ± 6.4**	57.5 ± 21.5
Zone 3 (group 3)	56	**52.4 ± 5.9**	47.8 ± 20.6
Zone 4 (group 4)	5	70.2 ± 1.9	61.0 ± 25.7
Substudy III			
PMC Zone (PMC group)	44	46.1 ± 13.2	46.3 ± 15.4
Non-PMC zone (Non-PMC group)	37	**51.8 ± 11.0**	54.0 ± 26.7

Orientation of sagittal plane =0°; Orientation of coronal plane =90°

Note: for better understanding, this table record all the direction of correcting force and PMC-orientation as absolute values (the angle between the direction of correcting force & PMC and the sagittal plane) no matter is was either clockwise (+) or counter-clockwise (-) rotation seeing from the top view. In the real case, the values were considered the positive (+) for the left curve and considered the negative (-) for the right curve.

(2) The sagittal thoracic kyphosis was significantly reduced only in some analysis groups but lumbar lordosis was diminished in all the analysed groups (except some groups involving with small sample size).

Compared with the sagittal thoracic kyphosis, lumbar lordosis was significantly decreased in almost all the analysed groups (except some groups with a small sample size). There may be two additional reasons besides the effect of "dorsolateral to ventromedial"

correcting force. Increased intra-abdominal pressure could effectively correct the lumbar lordosis (the orthosis selected in this study was rigid Hong Kong orthosis with an abdominal pad). Moreover, the lumbar region has a more flexible anatomical structure, allowing lateral and forward/backward bending and axial rotation, which makes it easier to be re-modeled/re-aligned. By comparison, besides the soft issues around, the thoracic region is stabilized by more fixed facet joints and ribs combined with costal muscles, making it challenging to be re-aligned.

(3) The degree of the curve rotated towards the coronal plane (PMC-orientation) was not significantly altered after fitting orthosis.

The degree of the curve rotated towards the coronal plane (PMC-orientation) only wavered in all the analysed groups in the three substudies after fitting orthosis (p>0.05). Similar results were reported earlier [155,179]. A poor correction was observed in VAR and rib hump [48,49]. These results suggested not enough effect of the orthosis on the correction of transverse deformities such as PMC-orientation, VAR, and rib hump. Spinal deformities are corrected using external forces applied on and transferred to the spine through ribs and soft tissues. Because of the complicated anatomical structure of ribs and soft issues, the magnitude and direction of correcting force can be altered during the transfer, and this may be one reason that spinal deformities cannot be corrected as expected.

In comparison with groups A and 2, groups E and 3 (showing relatively inferior clinical efficacy based on coronal-Cobb & PMC-Cobb) appeared to have a slightly greater reduction in the PMC-orientation. As shown in Table 6.22, groups E and 3 had correcting force closer to the coronal plane than groups A and 2 (groups E & 3 *vs.* groups A & 2 = 51.1° & 52.4° *vs.* 36.9°& 33.0°). A more lateral correcting force may generate a greater lateromedial component, which may better push the curve segment forwards the sagittal plane. No significant reduction being found may be due to not enough lateromedial correcting force, but the possibility of the inappropriate direction of correcting force could not be excluded.

(4) Whether the PMC concept improved clinical efficacy.

As described, PMC reflects the plane presenting the maximum spinal curvature. Theoretically, a correcting force applied in or closer to the PMC may provide better correction for the spinal curve. However, substudy III showed that correcting force in the PMC zone did not provide superior clinical efficacy to that in the non-PMC zone. Besides, no apparent relationship was found between the clinical efficacy and the proximity degree of the direction of correcting force and PMC-orientation (Table 6.22). This may be due to the complexity of anatomical structures of the spine, ribs, and soft issues around, and external correcting force may not act on the spine as expected (lie in PMC) after transferring through ribs and relevant soft tissues.

Although the correcting force in the PMC zone did not provide improved clinical efficacy as expected in this substudy, the application of PMC in correction evaluation of treatment should be valued. In a normal spine, there exist physiological curves in thoracic and lumbar regions, namely, sagittal thoracic normal-kyphosis (10°–40°) and lumbar normal-lordosis (40°–60°). The PMC overlaps with the sagittal plane (PMC-Cobb = sagittal thoracic normal-kyphosis/lumbar normal-lordosis; PMC-orientation = sagittal plane =0°; coronal-Cobb=0°). In a scoliotic spine, the thoracic/lumbar segment rotates towards the coronal plane, producing a coronal curve with or without alternating the sagittal thoracic kyphosis / lumbar lordosis. The coronal-Cobb and sagittal thoracic kyphosis / lumbar lordosis could be affected by both “actual” curve magnitude (PMC-Cobb) and the degree of a curve rotated towards the coronal plane (PMC-orientation). Decreased coronal-Cobb could result from decreased PMC-Cobb or PMC-orientation; decreased sagittal Cobb could decrease PMC-Cobb or increase PMC-orientation. For the scoliotic case without changes in the magnitude of the physiological curves (thoracic normal-kyphosis & lumber normal-lordosis), the PMC-Cobb would reflect the magnitude of the physiological curve, and PMC-orientation would present the degree of the curves rotated towards the coronal plane. In this case, orthotic intervention may target the PMC-orientation other than the PMC-Cobb or coronal-Cobb. Otherwise, pursuing decreased curve magnitude alone may decrease the magnitude of thephysiological curves, which may cause thoracic hypo-

kyphosis or lumbar hypo-lordosis. Hence, the PMC should be considered when assessing AIS and evaluating the correction of treatments.

As shown in Table 6.22, groups A and 2 had a direction of correcting force of 36.9° and 33.0°, respectively, suggesting that correcting force with a direction of 30°–40° may provide superior clinical efficacy as well as a significant reduction in sagittal thoracic kyphosis. By comparison, group E, group 3, and non-PMC group had a correcting force closer to the coronal plane (group E, group 3, non-PMC group = 51.1°, 52.4°, 51.8°). This indicates that correcting force with direction at around 50° offered slightly inferior clinical efficacy but did not cause a significant reduction in the sagittal thoracic kyphosis.

There were several limitations to this study. In substudy I, the pressure-pad shape was estimated from a transverse plane across the middle level of pressure area on the modified model of the patient's body used for spinal orthosis fabrication in the CAD/CAM system. The obtained pressure-pad shape may not always represent the shape of the pressure pads inside the spinal orthosis. Nevertheless, this substudy built a starting point for further investigation on the clinical efficacy of different pressure-pad shapes. Only the pressure pad on the convex side of the apical vertebra of the curve was considered while ignoring the counter pressure pads. In substudies II and III, the pressure of pad inside spinal orthosis applied on patient's body was assumed as hydrostatic pressure, and correcting force was estimated from a transverse plane, where the pressure-pad shape was identified in the substudy I. This may cause discrepancies between the directions of the estimated correcting force and the actual correcting force applied to the patient's body. Nevertheless, this substudy firstly estimated the correcting force from the positive models of patients' bodies in the CAD system, which would provide a new approach to understanding the correcting force applied by spinal orthoses. Furthermore, only the direction of correcting force on the convex side of the apical vertebra of the curve was studied while ignoring the counter-forces in the substudies II and III. Additionally, although the study recruited enough sample size for each substudy, some groups were not delivered with sufficient sample sizes due to the preference of spinal orthosis design in the local hospital where patients were selected. For instance, there were 2 and 7 patients' spinal orthoses designed with pressure-pad shape

B and D, respectively, among the selected 81 patients in substudy I; there were 3 and 5 patients' orthoses designed with correcting force in zone 2 and zone 4, respectively, among the selected 81 patients. A prospective study with more potential confounding factors controlled, such as patients' allocation, more number of correcting forces, patients' compliance to orthoses, will be conducted for the substudies I, II, and II when the COVID pandemic is ended.

6.5 Conclusion

Conclusions for each substudy were: (1) shapes A and E may be more beneficial to the correction of curves with sagittal thoracic hyper-kyphosis and hypo/normal-kyphosis, respectively. (2) correcting force in zones 2 and 3 may be more helpful for the correction of curves with sagittal thoracic hyper-kyphosis and hypo/normal-kyphosis, respectively. (3) correcting force in PMC zone seemed not demonstrate superior clinical efficacy to that in the non-PMC zone. Generally, correcting force with a direction at 30°–40° regarding the sagittal plane may be more suitable for curves with sagittal thoracic hyper-kyphosis. In comparison, correcting force with direction at around 50° regarding the sagittal plane may benefit curves with thoracic hypo/normal-kyphosis. These findings provided a foundation for continuous studies regarding optimizatioon of biomechanical design of spinal orthosis, enhancing the orthotic management of AIS. The Future prospective study for each substudy was recommended with more potential confounding factors controlled.

CHAPTER 7 CONCLUSIONS

Adolescent idiopathic scoliosis (AIS) has been a common disease among adolescents, which would affect their health physically and psychologically, and become a concern to families. AIS has been recognized as a three-dimensional spinal deformity for decades. coronal-Cobb serves as the golden standard in the assessment of AIS though it may underestimate its severity and not fully reveal the three-dimensional characteristics of AIS. Several three-dimensional descriptors like the best-fit plane, end-apical-end plane, and plane of maximum were proposed for AIS assessment. However, they were not commonly used clinically due to the time consumption and special skills needed of the assessment methods and the complexity of their concepts. By comparison, the plane of maximum curvature is closer to the coronal-Cobb as they reflect the spinal curvature in a vertical plane that makes the plane of maximum curvature easier to be understood and offered for meaningful applications.

In order to enhance the assessment and management of AIS, this study was to estimate the plane of maximum curvature and apply the plane of maximum curvature to enhance the orthotic management of AIS. Part I of the study proposed a computational method for estimating the plane of maximum curvature and verified it with the CT images, and analysed 3D characteristics of scoliotic spine in the standing and prone positions. Part II of the study investigated the optimal biomechanical design of spinal orthosis in terms of pressure pad shape, correcting force direction, and concept of plane of maximum curvature, for the patients with AIS using the plane of maximum curvature. The major findings are summarized as follows:

Part I

i. The proposed computational method could provide a reliable and valid plane of maximum curvature for the patients with AIS. With future effort, it believes that this method may serve as a useful tool for the three-dimensional assessment and management of AIS.

ii. The CT images served for validation references in providing reliable estimation of the plane of maximum curvature that could supplement the coronal-Cobb in managing AIS. With the development of techniques, its radiation dose could be reduced to a safer level for a broader range of patients.

iii. Prone spinal curvature was found notably smaller than but correlated with the standing spinal curvature, while the degree of the curve rotated towards the coronal plane was similar in the prone and standing positions, especially for the thoracic curves. This suggested that the gravity mainly alters the spinal curvature but did not significantly change the vertebral rotation.

Part II

iv. Shapes A and E could be more beneficial to control curves with thoracic hyper-kyphosis and hypo-/normal kyphosis, respectively.

v. The correcting force in zones 2 and 3 could be more effective in controlling the curves with thoracic hyper-kyphosis and hypo-/normal kyphosis, respectively.

vi. The correcting force in the PMC zone did not demonstrate superior effect to the non-PMC zone based on current findings.

vii. Generally, correcting force with the direction at 30°–40° and around 50° regarding the sagittal plane may be more suitable for curves with thoracic hyper-kyphosis and hypo-/normal kyphosis, respectively.

Three-dimensional assessment of AIS was recognized clinically. Although coronal-Cobb may underestimate the severity of spinal curvature and does not reveal the three-dimensional characteristics of AIS, it serves as a golden standard in assessment and management of AIS while coronal-Cobb was only a component of "actual" spinal curvature. By comparison, the plane of maximum curvature could have more potential to describe the three-dimensional deformities of AIS. It was applied to the 3D assessment of AIS and correction evaluation of spinal orthosis earlier; however, it was only limited to research studies but not clinical practice. This study proposed a computational method and converted it into a user-friendly software that makes it easier to obtain the plane of maximum curvature in clinical practice. Optimal pressure-pad shape and correcting-force

direction of spinal orthoses were investigated by utilizing the plane of maximum curvature. This would provide an insight into the 3D correction of spinal orthoses with different pressure pad shapes and correctingforce directions. Although spinal orthoses designed with the plane of maximum curvature concept did not demonstrate superior clinical efficacy to those without the plane of maximum curvature concept as expected, this study first applied the concept of the plane of maximum curvature in the design of spinal orthosis. The findings would provide a foundation for future studies. Limitations to the study should be noted. For instance, study only focused on the correcting force direction on the convex side of the spinal curve while ignoring confounding factors, like correcting force magnitude, counter-forces, and spinal flexibility. Nevertheless, this study first explored the optimal biomechanical design of spinal orthoses in terms of pressure pad shape, correcting force direction, and plane of maximum curvature concept, which would build a foundation for optimizing the design of spinal orthosis, enhancing the orthotic management of AIS. Future prospective study with more potential baffling factors controlled was suggested to further confirm the findings of this study.

APPENDICES

APPENDIX A -- CONSENT TO PARTICIPATE IN RESEARCH

CONSENT TO PARTICIPATE IN RESEARCH

Project Title: Estimation of Plane of Maximum Curvature for Enhancement of Orthotic Management of Adolescent Idiopathic Scoliosis (AIS)

I _____ hereby consent to participate in the captioned research conducted by Dr. Man-sang Wong (Associate Professor of the Interdisciplinary Division of Biomedical Engineering, The Hong Kong Polytechnic University), and assisted-conducted by Miss Huidong WU.

I understand that the information obtained from this research may be used in future research and published. However, my right to privacy will be retained, i.e. my personal details will not be revealed.

The procedure as set out in the attached information sheet has been fully explained. I understand the benefit and risks involved. My participation in the project is voluntary.

I acknowledge that I have the right to question any part of the procedure and can withdraw at any time without penalty of any kind.

If you would like more information about this study, please contact Dr. Man-sang WONG at 2766-7680.

Name of participant: _____

Signature of participant: _____

Date: _____

Name of researcher: _____

Signature of researcher: _____

Date: _____

Name of supervisor: _____

Signature of supervisor: _____

Date: _____

APPENDIX B -- CONSENT TO PARTICIPATE IN RESEARCH (CHINESE VERSION)

參與研究同意書

項目名稱: 關於最大側彎平面的預測及其對於青少年特發性脊柱側彎矯形管理的應用

本人 _____特此同意參加由香港理工大學生物醫學工程跨領域學部 黃文生 副教授負責執行及加以說明的研究項目，並且該項目將由 黃文生 副教授的博士研究生 吳會東 來協助執行。

我理解此研究所獲得的資料可用於未來的研究和學術交流。然而我有權保護自己的隱私，我的個人資料將不能被洩漏。

我對所附資料的有關步驟已經得到充分的解釋。我是自願參加與這項研究。

我理解我有權在研究過程中提出問題，并可在任何時候決定退出研究而不會受到任何不正常的待遇或責任追究。

如果 閣下想獲得更多有關這項研究的資料, 請與 黃文生 副教授聯絡，辦公室電話: 2766-7680.

參加者姓名：_____

參加者簽名：_____

日期：_____

研究人員姓名：_____

研究人員簽名：_____

日期：_____

導師姓名：_____

導師簽名：_____

日期：_____

APPENDIX C -- INFORMATION SHEET

INFORMATION SHEET

Project Title: Estimation of Plane of Maximum Curvature for Enhancement of Orthotic Management of Adolescent Idiopathic Scoliosis (AIS)

You are invited to participate in a study conducted by Dr. Man-sang Wong, Associate Professor of the Interdisciplinary Division of Biomedical Engineering, The Hong Kong Polytechnic University. Miss Huidong WU who is a PhD student of Dr. Man-sang Wong, will be the assistant in this study.

The aim of this study is going to apply ultrasound technique to estimate the plane of maximum curvature in scoliotic spine, which will be further used for enhancing the orthotic management for patients with adolescent idiopathic scoliosis, in a non-invasive approach. The 3D Ultrasound System is a specially designed system specifically used for the screening of scoliosis, which is safe for human. The ultrasound images obtained from the ultrasound system will be analysed to estimate the plane of maximum curvature that will be applied to orthotic management for patients with adolescent idiopathic scoliosis.

Subjects can withdraw from the study at any time without affecting their continuous treatment.
The results of this study can contribute in scientific practice of assessment and orthotic intervention and form a data base for further developments of orthotic treatment protocol for adolescent idiopathic scoliosis.

All information related to you will remain confidential, and will be identifiable by codes only known to the researcher. Subjects are at minimum risk with this study. Minimal risk means that the risks of harm anticipated in the proposed research are not greater considering probability and magnitude, than those ordinarily encountered in daily life.

You have every right to withdraw from the study before or during the measurement without penalty of any kind.

If you have any complaints about the conduct of this research study, please do not hesitate to contact Miss Ivy CHAU, Secretary of the Human Subjects Ethics Sub-Committee of The Hong Kong Polytechnic University in person or in writing (c/o Room M1303, Human Resources Office of the Hong Kong Polytechnic University) or Human Research Ethics Committee for Non-Clinical Faculties, the University of Hong Kong.

If you would like more information about this study, please contact Dr. Man-sang WONG at 2766-7680.

Thank you for your interest in participating in this study.

Principal Investigator: Dr. Man-sang WONG

APPENDIX D -- INFORMATION SHEET (CHINESE VERSION)

相關資料

項目名稱:
關於最大側彎平面的預測及其對於加強青少年特發性脊柱側彎矯形管理的應用

誠邀閣下參加由香港理工大學生物醫學工程跨領域學部 黃文生副教授負責執行的研究項目。此項目將由 黃文生 副教授的博士研究生 吳會東 來協助執行。

此研究的目標是使用三維超聲和影像自動識別技術來測量青少年特發性脊柱側彎病人的脊柱柔韌性和評估矯形器初始矯正效果。閣下只需要在佩戴脊柱矯形器前和佩戴脊柱矯形器時接受一項簡單的三維超聲檢查。三維超聲是在普通超聲的儀器上配置三維定位系統用於追蹤超聲掃描的探頭在三維空間中的位置，從而把二維的超聲圖像重建成為三維的圖像。此設備中的三維定位系統是用電磁波信號進行追蹤和重建的，系統中所用的信號對人體無害。由超聲儀器所測的三維脊柱圖片将会被用来评估脊柱柔韌性和矯形器的初始矯正效果。

所有的參加者都有權在任何時候選擇退出此項目，並且不影響其後續的治療。超聲波檢查已經使用多年，到目前為止還沒有出現任何安全問題報告，因此在測試的過程中將不會令閣下有任何不必要的不適。

此研究得出的結果可在矯形器的治療科學運用做出貢獻及能形成一個數據庫以便研究人員進一步研發能更好的治療青春期特發性脊柱側彎的矯形器。

凡有關閣下的資料均會保密，一切資料的編碼只有研究人員知道。

閣下享有充分的權利在研究開始之前或之後決定退出這項研究，而不會受到任何對閣下不正常的待遇或責任追究。

如果 閣下有任何對這項研究的不滿，請隨時親自或寫信聯絡香港理工大學-人事倫理委員會秘書 周艾維（地址：香港理工大學人力資源辦公室 M1303 室轉交）或 _____ 。

如果 閣下想獲得更多有關這項研究的資料, 請與 黃文生 副教授聯絡，辦公室電話: 2766-7680.

謝謝 閣下參與這項研究。

首席調查員:黃文生 副教授

APPENDIX E ETHICAL APPROVAL

THE HONG KONG POLYTECHNIC UNIVERSITY
香港理工大學

To	Wong Man Sang (Department of Biomedical Engineering)		
From	Sun Lei, Chair, Departmental Research Committee		
Email	lei.sun@	Date	06-Mar-2018

Application for Ethical Review for Teaching/Research Involving Human Subjects

I write to inform you that approval has been given to your application for human subjects ethics review of the following project for a period from 01-Sep-2017 to 01-Sep-2019:

Project Title:	Estimation of Plane of Maximum Curvature for Enhancement of Orthotic Management of Adolescent Idiopathic Scoliosis (AIS)
Department:	Department of Biomedical Engineering
Principal Investigator:	Wong Man Sang
Project Start Date:	01-Sep-2017
Reference Number:	HSEARS20170807003

You will be held responsible for the ethical approval granted for the project and the ethical conduct of the personnel involved in the project. In the case of the Co-PI, if any, has also obtained ethical approval for the project, the Co-PI will also assume the responsibility in respect of the ethical approval (in relation to the areas of expertise of respective Co-PI in accordance with the stipulations given by the approving authority).

You are responsible for informing the Human Subjects Ethics Sub-committee in advance of any changes in the proposal or procedures which may affect the validity of this ethical approval.

Sun Lei

Chair

Departmental Research Committee

REFERENCES

1. Rolton D, Nnadi C, Fairbank J. Scoliosis: a review. Paediatrics and Child Health. 2014;24(5):197-203.

2. Miller MD, Thompson SR, Hart JA. Review of orthopaedics: Elsevier Health Sciences; 2012.

3. Stokes IA, Bigalow LC, Moreland MS. Three-dimensional spinal curvature in idiopathic scoliosis. J Orthop Res. 1987;5(1):102-13.

4. Propst-Proctor SL, Bleck EE. Radiographic determination of lordosis and kyphosis in normal and scoliotic children. Journal of Pediatric Orthopaedics. 1983;3(3):344-6.

5. Konieczny MR, Senyurt H, Krauspe R. Epidemiology of adolescent idiopathic scoliosis. J Child Orthop. 2013;7(1):3-9.

6. Choudhry MN, Ahmad Z, Verma R. Adolescent Idiopathic Scoliosis. Open Orthopaedics Journal. 2016;10:143-54.

7. Lonner B, Yoo A, Terran JS, Sponseller P, Samdani A, Betz R, et al. Effect of spinal deformity on adolescent quality of life: comparison of operative scheuermann kyphosis, adolescent idiopathic scoliosis, and normal controls. Spine. 2013;38(12):1049-55.

8. Yang JH, Suh SW, Sung PS, Park WH. Asymmetrical gait in adolescents with idiopathic scoliosis. Eur Spine J. 2013;22(11):2407-13.

9. Mahaudens P, Detrembleur C, Mousny M, Banse X. Gait in adolescent idiopathic scoliosis: energy cost analysis. Eur Spine J. 2009;18(8):1160-8.

10. Lam TP, Hung VWY, Yeung HY, Tse YK, Chu WCW, Ng BK, et al. Abnormal bone quality in adolescent idiopathic scoliosis: a case-control study on 635 subjects and 269 normal controls with bone densitometry and quantitative ultrasound. Spine. 2011;36(15):1211-7.

11. Johnston CE, Richards BS, Sucato DJ, Bridwell KH, Lenke LG, Erickson M. Correlation of preoperative deformity magnitude and pulmonary function tests in adolescent idiopathic scoliosis. Spine. 2011;36(14):1096-102.

12. Koumbourlis AC. Scoliosis and the respiratory system. Paediatr Respir Rev. 2006;7(2):152-60.

13. Martinez-Llorens J, Ramirez M, Colomina MJ, Bago J, Molina A, Caceres E, et al. Muscle dysfunction and exercise limitation in adolescent idiopathic scoliosis. Eur Respir J. 2010;36(2):393-400.

14. Wright N. Imaging in scoliosis. Arch Dis Child. 2000;82(1):38-40.

15. Kotwicki T. Evaluation of scoliosis today: examination, x-rays and beyond. Disabil Rehabil. 2008;30(10):742-51.

16. Kotwicki T, Negrini S, Grivas T, Rigo M, Maruyama T, Durmala J, et al. Methodology of evaluation of morphology of the spine and the trunk in idiopathic scoliosis and other spinal deformities - 6th SOSORT consensus paper. Scoliosis. 2009;4:26.

17. Göçen S, Havitçioglu H. Effect of rotation on frontal plane deformity in idiopathic scoliosis. Orthopedics. 2001;24(3):265-8.

18. Lindahl O, Movin A. Measurement of the deformity in scoliosis. Acta Orthop Scand. 1968;39(3):291-302.

19. Villemure I, Aubin CE, Grimard G, Dansereau J, Labelle H. Progression of vertebral and spinal three-dimensional deformities in adolescent idiopathic scoliosis: a longitudinal study. Spine. 2001;26(20):2244-50.

20. S Delorme, Labelle H, Aubin C, Guise Jd, Rivard C, Poitras B, et al. A Three-Dimensional Radiographic Comparison of Cotrel–Dubousset and Colorado Instrumentations for the Correction of Idiopathic Scoliosis. Spine. 2000;25(2):205-10.

21. Sangole AP, C E Aubin, Labelle H, Stokes IAF, Lenke LG, Jackson R, et al. Three-dimensional classification of thoracic scoliotic curves. Spine. 2008;34(1):91-9.

22. Lenke LG. What's new in the surgical care of adolescent idiopathic scoliosis (AIS). ArgoSpine News J 2012;24(1-2):62-6.

23. Stokes IAF. Three-dimensional terminology of spinal deformity: a report presented to the scoliosis research society by the scoliosis research society working group on 3-D terminology of spinal Deformity. Spine. 1994;19(2):236-48.

24. Labelle H, Aubin CE, Jackson R, Lenke L, Newton P, Parent S. Seeing the Spine in 3D: How Will It Change What We Do? J Pediatr Orthop. 2011;31(1):S37–S45.

25. Wu HD, He C, Chu WC-W, Wong MS. Estimation of plane of maximum curvature for the patients with adolescent idiopathic scoliosis via a purpose-design computational method. European Spine Journal. 2020.

26. Koreska J, Smith J. Portable desktop computer-aided digitiser system for the analysis of spinal deformities. Medical and Biological Engineering and Computing. 1982;20(6):715-26.

27. Trac S, Zheng R, Hill DL, Lou E. Intra- and interrater reliability of Cobb angle measurements on the plane of maximum curvature using ultrasound imaging method. Spine Deform. 2019;7(1):18-26.

28. Tins B. Technical aspects of CT imaging of the spine. Insights Imaging. 2010;1(5-6):349-59.

29. Brink RC, Schlosser TPC, Colo D, Vincken KL, Stralen Mv, Hui SCN, et al. Asymmetry of the vertebral body and pedicles in the true transverse plane in adolescent idiopathic scoliosis: a CT-based study. Spine Deform. 2017;5(1):37-45.

30. Davis CM, Grant CA, Pearcy MJ, Askin GN, Labrom RD, Izatt MT, et al. Is there asymmetry between the concave and convex pedicles in adolescent idiopathic scoliosis? A CT investigation. Clin Orthop Relat Res. 2017;475(3):884-93.

31. Brink RC, Schlosser TPC, Stralen Mv, Vincken KL, Kruyt MC, Hui SCN, et al. Anterior-posterior length discrepancy of the spinal column in adolescent idiopathic scoliosis-a 3D CT study. Spine J. 2018;18(12):2259-65.

32. Koreska J, Smith JM. Portable desktop computer-aided digitiser system for the analysis of spinal deformities. Med Biol Eng Comput. 1982;20(6):715-26.

33. Stokes IAF, Bigalow LC, Moreland MS. Three-dimensional spinal curvature in idiopathic scoliosis. J orthop Res. 1987;5(1):102-13.

34. Torell G, Nachemson A, Haderspeck-Grib K, Schultz A. Standing and supine Cobb measures in girls with idiopathic scoliosis. Spine. 1985;10(5):425-7.

35. Wessberg P, Danielson BI, Jan Wille´n. Comparison of Cobb angles in idiopathic scoliosis on standing radiographs and supine axially loaded MRI. Spine. 2006;31(26):3039-44.

36. Harmouche R, Cheriet F, Labelle H, Dansereau J. 3D registration of MRI and x-ray spine images using an articulated model. Comput Med Imaging Graph. 2012;36(5):410-8.

37. Lee MC, Solomito M, Patel A. Supine magnetic resonance imaging Cobb measurements for idiopathic scoliosis are linearly related to measurements from standing plain radiographs. Spine. 2013;38(11):E656-61.

38. Keenan BE, Izatt MT, Askin GN, Labrom RD, Pearcy MJ, Adam CJ. Supine to standing Cobb angle change in idiopathic scoliosis: the effect of endplate pre-selection. Scoliosis. 2014;9(1):16.

39. Shi B, Mao S, Wang Z, Lam TP, Yu FWP, Ng BKW, et al. How does the supine MRI correlate with standing radiographs of different curve severity in adolescent idiopathic scoliosis? Spine. 2015;40(15):1206-12.

40. Vavruch L, Tropp H. A Comparison of Cobb angle: standing versus supine images of late-onset idiopathic scoliosis. Pol J Radiol. 2016;81:270-6.

41. Brink RC, Colo D, Schlosser TPC, Vincken KL, van Stralen M, Hui SCN, et al. Upright, prone, and supine spinal morphology and alignment in adolescent idiopathic scoliosis. Scoliosis Spinal Disord. 2017;12:6.

42. Hasegawa K, Okamoto M, Hatsushikano S, Caseiro G, Watanabe K. Difference in whole spinal alignment between supine and standing positions in patients with adult spinal deformity using a new comparison method with slot-scanning three-dimensional X-ray imager and computed tomography through digital reconstructed radiography. BMC Musculoskelet Disord. 2018;19(1):437.

43. Yang C, Li Y, Zhao Y, Zhu X, Li M, Liu G. Adult degenerative scoliosis: can Cobb angle on a supine posteroanterior radiograph be used to predict the Cobb angle in a standing position? Medicine (Baltimore). 2016;95(6):e2732.

44. Yazici M, Acaroglu ER, Alanay A, Deviren V, Cila A, Surat A. Measurement of vertebral rotation in standing versus supine position in adolescent idiopathic scoliosis. J Pediatr Orthopaed. 2001;21(2):252-6.

45. Chen W. Application of ultrasound to measure coronal curvature and vertebral rotation in adolescent idiopathic scoliosis. 2014.

46. Goldberg CJ, Dowling FE, Hall JE, Emans JB. A statistical comparison between natural history of idiopathic scoliosis and brace treatment in skeletally immature adolescent girls. Spine. 1993;18(7):902-8.

47. Goldberg CJ, Moore DP, Fogarty EE, Dowling FE. Adolescent idiopathic scoliosis the effect of brace treatment on the incidence of surgery. Spine. 2001;26(1):42-7.

48. Goldberg CJ, Moore DP, Fogarty EE, Dowling FE. Adolescent Idiopathic Scoliosis: The Effect of Brace Treatment on the Incidence of Surgery. Spine (Phila Pa 1976). 2001;26(1):42-7.

49. Labelle H, Dansereau J, Bellefleur C, Poitras B. Three- Dimensional Effect of the Boston Brace on the Thoracic Spine and Rib Cage. Spine (Phila Pa 1976). 1996; 21(1):59–64.

50. Nie WZ, Ye M, Liu ZD, Wang CT. The patient-specific brace design and biomechanical analysis of adolescent idiopathic scoliosis. Journal of Biomechanical Engineering. 2009;131(4):041007 (7 pp.)- (7 pp.).

51. Aulisa AG, Guzzanti V, Marzetti E, Giordano M, Falciglia F, Aulisa L. Brace treatment in juvenile idiopathic scoliosis: a prospective study in accordance with the SRS criteria for bracing studies - SOSORT award 2013 winner. Scoliosis. 2014;9:3.

52. Nachemson A, Peterson L. Effectiveness of Treatment with A Brace in Girls Who Have Adolescent Idiopathic Scoliosis. J Bone Joint Surg. 1995;77(6):815–22.

53. Rigo M, Negrini S, Weiss HR, Grivas TB, Maruyama T, Kotwicki T, et al. 'SOSORT consensus paper on brace action: TLSO biomechanics of correction (investigating the rationale for force vector selection)'. Scoliosis. 2006;1:11.

54. Pasha S, Cahill PJ, Dormans JP, Flynn JM. Characterizing the differences between the 2D and 3D measurements of spine in adolescent idiopathic scoliosis. Eur Spine J. 2016;25(10):3137-45.

55. Berthonnaud E, Dimnet J, Hilmi R. Classification of pelvic and spinal postural patterns in upright position. specific cases of scoliotic patients. Comput Med Imag Grap. 2009;33(8):634-43.

56. Bernard JC, Berthonnaud E, Deceuninck J, Journoud-Rozand L, Notin G, Chaleat-Valayer E. Three-dimensional reconstructions of Lenke 1A curves. Scoliosis. 2018;13:5.

57. Stokes IAF. Axial rotation component of thoracic scoliosis. J orthop Res. 1989;7(5):702-8.

58. Hout JAvd, Rhijn LWv, Munckhof RJvd, Ooy Av. Interface corrective force measurements in Boston brace treatment. Eur Spine J. 2002;11:332-5.

59. Moalej S, Asadabadi M, Hashemi R, Khedmat L, Tavacolizadeh R, Vahabi Z, et al. Screening of scoliosis in school children in Tehran: The prevalence rate of idiopathic scoliosis. J Back Musculoskelet Rehabil. 2018;31(4):767-74.

60. Herkowitz HN, Garfin SR, Balderston RA, Eismont FJ, Bell GR, Wiesel SW. Rothman-Simeone: the spine 4th edition. USA: WB Saunders Inc; 1998.

61. Deepak AS, Ong JY, Choon D, Lee CK, Chiu CK, Chan C, et al. The Clinical Effectiveness of School Screening Programme for Idiopathic Scoliosis in Malaysia. Malays Orthop J. 2017;11(1):41-6.

62. Vasiliadis ES, Grivas TB, Kaspiris A. Historical overview of spinal deformities in ancient Greece. Scoliosis. 2009;4:6.

63. Negrini S, Donzelli S, Aulisa AG, Czaprowski D, Schreiber S, Mauroy JCd, et al. 2016 SOSORT guidelines: orthopaedic and rehabilitation treatment of idiopathic scoliosis during growth. Scoliosis Spinal Disord. 2018;13:3.

64. Altaf F, Gibson A, Dannawi Z, Noordeen H. Adolescent idiopathic scoliosis. BMJ. 2013;346:f2508.

65. Kleinberg S. The operative treatment of scoliosis. Arch Surg. 1922;5(3):631– 45.

66. Hresko MT. Clinical practice. Idiopathic scoliosis in adolescents. N Engl J Med. 2013;368(9):834-41.

67. Ogilvie JW, Braun J, Argyle V, Nelson L, Meade M, Ward K. The search for idiopathic scoliosis genes. Spine. 2006;31(6):679-81.

68. Nakamura Y, Nagai T, Iida T, Ozeki S, Nohara Y. Epidemiological aspects of scoliosis in a cohort of Japanese patients with Prader-Willi syndrome. Spine J. 2009;9(10):809–16.

69. Kamtsiuris P, Atzpodien K, Ellert U, Schlack R, Schlaud M. Prevalence of somatic diseases in German children and adolescents. Results of the German health interview and examination survey for children and adolescents (KiGGS). Bundesgesundheitsbla. 2007;50(5-6):686–700.

70. Ratahi ED, Crawford HA, Thompson JM, arnes BMJ. Ethnic variance in the epidemiology of scoliosis in New Zealand. J Pediatr Orthop. 2002;22(6):784-7.

71. Daruwalla JS, Balasubramaniam PP, Chay SO, Rajan U, Lee HP. Idiopathic scoliosis, prevalence and ethnic distribution in Singapore schoolchildren. J Bone Joint Surg Br. 1985;67(2):182-4.

72. Wang W, Zhu Z, Zhu F, Sun C, Wang Z, Sun X, et al. Different curve pattern and other radiographic characteristics in male and female patients with adolescent idiopathic scoliosis. Spine. 2012;37(18):1586–92.

73. Suh SW, Modi HN, Yang JH, Hong JY. Idiopathic scoliosis in Korean schoolchildren: a prospective screening study of over 1 million children. Eur Spine J. 2011;20(7):1087-94.

74. Richards BS, Bernstein RM, D'Amato CR, Thompson GH. Standardization of criteria for adolescent idiopathic scoliosis brace studies: SRS committee on bracing and nonoperative management. Spine. 2005;30(18):2068-75.

75. Weinstein SL, Dolan LA, Spratt KF, Peterson KK, Spoonamore MJ, Ponseti IV. Health and function of patients with untreated idiopathic scoliosis. A 50-year natural history study. JAMA. 2003;289(5):559-67.

76. Duval-Beaupère G. Maturation indices in the surveillance of scoliosis. Rev Chir Orthop Reparatrice Appar Mot. 1970;56(1):59-76.

77. Duval-Beaupere G. Maturation parameters in scoliosis. Rev Chir Orthop Reparatrice Appar Mot. 1970;56:59.

78. Duval-Beaupere G. Pathogenic relationship between scoliosis and growth. In: Zorab PA, ed. Scoliosis and Growth: Churchill Livingstone; 1971.

79. Kesling KL, Reinker KA. Scoliosis in twins: a meta-analysis of the literature and report of six cases. Spine. 1997;22(17):2009.

80. Sanders JO. Maturity indicators in spinal deformity. J Bone Joint Surg. 2007;89-A(suppl 1):14-20.

81. Charles Y, Daures J, Rosa VD. Progression risk of idiopathic juvenile scoliosis during pubertal growth. Spine. 2006;31(17):1933-42.

82. Risser JC. The classic: the Iliac apophysis: an invaluable sign in the management of scoliosis. Clin Orthop Relat Res. 2010;468(3):646-53.

83. Lonstein JE, Carlson JM. The prediction of curve progression in untreated idiopathic scoliosis during growth. J Bone Joint Surg. 1984;66(7):1061-71.

84. Fairbank MJ. Historical perspective: William Adams, the forward bending test, and the spine of gideon algernon. Spine. 2004;29(17):1953-5.

85. Coté P, Kreitz BG, Cassidy JD, Dzus AK, Martel J. A study of the diagnostic accuracy and reliability of the scoliometer and adam's forward bend test. Spine. 1998;279(23):796-802.

86. Brink Y, Louw QA. Clinical instruments: reliability and validity critical appraisal. J Eval Clin Pract. 2012;18(6):1126-32.

87. Asher M, Min L, Burton D, Manna B. The reliability and concurrent validity of the Scoliosis Research Society-22 patient questionnaire for idiopathic scoliosis. Spine. 2003;28(1):63-9.

88. Lee JS, Lee DH, Suh KT, Kim I, Lim JM, Goh TS. Validation of the Korean version of the Scoliosis Research Society-22 Questionnaire. Eur Spine J. 2011;20(10):1751-6.

89. Danielsson AJ, Romberg K. Reliability and validity of the Swedish version of the Scoliosis Research Society-22 (SRS-22r) patient questionnaire for idiopathic scoliosis. Spine. 2013;38(21):1875-84.

90. Lonjon G, Ilharreborde B, Odent T, Moreau S, Glorion C, Mazda K. Reliability and validity of the French-Canadian version of the Scoliosis Research Society 22 questionnaire in France. Spine. 2014;39(1):E26-34.

91. Haidar RK, Kassak K, Masrouha K, Ibrahim K, Mhaidli H. Reliability and validity of an adapted arabic version of the Scoliosis Research Society-22r questionnaire. Spine. 2015;40(17):E971-E7.

92. Vasiliadis E, Grivas T, Gkoltsiou K. Development and preliminary validation of brace questionnaire (BrQ): a new instrument for measuring quality of life of brace treated scoliotics. Scoliosis. 2006;1(1):1-8.

93. Weiss HR, editor Reproducibility and criterion validity of the BSSQstress questionnaire for patients with scoliosis.2006.

94. Kotwicki T, Kinel E, Stryła W, Szulc A. Estimation of the stress related to conservative scoliosis therapy: an analysis based on BSSQ questionnaires. Scoliosis and Spinal Disorders. 2007;2(1):1-6.

95. Botenshelmus C, Klein R, Stephan C. The reliability of the bad sobernheim stress questionnaire (BSSQbrace) in adolescents with scoliosis during brace treatment. Scoliosis and Spinal Disorders. 2006;1(1):22.

96. Weiss HR, editor How much stress do adolescents with scoliosis have because of their brace? Proceedings of the 3rd International Conference on Conservative Management of Spinal Deformites; 2006; Poznan.

97. O'Brien MF, Kuklo TR, Blanke KM, Lenke LG, Spinal Deformity Study G. Radiographic measuremnt manual. Medtronic Sofamor Danek USA, Inc. 2008.

98. Knott P, Pappo E, Cameron M, deMauroy JC, Rivard C, Kotwicki T, et al. SOSORT 2012 consensus paper: reducing x-ray exposure in pediatric patients with scoliosis. Scoliosis. 2014;9(1):4.

99. Ronckers CM, Land CE, Miller JS, Stovall M, Lonstein JE, Doody MM. Cancer mortality among women frequently exposed to radiographic examinations for spinal disorders. Radiat Res. 2010;174(1):83-90.

100. McKenna C, Wade R, Faria R, Yang R, Stirk L, Gummerson N, et al. EOS 2D/3D X-ray imaging system: a systematic review and economic evaluation. Health Technol Assess. 2012;16(14):1-188.

101. Desche^nes S, Charron G, Beaudoin G, Labelle H, Jose´e D, Miron MC, et al. Diagnostic Imaging of Spinal Deformities: Reducing Patients Radiation Dose With a New Slot-Scanning X-ray Imager. Spine (Phila Pa 1976). 2010;35(9):989 –94

102. Wade R, Yang H, McKenna C, Faria R, Gummerson N, Woolacott N. A systematic review of the clinical effectiveness of EOS 2D/3D X-ray imaging system. Eur Spine J. 2013;22(2):296-304.

103. Donzelli S, Zaina F, Lusini M, Minnella S, Respizzi S, Balzarini L, et al. The three dimensional analysis of the Sforzesco brace correction. Scoliosis. 2016;11:34.

104. Somoskeoy S, Tunyogi-Csapo M, Bogyo C, Illes T. Accuracy and reliability of coronal and sagittal spinal curvature data based on patient-specific three-dimensional models created by the EOS 2D/3D imaging system. Spine J. 2012;12(11):1052-9.

105. Al-Aubaidia Z, Lebelb D, Oudjhaneb K, Zellerb R. Three-dimensional imaging of the spine using the EOS system: is it reliable? A comparative study using computed tomography imaging. J Pediatr Orthopaed. 2013;22(5):409-12.

106. Bagheri A, Liu XC, Tassone C, Thometz J, Tarima S. Reliability of three-dimensional spinal modeling of patients with idiopathic scoliosis using EOS system. Spine Deform. 2018;6(3):207-12.

107. Gille O, Champain N, Benchikh-El-Fegoun A, Vital J-M, Skalli W. Reliability of 3D Reconstruction of the Spine of Mild Scoliotic Patients. Spine
. 2007;32(5):568-73.

108. Carreau JH, Bastrom T, Petcharaporn M, Schulte C, Marks M, Illes T, et al. Computer-generated, three-dimensional spine model from biplanar radiographs: a validity study in idiopathic scoliosis curves greater than 50 degrees. Spine Deform. 2014;2(2):81-8.

109. Tabard-Fougere A, Bonnefoy-Mazure A, Hanquinet S, Lascombes P, rmand A, Dayer R. Validity and reliability of spine rasterstereography in patients with adolescent idiopathic scoliosis. Spine. 2017;42(2):98-105.

110. Hirsch C, Ilharreborde B, Mazda K. Flexibility analysis in adolescent idiopathic scoliosis on side-bending images using the EOS imaging system. Orthop Traumatol Surg Res. 2016;102(4):495-500.

111. Ilharreborde B, Dubousset J, Le HJC. Use of EOS imaging for the assessment of scoliosis deformities: application to postoperative 3D quantitative analysis of the trunk. Eur Spine J. 2014;23 Suppl 4:S397-405.

112. Illes T, Somoskeoy S. Comparison of scoliosis measurements based on three-dimensional vertebra vectors and conventional two-dimensional measurements: advantages in evaluation of prognosis and surgical results. Eur Spine J. 2013;22(6):1255-63.

113. Courvoisier A, Vialle R, Skalli W. EOS 3D Imaging: assessing the impact of brace treatment in adolescent idiopathic scoliosis. Expert Rev Med Devices. 2014;11(1):1-3.

114. Adam CJ, Izatt MT, Harvey JR, Askin GN. Variability in Cobb angle measurements using reformatted computerized tomography scans. Spine. 2005;30(14):1664-9.

115. Abul-Kasim K, Karlsson M, Hasserius R, Ohlin A. Measurement of vertebral rotation in adolescent idiopathic scoliosis with low-dose CT in prone position - method description and reliability analysis. Scoliosis. 2010;5(1):4.

116. Abul-Kasim K, Ohlin A, Strombeck A, Maly P, Sundgren PC. Radiological and clinical outcome of screw placement in adolescent idiopathic scoliosis: evaluation with low-dose computed tomography. Eur Spine J. 2010;19(1):96-104.

117. Asghar J, Samdani AF, Pahys JM, D'Andrea LP, Guille JT, Clements DH, et al. Computed tomography evaluation of rotation correction in adolescent idiopathic

scoliosis: a comparison of an all pedicle screw construct versus a hook-rod system. Spine. 2009;34(8):804-7.

118. Sarwahi V, Sugarman EP, Wollowick AL, Amaral TD, Harmon ED, Thornhill B. Scoliosis surgery in patients with adolescent idiopathic scoliosis does not alter lung volume: a 3-dimensional computed tomography-based study. Spine. 2014;39(6):E399-405.

119. Kwan MK, Chiu CK, Gani SM, Wei CC. Accuracy and Safety of Pedicle Screw Placement in Adolescent Idiopathic Scoliosis Patients: A Review of 2020 Screws Using Computed Tomography Assessment. Spine (Phila Pa 1976). 2017;42(5):326-35.

120. Wang Q, Li M, Lou EHM, Wong MS. Reliability and validity study of clinical ultrasound imaging on lateral curvature of adolescent idiopathic scoliosis. PLoS One. 2015;10(8):e0135264.

121. Schmitz A, Jaeger UE, Koenig R, Kandyba J, Wagner UA, Giesecke J, et al. A new MRI technique for imaging scoliosis in the sagittal plane. Eur Spine J. 2001;10(2):114-7.

122. Wang Q, Li M, Lou EH, Chu WC, Lam TP, Cheng JC, et al. Validity study of vertebral rotation measurement using 3-D ultrasound in adolescent idiopathic scoliosis. Ultrasound Med Biol. 2016;42(7):1473-81.

123. Freund M, Hähnel S, Thomsen M, Sartor K. Treatment planning in severe scoliosis: the role of MRI. Neuroradiology. 2001;43(6):481-4.

124. Ozturk C, Karadereler S, Ornek I, Enercan M, Ganiyusufoglu K, Hamzaoglu A. The role of routine magnetic resonance imaging in the preoperative evaluation of adolescent idiopathic scoliosis. Int Orthop. 2010;34(4):543-6.

125. Rajwani T, Bagnall KM, Lambert R, Videman T, Kautz J, Moreau M, et al. Using Magnetic Resonance Imaging to Characterize Pedicle Asymmetry in Both Normal Patients and Patients With Adolescent Idiopathic Scoliosis. Spine. 2004;29(7):E145-E52.

126. Nakahara D, Yonezawa I, Kobanawa K, Sakoda J, Nojir H, Kamano S, et al. Magnetic resonance imaging evaluation of patients with idiopathic scoliosis: a prospective study of four hundred seventy-two outpatients. Spine. 2011;36(7):E482-5.

127. Diab M, Landman Z, Lubicky J, Dormans J, Erickson M, Richards BS, et al. Use and outcome of MRI in the surgical treatment of adolescent idiopathic scoliosis. Spine (Phila Pa 1976). 2011;36(8):667-71.

128. Young M, Lou E. Reliability and accuracy of ultrasound measurements with and without the aid of previous radiographs in adolescent idiopathic scoliosis (AIS). Eur Spine J 2015;24:1427–33.

129. Rui Zheng, Chan ACY, Chen W, Douglas L. Hill, Lawrence H. Le, Douglas Hedden, et al. Intra- and Inter-rater Reliability of Coronal Curvature Measurement for Adolescent Idiopathic Scoliosis Using Ultrasonic Imaging MethoddA Pilot Study. Spine Deformity. 2015;3: 151-8.

130. Zheng R, Young M, Hill D, Le LH, Hedden D, Moreau M, et al. Improvement on the accuracy and reliability of ultrasound coronal curvature measurement on adolescent idiopathic scoliosis with the aid of previous radiographs. Spine. 2016;41(5):404-11.

131. Khodaei M, Hill D, Zheng R, Le LH, Lou EHM. Intra- and inter-rater reliability of spinal flexibility measurements using ultrasonic (US) images for non-surgical candidates with adolescent Idiopathic scoliosis: a pilot study. Eur Spine J. 2018;27(9):2156-64.

132. Wang Q, Li M, Lou EHM, Wong MS. Reliability and Validity Study of Clinical Ultrasound Imaging on Lateral Curvature of Adolescent Idiopathic Scoliosis. Plos One. 2015.

133. Cheung CWJ, Zhou GQ, Law SY, Mak TM, Lai KL, Zheng YP. Ultrasound volume projection imaging for assessment of scoliosis. IEEE T Med Imaging. 2015a;34(8):1760-8.

134. Zheng Y-P, Lee TT-Y, Lai KK-L, Yip BH-K, Zhou G-Q, Jiang W-W, et al. A reliability and validity study for Scolioscan: a radiation-free scoliosis assessment system using 3D ultrasound imaging. Scoliosis and Spinal Disorders. 2016.

135. Rob C. Brink, Wijdicks SPJ, Brink RC, Tom P.C. Schlösser, Kruyt MC, Frederik J.A. Beek, et al. A reliability and validity study for different coronal angles using ultrasound imaging in adolescent idiopathic scoliosis. Spine J. 2017.

136. Li M, Ng B, Cheng J, Ying M, Zheng YP, Lam TP, et al. Could clinical ultrasound improve the fitting of spinal orthosis for the patients with AIS? Eur Spine J. 2012;21:1926–35.

137. Li M, Cheng J, Ying M, Ng B, Lam T-p, Wong M-s. A Preliminary Study of Estimation of Cobb's Angle From the Spinous Process Angle Using a Clinical Ultrasound Method. Spine Deformity. 2015;3: 476-82.

138. Cheung C-WJ, Zhou G-Q, Law S-Y, Lai K-L, Jiang W-W, Zheng Y-P. Freehand three-dimensional ultrasound system for assessment of scoliosis. Journal of Orthopaedic Translation. 2015;3:123-33.

139. Chen W, Lou E, Le LH. A reliable semi-automatic program to measure the vertebral rotation using the center of lamina for adolescent idiopathic scoliosis. In: 5th

international conference on biomedical engineering in Vietnam. IFMBE Proceedings2015. p. 159-62.

140. Cheung CWJ, Law SY, Zheng YP, editors. Development of 3-D ultrasound system for assessment of adolescent idiopathic scoliosis (AIS): and system validation. 35th Annual International Conference of the IEEE EMBS; 2013; Osaka, Japan.

141. Chen W, Le LH, Lou EH. Reliability of the axial vertebral rotation measurements of adolescent idiopathic scoliosis using the center of lamina method on ultrasound images: in vitro and in vivo study. Eur Spine J. 2016;25(10):3265-73.

142. Brink RC, Wijdicks SPJ, Schlösser TP, Kruyt MC, Beek FJA, Castelein RM, et al. A reliability and validity study for different coronal angles using ultrasound imaging in adolescent idiopathic scoliosis. Spine journal. 2018;18(6):979-85.

143. Zheng R, Hill D, Hedden D, Moreau M, Le LH, Raso J, et al. Assessment of curve flexibility on scoliotic surgical candidates using ultrasound imaging method. Ultrasound Med Biol. 2017;43(5):934-42.

144. He C, To MK, Cheung JP, Cheung KM, Chan CK, Jiang WW, et al. An effective assessment method of spinal fexibility to predict the initial in-orthosis correction on the patients with adolescent idiopathic scoliosis (AIS). PLoS One. 2017;12(12):e0190141-.

145. Lou E, Zheng R, Le L, Hill D, Raso J, Hedden D, et al. Curve flexibility assessment on AIS surgical candidates using ultrasonic imaging method - a preliminary study. Scoliosis. 2015;10(Suppl 1):O39.

146. Zheng R, Hill D, Hedden D, Moreau M, Southon S, Lou E. Assessment of curve progression on children with idiopathic scoliosis using ultrasound imaging method. Eur Spine J. 2018;27(5):1-6.

147. Lou E, Chan A, Donauer A, Tilburn M, Hill D. Ultrasound-assisted brace casting for adolescent idiopathic scoliosis. Scoliosis. 2015;10(Suppl 1):O38.

148. Meadows DM, Johnson WO, Allen JB. Generation of surface contours by moiré patterns. Appl Opt. 1970;9(4):942-7.

149. Klos SS, Liu XC, Lyon RM, Tassone JC, Thometz JC. Reliability of a functional classification system in the monitoring of patients with idiopathic scoliosis. Spine. 2007;32(15):1662-6.

150. Pazos V, Cheriet F, Danserau J, Ronsky J, Zernicke RF, Labelle H. Reliability of trunk shape measurements based on 3-D surface reconstructions. Eur Spine J. 2007;16(11):1882–91.

151. Seoud L, Cheriet F, Labelle H, Dansereau J. Anovel method for 3-D reconstruction of scoliotic ribs from frontal and lateral radiographs. IEEE Trans Biomed Eng. 2011;58(5):1135–46.

152. Zubovic A, Davies N, Berryman F, Pynsent P, Quraishi N, Lavy C, et al. New method of scoliosis deformity assessment: ISIS2 system. Stud Health Technol Inform. 2008;140:157–60.

153. Hong A, Jaswal N, Westover L, Parent EC, Moreau M, Hedden D, et al. Surface topography classification trees for assessing severity and monitoring progression in adolescent idiopathic scoliosis. Spine. 2017;42:E781-E7.

154. Fortin D, Cheriet F, Beauséjour M, Debanné P, Joncas J, Labelle H. A 3D visualization tool for the design and customization of spinal braces. Comput Med Imaging Graph. 2007;31(8):612–24.

155. Labelle H, Bellefleur C, Joncas J, Aubin CE, Cheriet F. Preliminary evaluation of a computer-assisted tool for the design and adjustment of braces in idiopathic scoliosis: a prospective and randomized study. Spine. 2007;32(8):835-84.

156. Berryman F, Pynsent P, Fairbank J, Disney S. A new system for measuring three-dimensional back shape in scoliosis. Eur Spine J. 2008;17(5):663–72.

157. McArdle FJ, Griffiths CJ, Macdonald AM, Gibson MJ. Monitoring the thoracic sagittal curvature in kyphoscoliosis with surface topography: a trend analysis of 57 patients. Stud Health Technol Inform. 2002;91:199-203.

158. Frerich JM, Hertzler K, Knott P, Mardjetko S. Comparison of radiographic and surface topography measurements in adolescents with idiopathic scoliosis. Open Ortho J. 2012;6:261–5.

159. Mardjetko S, Knott P, Rollet M, Baute S, Riemenschneider M, Muncie L. Evaluating the reproducibility of the formetric 4D measurements for scoliosis. Eur Spine J. 2010;19(3):S241–S2.

160. Mohokum M, Mendoza S, Udo W, Sitter H, Paletta JR, Skwara A. Reproducibility of rasterstereography for kyphotic and lordotic angles, trunk length, and trunk inclination: a reliability study. Spine. 2010;35(14):1353-8.

161. Knott P, Mardjetko S, Tager D, Hund R, Thompson S. The influence of Body Mass Index (BMI) on the reproducibility of surface topography measurements. Scoliosis. 2012;7(1):O18.

162. Hackenberg L, Hierholzer E, Bullmann V, Liljenqvist U, Götze C. Rasterstereographic Analysis of Axial Back Surface Rotation in Standing versus Forward Bending Posture in Idiopathic Scoliosis. Eur Spine J. 2006;15(7):1144-9.

163. Kotwicki T, Negrini S, Grivas TB, Rigo M, Maruyama T, Durmala J, et al. Methodology of evaluation of morphology of the spine and the trunk in idiopathic scoliosis and other spinal deformities - 6th SOSORT consensus paper. Scoliosis. 2009;4(1):1-16.

164. Delorme S, Labelle H, Aubin CE, Guise JAd, Rivard CH, Poitras B, et al. A three-dimensional radiographic comparison of Cotrel–Dubousset and Colorado instrumentations for the correction of idiopathic scoliosis. Spine. 2000;25(2):205-10.

165. Perdriolle R, Borgne PL, Dansereau J, Guise J, Labelle H. Idiopathic scoliosis in three dimensions: a succession of two-dimensional deformities? Spine. 2001;26(24):2719-26.

166. Delorme S, Labelle H, Aubin CE, Guise JAd, Rivard CH, Poitras B, et al. Intraoperative comparison of two instrumentation techniques for the correction of adolescent idiopathic scoliosis: rod rotation and translation. Spine. 1999;24(19):2011-.

167. Sangole A, Aubin C, Labelle H, Lenke L, Jackson R, Newton P, et al. The central hip vertical axis: a reference axis for the scoliosis research society three-dimensional classification of idiopathic scoliosis. Spine. 2010;35(12):E530-E4.

168. Wu HD, Wong MS. Assessment of Maximum Spinal Deformity in Scoliosis: A literature Review. Journal of Medical and Biological Engineering. 2020;40:621-9.

169. Berthonnaud E, Hilmi R, Dimnet J. Geometric structure of 3D spinal curves: plane regions and connecting zones. ISRN Orthopedics. 2012;2012:1-10.

170. Labelle H, Aubin CE, Jackson R, Lenke L, Newton P, Parent S. Seeing the spine in 3D: how will it change what we do? J Pediatr Orthopaed. 2011;31(1):S37-S45.

171. Kohashi Y, Oga M, Sugioka Y. A new method using top views of the spine to predict the progression of curves in idiopathic scoliosis during growth. Spine. 1996;21(2):212-7.

172. Thong W, Parent S, Wu J, Aubin C, Labelle H, Kadoury S. Three-dimensional morphology study of surgical adolescent idiopathic scoliosis patient from encoded geometric models. Eur Spine J. 2016;25(10):3104-13.

173. Duong L, Mac-Thiong JM, Cheriet F, Labelle H. Three-dimensional subclassification of Lenke type 1 scoliotic curves. J Spinal Disord Tech. 2009;22(2):135–43.

174. Stokes IAF, Sangole AP, Aubin CE. Classification of scoliosis deformity three-dimensional spinal shape by cluster analysis. Spine. 2009;34(6):584-90.

175. Kumar S, Nayak KP, Hareesha KS. Quantification of spinal deformities using combined SCP and geometric 3D reconstruction. Biomed Signal Proces. 2017;31:181-8.

176. Nault ML, Mac-Thiong JM, Roy-Beaudry M, Turgeon I, Deguise J, Labelle H, et al. Three-dimensional spinal morphology can differentiate between progressive and nonprogressive patients with adolescent idiopathic scoliosis at the initial presentation: a prospective study. Spine. 2014;39(10):E601-E6.

177. Labelle H, Dansereau J, Bellefleur C, Jequier JC. Variability of geometric measurements from three-dimensional reconstructions of scoliotic spines and rib cages. Eur Spine J. 1995;4(2):88-94.

178. Labelle H, Dansereau J, Bellefleur C, Poitras B, Rivard CH, Stokes IA, et al. Comparison between preoperative and postoperative three-dimensional reconstructions of idiopathic scoliosis with the Cotrel-dubousset procedure. Spine. 1995;20(23):2487-92.

179. Labelle H, Dansereau J, Bellefleur C, Poitras B. Three-dimensional effect of the Boston brace on the thoracic spine and rib cage. Spine. 1996;21(1):59-64.

180. Papin P, Labelle H, Delorme S, Aubin CE, Guise JAd, Dansereau J. Long-term three-dimensional changes of the spine after posterior spinal instrumentation and fusion in adolescent idiopathic scoliosis. Eur Spine J. 1999;8(1):16-21.

181. Delorme S, Labelle H, Poitras B, Rivard CH, Coillard C, Dansereau J. Pre-, intra-, and postoperative three-dimensional evaluation of adolescent idiopathic scoliosis. J Spinal Disord. 2000;13(2):93–101.

182. Moura DC, Boisvert J, Barbosa JG, Labelle H, Tavares JM. Fast 3D reconstruction of the spine from biplanar radiographs using a deformable articulated model. Med Eng Phys. 2011;33(8):924-33.

183. Kadoury S, Labelle H. Classification of three-dimensional thoracic deformities in adolescent idiopathic scoliosis from a multivariate analysis. Eur Spine J. 2012;21(1):40-9.

184. Deacon P, Flood BM, Dickson RA. Idiopathic scoliosis in three dimensions: a radiographic and morphometric analysis. J Bone Joint Surg Br. 1984;66(4):509-12.

185. Vo QN, Lou EHM, Le LH. 3D ultrasound imaging method to assess the true spinal deformity. Engineering in medicine and biology society (EMBC), 2015 37th annual international conference of the IEEE. 2015.

186. Zheng YP, Lee TTY, Lai KKL, Yip BHK, Zhou GQ, Jiang WW, et al. A reliability and validity study for Scolioscan: a radiation-free scoliosis assessment system using 3D ultrasound imaging. Scoliosis. 2016;11:13.

187. Zheng R, Chan AC, Chen W, Hill DL, Le LH, Hedden D, et al. Intra- and inter-rater reliability of coronal curvature measurement for adolescent idiopathic scoliosis using ultrasonic imaging method - A pilot study. Spine Deform. 2015;3(2):151-8.

188. Young M, Hill DL, Zheng R, Lou E. Reliability and accuracy of ultrasound measurements with and without the aid of previous radiographs in adolescent idiopathic scoliosis (AIS). Eur Spine J. 2015;24(7):1427-33.

189. Berthonnaud E, Papin P, Deceuninck J, Hilmi R, Bernard JC, Dimnet J. The use of a photogrammetric method for the three-dimensional evaluation of spinal correction in scoliosis. Int Orthop. 2016;40(6):1187–96.

190. Sawatzky B, Tredwell SJ, Jang SB, Black AH. Effects of three-dimensional assessment on surgical correction and on hook strategies in multi-hook instrumentation for adolescent idiopathic scoliosis. Spine. 1998;23(2):201-5.

191. Stephen TJ, Bonita SJ, Barbara HL. Rotations of a helix as a model for correction of the scoliotic spine. Spine. 1999;24(12):1223-7.

192. Sawatzky BJ, Jang SB, Tredwell SJ, Black A, Reilly CW, Booth KS. Intra-operative analysis of scoliosis surgery in 3-D. Comput Method Bio Mec. 1998;1(3):211-21.

193. Humbert L, Guise JAD, Aubert B, Godbout B, Skalli W. 3D reconstruction of the spine from biplanar x-rays using parametric models based on transversal and longitudinal inferences. Med Eng Phys. 2009;31(6):681-7.

194. Kadoury S, Cheriet F, Labelle H. Personalized x-ray 3-D reconstruction of the scoliotic spine from hybrid statistical and image-based models. IEEE T Med Imaging. 2009;28(9):1422-35.

195. Kadoury S, Cheriet F, Laporte C, Labelle H. A versatile 3D reconstruction system of the spine and pelvis for clinical assessment of spinal deformities. Med Biol Eng Comput. 2007;45(6):591-602.

196. Kadoury S, Cheriet F, Dansereau J, Labelle H. Three-dimensional reconstruction of the scoliotic spine and pelvis from uncalibrated biplanar x-ray images. J Spinal disord Tech. 2007;20(2):160–8.

197. Delorme S, Petit Y, Guise JAd, Labelle H, Aubin CE, Dansereau J. Assessment of the 3-d reconstruction and high-resolution geometrical modeling of the human skeletal trunk from 2-D radiographic images. IEEE T Bio-Med Eng. 2003;50(8):989-98.

198. Cheriet F, Dansereau J, Petit Y, Aubin CE, Labelle H, Guise AUd. Towards the self-calibration of a multi-view radiographic imaging system for the 3D reconstruction of the human spine and rib cage. Int J Pattern Recog N. 1999;13(5):761-79.

199. Stokes IAF, Shuma-Hartswick D, Moreland MS. Spine and back-shape changes in scoliosis. Acta orthop scand. 1988;59(2):128-33.

200. Cobb JR. Outline for the study of scoliosis. AAOS Instr Course Lect. 1948;5:261-75.

201. Shen J, Kadoury S, Labelle H, Parent S. Geometric torsion in adolescent idiopathic scoliosis: a surgical outcomes study of Lenke type 1 patients. Spine. 2016;41(24):1903-7.

202. Shen J, Kadoury S, Labelle H, Roy-Beaudry M, Aubin CE, Parent S. Geometric torsion in adolescent idiopathic scoliosis: a new method to differentiate between Lenke 1 subtypes. Spine. 2017;42(9):E532-E8.

203. Rowe DE, Kalamazoo M. The Scoliosis Research Society Brace Mannual.

204. Fusco C, Zaina F, Atanasio S, Romano M, Negrini A, Negrini S. Physical exercises in the treatment of adolescent idiopathic scoliosis: an updated systematic review. Physiother Theory Pract. 2011;27(1):80-114.

205. Negrini S, Antonini G, Carabalona R, Minozzi S. Physical exercises as a treatment for adolescent idiopathic scoliosis. A systematic review. Pediatr Rehabil. 2003;6(3-4):227-35.

206. Lenssinck M-LB, Frijlink AC, YBerger M, Bierma-Zeinstra SM, Verkerk K, Verhagen AP. Effect of bracing and other conservative interventions in the treatment of idiopathic scoliosis in adolescents: a systematic review of clinical trials. Phys Ther. 2005;85(12):1329-39.

207. Negrini S, Fusco C, Minozzi S, Atanasio S, Zaina F, Romano M. Exercises reduce the progression rate of adolescent idiopathic scoliosis: results of a comprehensive systematic review of the literature. Disabil Rehabil. 2008;30(10):772-85.

208. Romano M, Minozzi S, Zaina F, altikov JB, Chockalingam N, Kotwicki T, et al. Exercises for adolescent idiopathic scoliosis: a Cochrane systematic review. Spine. 2013;38(14):E883-93.

209. Otman S, Kose N, Yakut Y. The efficacy of Schroths 3-dimensional exercise therapy in the treatment of adolescent idiopathic scoliosis in Turkey. Saudi Med J. 2005;26(9):1429.

210. Mooney V, Gulick J, Pozos R. A preliminary report on the effect of measured strength training in adolescent idiopathic scoliosis. J Spinal Disord. 2000;13(2):102–7.

211. Weiss HR, Weiss G, Petermann F. Incidence of curvature progression in idiopathic scoliosis patients treated with scoliosis in-patient rehabilitation (SIR): an age- and sex-matched controlled study. Pediatr Rehabil. 2003;6(1):23-30.

212. Weiss RH. The effect of an exercise program on vital capacity and rib mobility in patients with idiopathic scoliosis. Spine. 1991;16(1):88-93.

213. Moe JH. Indications for milwaukee brace non-operative treatment in idiopathic scoliosis. Clin Orthop Relat R. 1973;93:38-43.

214. Wong M, Evans J. Biomechanical evaluation of the Milwaukee brace. Prosthetics and orthotics international. 1998;22(1):54-67.

215. Mulcahy T, Galante J, DeWald R, Schultz A, Hunter J. A follow-up study of forces acting on the Milwaukee brace on patients undergoing treatment for idiopathic scoliosis. Clinical Orthopaedics and Related Research®. 1973;93:53–68.

216. Negrini S, Atanasio S, Negrini A, Parzini S. The evidence-based ISICO approach to spinal deformities. Milan: Carlo Crivelli; 2007.

217. Pham V, Houilliez A, Schill A, Carpentier A, Herbaux B, Thevenon A. Study of the pressures applied by a Chêneau brace for correction of adolescent idiopathic scoliosis. Prosthetics and orthotics international. 2008;32(3):345-55.

218. Kotwicki T, Cheneau J. Biomechanical action of a corrective brace on thoracic idiopathic scoliosis: Cheneau 2000 orthosis. Disability and Rehabilitation: Assistive Technology. 2008;3(3):146-53.

219. Dobrinka D, Đurđica S-P, Goran T, Nataša T, Vladimira Š-K. Cheneau Brace In The Treatment Of Idiopathic Scoliosis. Scripta Medica. 2014;45(2).

220. Rigo M, Weiss H. The Chêneau concept of bracing-Biomechanical aspects. Studies in health technology and informatics. 2008;135:303.

221. Weiss HR, Rigo M. The cheneau concept of bracing--actual standards. Studies in health technology and informatics. 2008;135:291-302.

222. van den Hout JA, van Rhijn LW, van den Munckhof RJ, van Ooy A. Interface corrective force measurements in Boston brace treatment. Eur Spine J. 2002;11(4):332-5.

223. Grivas TB, Rodopoulos GI, Bardakos NV. Night-time braces for treatment of adolescent idiopathic scoliosis. Disabil Rehabil Assist Technol. 2008;3(3):120-9.

224. Yrjonen T, Ylikoski M, Schlenzka D, Kinnunen R, Poussa M. Effectiveness of the Providence nighttime bracing in adolescent idiopathic scoliosis: a comparative study of 36 female patients. Eur Spine J. 2006;15(7):1139-43.

225. Emrani M, Kirdeikis R, Igwe P, Hill D, Adeeb S. Surface reconstruction of torsos with and without scoliosis. J Biomech. 2009;42(13):2200-4.

226. Wong MS, Cheng JCY, Lam TP, Ng BKW, Sin SW, Lee-Shum SLF, et al. The effect of rigid versus flexible spinal orthosis on the clinical efficacy and acceptance of the patients with adolescent idiopathic scoliosis. Spine. 2008;33(12):1360-5.

227. Coillard C, Leroux MA, Zabjek KF, Rivard CH. SpineCor - a non-rigid brace for the treatment of idiopathic scoliosis: post-treatment results. Eur Spine J. 2003;12(2):141-8.

228. Coillard C, Vachon V, Circo AB, Beause´jour M, Rivard CH. Effectiveness of the SpineCor Brace Based on the New Standardized Criteria Proposed by the Scoliosis Research Society for Adolescent Idiopathic Scoliosis. J Pediatr Orthop. 2007;27(4):376-9.

229. Coillard C, Circo AB, Rivard CH. A prospective randomized controlled trial of the natural history of idiopathic scoliosis versus treatment with the spinecor brace. Eur J Phys Rehabil Med. 2014;50(5):479-87.

230. Weiss HR, Weiss GM. Brace treatment during pubertal growth spurt in girls with idiopathic scoliosis (IS): a prospective trial comparing two different concepts. Pediatr Rehabil. 2005;8(3):199-206.

231. Wiemann JM, Shah SA, Price CT. Nighttime bracing versus observation for early adolescent idiopathic scoliosis. J Pediatr Orthop. 2014;34:603–6.

232. d'Amato CR, Griggs S, McCoy B. Nighttime Bracing With the Providence Brace in Adolescent Girls With Idiopathic Scoliosis. Spine. 2007;26(18):2006-12.

233. Gepstein R, Leitner Y, Zohar E, Angel I, Shabat S, Pekarsky I, et al. Effectiveness of the Charleston bending brace in the treatment of single-curve idiopathic scoliosis. J Pediatr Orthopaed. 2002;22:84-7.

234. Price CT, Scott DS, Reed FE, Riddick MF. Nighttime brace for adolescent liopathic scoliosis with the Charleston bending brace: preliminary report. Spine. 1990;15(12):1294-9.

235. Lee CS, Hwang CJ, Kim D-J, Kim JH, Kim Y-T, Lee MY, et al. Effectiveness of the Charleston Night-time bending brace in the treatment of adolescent idiopathic scoliosis. J Pediatr Orthop. 2012;32:368–72.

236. Aulisa AG, Guzzanti V, Falciglia F, Giordano M, Marzetti E, Aulisa L. Lyon bracing in adolescent females with thoracic idiopathic scoliosis: a prospective study based on SRS and SOSORT criteria. BMC Musculoskelet Disord. 2015;16:316.

237. Lusini M, Donzelli S, Minnella S, Zaina F, Negrini S. Brace treatment is effective in idiopathic scoliosis over 45 degrees : an observational prospective cohort controlled study. Spine J. 2014;14(9):1951-6.

238. Weinstein SL, Dolan LA, Wright JG, Dobbs MB. Effects of bracing in adolescents with idiopathic scoliosis. N Engl J Med. 2013;369(16):1512-21.

239. Aulisa AG, Guzzanti V, Galli M, Perisano C, Falciglia F, Aulisa L. Treatment of thoraco-lumbar curves in adolescent females affected by idiopathic scoliosis with a progressive action short brace (PASB): assessment of results according to the SRS committee on bracing and nonoperative management standardization criteria. Scoliosis. 2009;4:21.

240. Negrini S, Donzelli S, Lusini M, Minnella S, Zaina F. The effectiveness of combined bracing and exercise in adolescent idiopathic scoliosis based on SRS and SOSORT criteria: a prospective study. BMC Musculoskel Dis. 2014;15(1):263.

241. Giorgi SD, Piazzolla A, Tafuri S, Borracci C, Martucci A, Giorgi GD. Cheneau brace for adolescent idiopathic scoliosis: long-term results. Can it prevent surgery? Eur Spine J. 2013;22 Suppl 6:S815-22.

242. Wiley JW, Thomson JD, Mitchell TM, Smith BG, Banta JV. Effectiveness of the Boston brace in treatment of large curves in adolescent idiopathic scoliosis. Spine. 2000;25(18):2326-32.

243. Willers U, Normelli H, Aaro S, Svensson O, Hedlund R. Long-term results of Boston brace treatment on vertebral rotation in idiopathic scoliosis. Spine. 1993;18(4):432-5.

244. Negrini S, Grivas T, Kotwicki T, Rigo M, Zaina F, international Society on Scoliosis O, et al. Guidelines on "Standards of management of idiopathic scoliosis with corrective braces in everyday clinics and in clinical research": SOSORT Consensus 2008. Scoliosis. 2009;4:2.

245. Aubin CE, Lobeau D, Labelle H, Maquinghen-Godillon AP, LeBlanc R, Dansereau J. Planes of maximum deformity in the scoliotic spine. In: IAF Stokes (ed) Research into spinal deformities 2, IOS Press, Amsterdam, pp 45-481999.

246. Currier DP. Elements of research in physical therapy. 3rd ed: William & Wikins, Baltimore; 1984.

247. Dawson B, Trapp RG. Basic and clinical biostatistics. 4th ed: Lange Medical Books/McGraw-Hill, New York; 2004.

248. Hong JY, Suh SW, Modi HN, Hur CY, Song HR, Ryu JH. Centroid method: reliable method to determine the coronal curvature of scoliosis: a case control study comparing with the Cobb method. Spine. 2011;36(13):E855-E61.

249. Tanure MC, Pinheiro AP, Oliveira AS. Reliability assessment of Cobb angle measurements using manual and digital methods. Spine J. 2010;10(9):769-74.

250. Wu H, Ronsky JL, Cheriet F, Harder J, Kupper JC, Zernicke RF. Time series spinal radiographs as prognostic factors for scoliosis and progression of spinal deformities. Eur Spine J. 2011;20(1):112-7.

251. Cecen GS, Gulabi D, Cecen A, Oltulu I, Guclu B. Computerized tomography imaging in adolescent idiopathic scoliosis: prone versus supine. Eur Spine J. 2016;25(2):467-75.

252. Z Al-Aubaidi, Lebel D, Oudjhane K, Zeller R. Three-dimensional imaging of the spine using the EOS system: is it reliable? A comparative study using computed tomography imaging. J Pediatr Orthop B. 2013;22(5):409-12.

253. Harmouche R, Cheriet F, Labelle H, Dansereau J. 3D registration of MR and X-ray spine images using an articulated model. Comput Med Imaging Graph. 2012;36(5):410-8.

254. Hu ML, Wu XR. Fluid mechanics, 3rd Edition. Wuhan: Wuhan University of Technology Press 2008.

255. Maruyama T, Kobayashi Y, Miura M, Nakao Y. Effectiveness of brace treatment for adolescent idiopathic scoliosis. Scoliosis. 2015;10(Suppl 2):S12.

256. Zheng Y, Dang Y, Yang Y, Li H, Zhang L, Lou EHL, et al. Whether orthotic management and exercise are equally effective to the patients with adolescent idiopathic scoliosis in minland China? A Randomized Controlled Trial Study. Spine. 2018; 43(9): E494-E503.

257. Gao C, Zheng Y, Fan C, Yang Y, He C and Wong MS. Could the clinical effectiveness be improved under the integration of orthotic intervention and scoliosis-specific exercise in managing adolescent idiopathic scoliosis? A Randomized Controlled Trial Study. Am J Phys Med Rehabil. 2019; 98(8):642-8.

- END -